KINETICS OF DIELS-ALDER REACTIONS OF CYCLOPENTADIENE WITH FEED IMPURITIES

A Dissertation
Presented to
The Academic Faculty

by

Lisa Kirsten Wiest

In Partial Fulfillment
of the Requirements for the Degree
Master of Science in the
School of Chemical and Biomolecular Engineering

Georgia Institute of Technology
August 2018

KINETICS OF DIELS-ALDER REACTIONS OF CYCLOPENTADIENE WITH FEED IMPURITIES

Approved by:

Dr. Carsten Sievers, Advisor
School of Chemical and Biomolecular Engineering
Georgia Institute of Technology

Dr. Charles Liotta, Advisor
School of Chemistry
Georgia Institute of Technology

Dr. AJ Medford
School of Chemical and Biomolecular Engineering
Georgia Institute of Technology

Date Approved: [April 23, 2018]

ACKNOWLEDGEMENTS

Firstly, I would like to thank Dr. Carsten Sievers and Dr. Charles Liotta for their guidance, advice, and support throughout my pursuit of this master's thesis. I would like to thank the two post-docs who helped me in preparing my thesis: Sarath Chand and Rui Xu. I would also like to thank all my group members, former and present: Chuck, Jungseob, Alex, Sireesha, Jason, Qandeel, Andrew, Mike, Yimeng, Sean, Mark, Sarath, and Zhou, as well as Elise and Marianna who were visiting students from Brazil. Additionally, I would like to thank my friends who started this journey at the same time: Min, Solah, Jungwoo, Jung, Garrett, Brian, Leo, Luc, Wenqin, and Scott. My final acknowledgement goes to those who supported me during my time in Atlanta, although not at Georgia Tech: my Church in Atlanta family and my Atlanta Kendo Kai friends, who helped keep me sane and reminded me that there is more to life than just a graduate degree.

TABLE OF CONTENTS

LIST OF TABLES

LIST OF FIGURES

LIST OF SYMBOLS AND ABBREVIATIONS

A	Pre-exponential factor
CPD	Cyclopentadiene
CPD-1P	Cyclopentadiene – 1-pentene co-dimer
CPD-ISP	Cyclopentadiene – isoprene co-dimer
CPD-tP	Cyclopentadiene – trans-1,3-pentadiene co-dimer
DCPD	Dicyclopentadiene
DISP	Isoprene dimer
Dtp	Trans-1,3-pentadiene dimer
E_A	Activation Energy
ISP	Isoprene

SUMMARY

In this thesis, I present a developed kinetic model of cyclopentadiene with feed impurities. The model is valid for multiple impurities: isoprene, trans-1,3-pentadiene, 1-pentene, and cyclopentene. The model was developed from experiments over a temperature range of 80 °C to 160 °C. Reaction rate constants across this range were calculated and related activation energies and pre-exponential factors were derived. Overall, the model affirms that CPD self-dimerization is the dominant reaction occurring in the C5 stream, followed by the co-dimerization between cyclopentadiene and isoprene. For impurities, co-dimerization with CPD occurs more readily than self-dimerization.

CHAPTER 1. INTRODUCTION

1.1 Diels-Alder Reaction

Diels-Alder chemistry was first published in 1928.[1] The Diels-Alder reaction requires a diene and dienophile which react to create a ring structure. This reaction is a subset of cycloaddition reactions and can also be referred to as a [2+4] cycloaddition reaction. Figure 1 shows a typical Diels-Alder reaction. Mechanistically, the Diels-Alder reaction occurs in one-step by the flow of electrons. This makes a Diels-Alder reaction suitable for a kinetic study where no elementary reactions need to be assumed. The Diels-Alder reaction is already the elementary reaction.

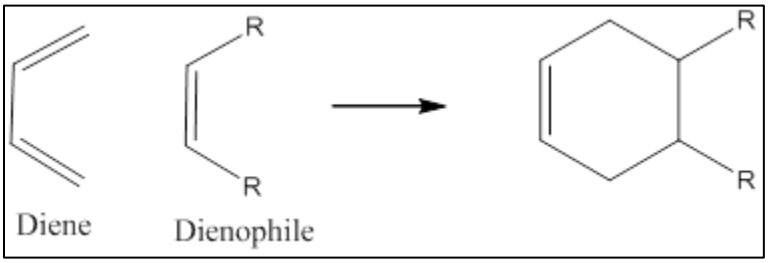

Figure 1: Typical Diels-Alder reaction.

1.2 Cyclopentadiene

The primary molecule studied in this thesis, cyclopentadiene (CPD), can act as both a diene and dienophile and thus can undergo a Diels-Alder reaction with itself. The Diels-Alder reaction of cyclopentadiene forms dicyclopentadiene (DCPD), which has two isomers: an endo-isomer (endo-DCPD) and an exo-isomer (exo-DCPD), as seen in Figure 2. Kinetically, the endo-isomer is preferentially formed.[2] However, the exo-isomer is thermodynamically more stable.[3] At typical reaction conditions, direct isomerization of

endo-DCPD to exo-DCPD does not occur.[4] The activation energy for the dimerization of CPD to endo-DCPD is low enough that the reaction occurs spontaneously ($\Delta G \leq 0$) even at room temperature.

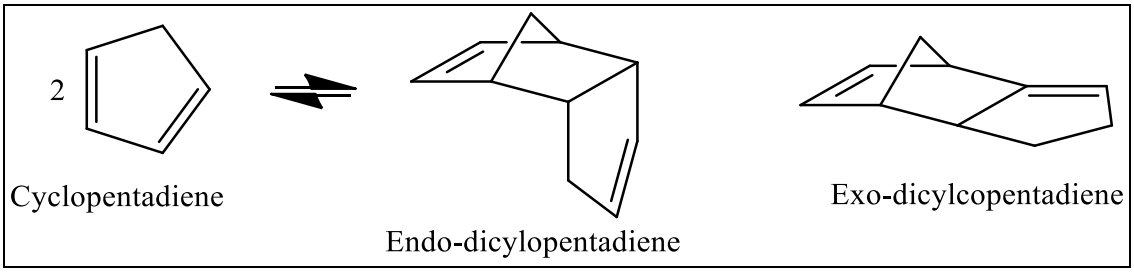

Figure 2: Dimerization of cyclopentadiene.

Industrially, cyclopentadiene is produced in reactive distillation in the petrochemical industry. It is the primary product in a C5 stream.[5] However, this stream will contain many feed impurities, such as cyclopentene, isoprene, methyl-1,3-cyclopentadiene isomers, and isoamylenes.[2, 5-7] The CPD is often reacted further to produce dicyclopentadiene which can be used in unsaturated polyester resins, as well as inks, adhesives, and paints.[8] DCPD is not only more industrially relevant than CPD, but it is easier to separate from most solvents due to its higher boiling point of 158 °C.

CHAPTER 2. EXPERIMENTAL SETUP

2.1 Materials

Dicyclopentadiene (95%, stabilized with butylated hydroxytoluene), toluene (>99.5%), cyclohexane (99.5%), trans-2-pentene (>99.0%), n-pentene (>98.5%), n-pentene (>98.0%), cyclopentene (>96.0%), cyclopentane (>98.0%), benzene (>99.0%), cyclooctane (>99.0%), and boron trifluoride diethyl etherate (> 46.5% BF_3 basis) were purchased from Sigma Aldrich. Isoprene (>99.0%, stabilized with 4-tert butylcatechol), trans-1,3-pentadiene (>93.0%, stabilized with 4-tert-butylcatechol), and cis-1,3-pentadiene (>97.0%) were purchased from TCI America. Cis-2-pentene (>95.0%) was purchased from Fisher Scientific.

2.2 Production of Cyclopentadiene

Due to the spontaneous reactivity of cyclopentadiene, it must be produced from dicyclopentadiene. The purchased dicyclopentadiene was cracked at 160 °C to produce pure cyclopentadiene. This cyclopentadiene was then stored at -35 °C. In order to maintain purity, the cyclopentadiene was distilled from a partially dimerized solution every two weeks.

2.3 Dimerization Reaction Conditions

Reaction solutions were prepared by adding an internal standard of cyclooctane, cyclopentadiene, and one or no feed impurities to a 25 mL volumetric flask by using an Eppendorf pipette. Toluene was added to the flask as a solvent. The volumetric flask was

mixed well and then 1.8 mL of solution was placed into each of nine separate 3 mL titanium reactor vials. The vials were sealed using PTFE tape to ensure they can withstand moderate pressure increases. These vials were placed in an aluminum heating block that was pre-heated to the desired reaction temperature. The setup is shown in Figure 3. Reactor vials were removed at specified times. Vials were quenched in an isopropyl alcohol and dry ice mixture (-78 °C) for 10 minutes to stop the reaction. Then reactor vials were placed in a freezer (-35 °C) until analyzed by GC as detailed in section 2.4. Each reaction was completed at least twice to ensure reproducibility and to determine appropriate error.

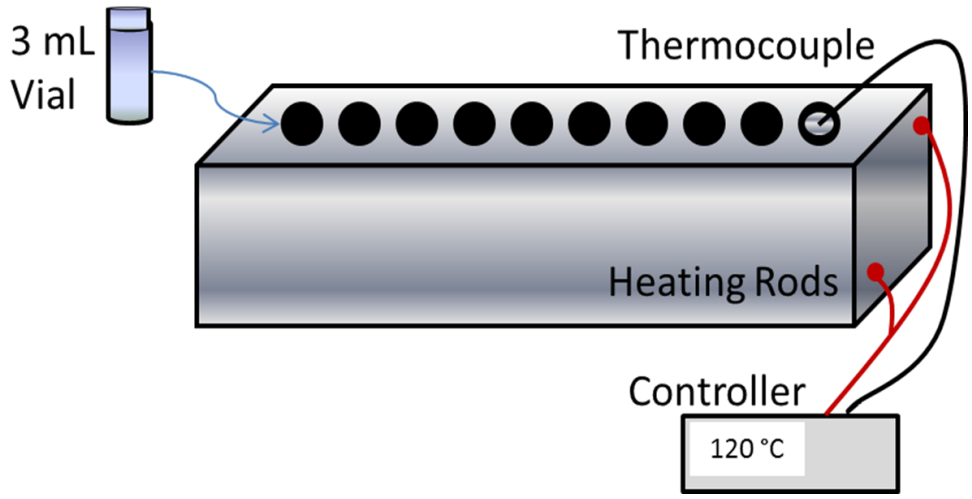

Figure 3: Dimerization reaction experimental setup.

2.3.1 Mixture Reaction Conditions

For the initial based mixture reactions, a reaction mixture was prepared according to the following table:

Table 1. Initial Mixture Composition

Chemical Name	Mol %
cyclopentadiene	25.47
cyclooctane	1.70
n-pentane	2.90
n-pentene	0.94
trans-2-pentene	2.34
cis-2-pentene	1.19
benzene	2.03
trans-1,3-pentadiene	0.68
cyclopentene	7.49
cyclopentane	2.03
toluene	53.23

2.4 Analytical Method

Reaction products were analyzed by Shimadzu GC-FID with an HP PONA 50m column in most cases. The injector temperature was 200 °C. The column was heated from 40 °C to 250 °C. Heating rates were dependent on the chemicals that were analyzed, as described in Appendix A.2 GC-FID Method Conditions. Some preliminary data was collected using a Shimadzu GC-MS and the method can be found in Appendix A.2 GC-FID Method Conditions

2.4.1 Internal Standard

Cyclooctane was used as an internal standard as it is not reactive with either cyclopentadiene or the impurities studied. It was added at a concentration of 0.15 M. A calibration curve of cyclooctane was prepared, resulting in a response factor of

28544793. This was used to calculate the concentration of cyclooctane in each sample. The initial sample was assumed to have a 100% mole balance in the 1.8 mL sample, and a ratio of the first cyclooctane concentration to the remaining samples was determined to calculate the total reaction volume. This reaction volume was then used to determine the total moles of carbon based on the concentrations of each individual component. The total moles of carbon for each sample after t = 0 min was compared to the initial t = 0 min sample to determine the carbon balance.

2.5 Kinetic Model

2.5.1 Cyclopentadiene Dimerization

The kinetic model assumed for the mixture of CPD in toluene, the solvent, is as follows:

$$2\ \text{CPD} \leftrightarrow \text{Endo-DCPD}\ (k_f, k_r)$$

$$2\ \text{CPD} \rightarrow \text{Exo-DCPD}\ (k_2)$$

At the temperatures studied, the conversion of cyclopentadiene to the endo isomer is reversible. However, the conversion of cyclopentadiene to exo-isomer is assumed to be irreversible, based on its thermal stability.[4]

$$\frac{dC_{CPD}}{dt} = k_r C_{Endo} - k_f {C_{CPD}}^2 - k_2 {C_{CPD}}^2 \qquad (1)$$

$$\frac{dC_{Endo}}{dt} = \frac{1}{2}(k_f {C_{CPD}}^2 - k_r C_{Endo}) \qquad (2)$$

$$\frac{dC_{Exo}}{dt} = \frac{1}{2} k_2 {C_{CPD}}^2 \qquad (3)$$

Based on rate constants k_f, k_r, and k_2, the activation energy and pre-exponential factor for these three reaction constants were determined from experiments at various temperatures (ranging between 80 °C and 160 °C). These values are calculated by fitting the experiment data to the Arrhenius equation listed below and solving for $E_{A,i}$ and A_i.

$$\ln(k_i) = \frac{E_{A,i}}{R}\left(\frac{1}{T}\right) + \ln(A_i) \qquad (4)$$

For reactions at 160 °C or higher, the formation of trimers was significant enough that it needed to be included in the kinetic model. Based on the long-term equilibration data detailed in section **Error! Reference source not found.**, the chemical equation and resulting rate equations were assumed to be as follows:

$$\text{Endo-DCPD} + \text{CPD} \rightarrow \text{Trimer}$$

$$\frac{dC_{CPD}}{dt} = k_r C_{Endo} - k_f {C_{CPD}}^2 - k_2 {C_{CPD}}^2 - k_{trimer} C_{CPD} C_{Endo} \qquad (5)$$

$$\frac{dC_{Endo}}{dt} = \frac{1}{2}\left(k_f {C_{CPD}}^2 - k_r C_{Endo}\right) - k_{trimer} C_{CPD} C_{Endo} \qquad (6)$$

$$\frac{dC_{trimer}}{dt} = k_{trimer} C_{CPD} C_{Endo} \qquad (7)$$

2.5.1.1 Computational Approach

In order to fit the experimental data to a computational model, initial values for the rate constants (k) were input based on expected order of magnitude. Using the first experimental concentration that is assumed to be at the desired reaction temperature (t = 10 min) and these initial k values, concentrations were numerically computed by using Euler's method with a time step of 1 min. The differences between the theoretical and

experimental concentrations were weighted by the standard deviation of each component's concentration over the entire experiment. The weighted residual sum squared error is minimized using Excel's Solver function. For the dimerization of CPD, an initial rate constant was determined by the slope of the first few points of $1/C_{CPD}$ versus time – assuming a second order reaction – and compared to the calculated k_f to ensure that the numerical method results had the same order of magnitude.

2.5.2 Isoprene Dimerization

Isoprene was one of the main impurities I wanted to study, as isoprene is known to readily polymerize.[9] Therefore, just as the reaction rate data was needed to determine the rate constants, activation energy, and pre-exponential factor for CPD dimerization, the rate constants for isoprene self-dimerization (and higher polymerization if significant) must be determined. Additionally, isoprene polymers of greater than 3 monomer units are not identified with the GC method described in Appendix A.2 GC-FID Method Conditions Therefore, decreases in the carbon balance are attributed to the formation of heavier isoprene polymers.

2.5.2.1 Isoprene Self-Dimerization

In the case of isoprene, there are 6 identified dimer products, seen in Figure 4. Identification is made on the basis of FID peaks with area changing over the time of the reaction and assisted by referring to the products identified by Krupka.[7] Of the identified products, there are three groups of two isomers each. The individual isomers cannot be distinguished and thus, data which refers to DISP 1 may have the structure of either DISP

1 or DISP 2 indicated below. For the kinetic model DISP 5 and DISP 6 were considered together to determine the rate constant.

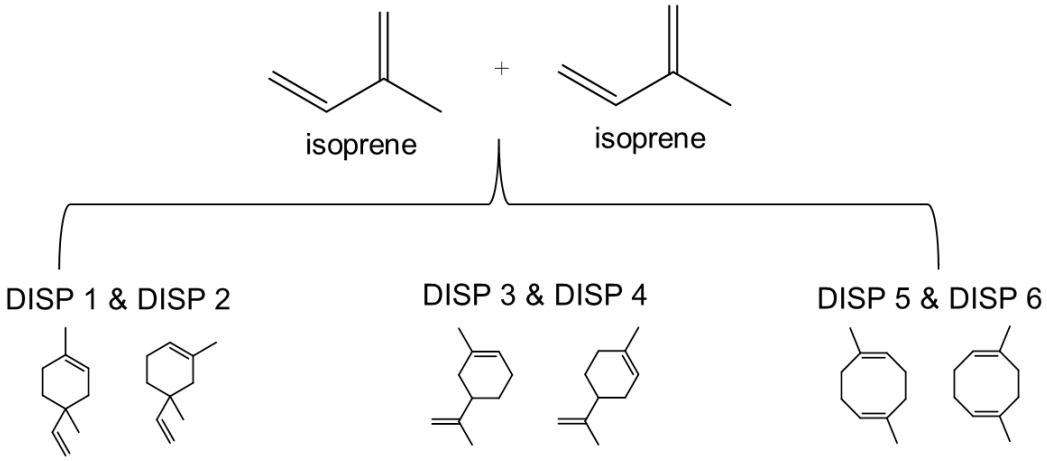

Figure 4: Isoprene dimers.

Rate constants are defined as follows:

$$\frac{dC_{DISPi}}{dt} = k_{DISPi}{C_{ISP}}^2 \qquad (7)$$

$$\frac{dC_{ISP}}{dt} = \sum_{i=1}^{6} -k_{DISPi}{C_{ISP}}^2 \qquad (8)$$

The rate constants were then solved for in the same manner as described in Section 2.5.1.1

The method described in this section is used for determining all other impurities self-dimerization kinetic data: (1) Determine impurity products, (2) Define appropriate rate equations, (3) Fit experimental data to model and determine kinetic parameters.

2.5.2.2 Co-dimerization Kinetic Model

After determining rate constants for CPD self-dimerization and isoprene, the rate constants for co-dimerization were determined. The rate constants for self-dimerization are calculated from the activation energy and pre-exponential factors calculated previously. Therefore, only the new rate constants (for co-dimerization) were fit in my model.

The co-dimerization of CPD and isoprene produced six co-dimers, labeled CPD-ISP 1 to CPD-ISP 6, as seen in Figure 5. These products were identified by FID peaks with area changing over the time of the reaction. In addition to the Diels-Alder mechanism for producing co-dimers, Krupka noted a Cope-rearrangement from CPD-ISP 2 to CPD-ISP 3.[7] The Cope rearrangement is a 1,5-diene isomerization that occurs when both ends of a σ bond change positions.[1]

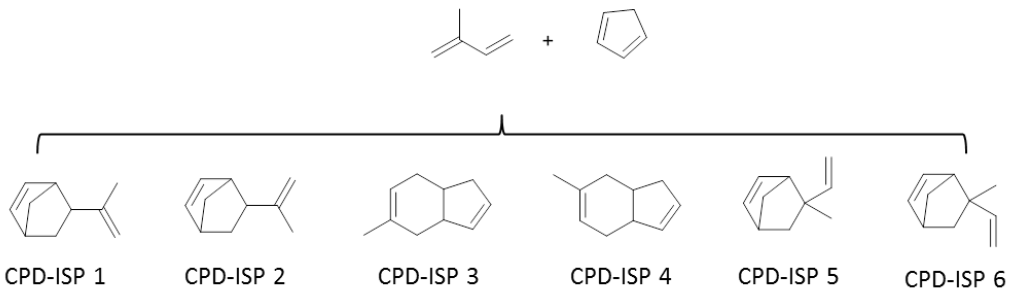

Figure 5: Cyclopentadiene-isoprene co-dimers.

The defined rate equations are as follows:

$$\frac{dC_{CPD-ISPi}}{dt} = k_{CPD-ISPi} C_{ISP} C_{CPD} \qquad (9.1)$$

$$\frac{dC_{CPD-ISP3}}{dt} = k_{CPD-ISP3} C_{ISP} C_{CPD} + k_{CI-2toCI-3} C_{CPD-ISP2} \quad (9.2)$$

$$\frac{dC_{CPD-ISP2}}{dt} = k_{CPD-ISP2}C_{ISP}C_{CPD} - k_{CI-2toCI-3}C_{CPD-ISP2} \quad (9.3)$$

$$\frac{dC_{ISP}}{dt} = \sum_{i=1}^{6} -k_{DISPi}{C_{ISP}}^2 + \sum_{j=1}^{6} -k_{CPD-ISPj}C_{ISP}C_{CPD} \quad (10)$$

$$\frac{dC_{CPD}}{dt} = k_r C_{Endo} - k_f {C_{CPD}}^2 - k_2 {C_{CPD}}^2 + \sum_{j=1}^{6} -k_{CPD-ISPj}C_{ISP}C_{CPD} \quad (11)$$

The rate constants were then solved for in the same manner as described in Section 2.5.1.1

The method described in this section is used for determining all other impurities co-dimerization kinetic data: (1) Determine co-dimerization products, (2) Define appropriate rate equations, (3) Fit experimental data to model for co-dimerization reactions only and determine co-dimerization kinetic parameters.

CHAPTER 3. RESULTS AND DISCUSSION

3.1 CPD Self-Dimerization

3.1.1 Reactor Vials Weight Consistency

At atmospheric pressure, a solution of cyclopentadiene and toluene evaporate at elevated temperatures due to relatively low boiling points. The boiling point of cyclopentadiene is 40 °C and the boiling point of toluene is 111 °C. Therefore, I analyzed the reactor weights before and after the experiment to ensure there that no gases left the reactor vial and that the entire sample was accounted for in the following GC analysis. The average weight of the reactor vial with feed reaction solution is 51.521 g. In the case of all samples the change of weight was 0.005 ± 0.002 g, which indicates the vials do not lose any reaction solution during the experiment.

3.1.2 GC Injector Temperature

In their research, Krupka et al. used an injector temperature of 250 °C.[10] A change in temperature will shift the thermodynamic equilibrium. The result of a shifted equilibrium would be that the sample we are actually analyzing – having undergone a reaction in the injector - is different from the experimental sample. Therefore, I examined the effect of the injector temperature on CPD dimerization and DCPD cracking.

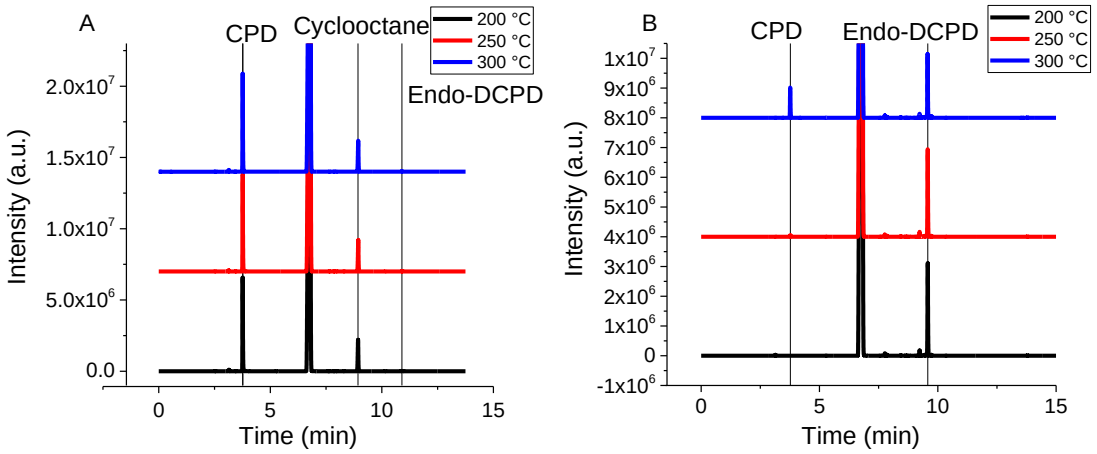

Figure 6: Injector temperature influence on (A) CPD dimerization and (B) DCPD cracking.

To study the dimerization of CPD in the injector, freshly prepared CPD in toluene with cyclooctane used as the internal standard were injected to the GC-FID at the temperatures of 200, 250, and 300 °C. In all three cases, only 1% endo-DCPD was found in the analyzed data, indicating that CPD does not undergo significant dimerization with the injector temperature ranges studied. The endo-DCPD is most likely due to small amounts of Endo-DCPD existing in the CPD solution.

To determine the effect of the injector temperature on the cracking of DCPD, DCPD containing a 5% BHT stabilizer with toluene as the solvent was injected to the GC-FID at 200, 250, and 300 °C. The peak areas between endo-DCPD (retention time ~ 9.6 min) and CPD (retention time ~ 3.7 min) at the 3 injection temperatures were analyzed. At an injector temperature of 300 °C, 32% of DCPD is lost to cracking. At 250 °C, the temperature used in prior literature,[2] 2% DCPD is lost to cracking. At 200 °C, there is no discernable CPD and thus no DCPD cracking observed. This indicates that

DCPD cracking increases with injector temperature. Thus, 200 °C was chosen as the injector temperature.

Initial experiments were run with an injector temperature of 300 °C, and the results are presented in Appendix B.3.

3.1.3 CPD Dimerization

CPD in toluene was reacted at 80, 100, 120, 130, and 140 °C to determine the self-dimerization rate constants, activation energy, and pre-exponential factor. Individual experimental data is presented in Appendix B.5 CPD Dimerization Data with 200 °C Injector Data

The activation energy for CPD to Endo-DCPD was calculated as 68.8 ± 0.7 kJ/mol. The pre-exponential factor is (8.49 ± 0.10) $\cdot 10^7$ 1/M·min. Previous literature has calculated 70.6 kJ/mol for cyclopentadiene in cyclohexane[2] and 67.9 kJ/mol for cyclopentadiene in toluene.[11]

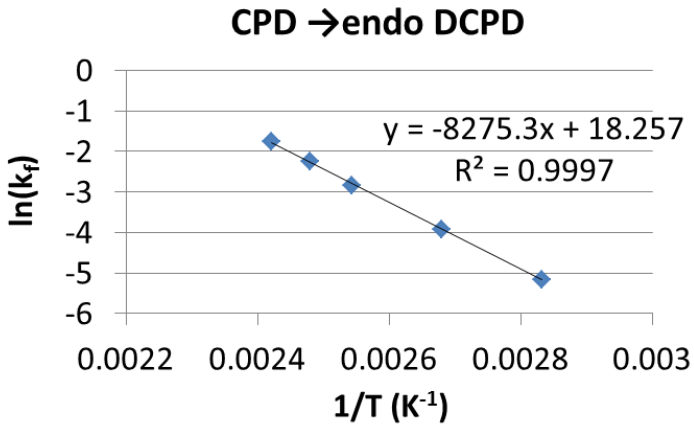

Figure 7: Arrhenius plot for CPD dimerization to endo-DCPD.

Krupka et al. restricted data collection to times where the cracking of DCPD (i.e. the reverse reaction of dimerization) was negligible. However, I have included the reverse reaction as well in order to determine the activation energy of the reverse reaction. The activation energy is 157.2 ± 3.9 kJ/mol, as determined from the slope of the Arrhenius plot shown in Figure 8. The pre-exponential factor is (7.02 ± 0.20) · 10^{16} 1/min.

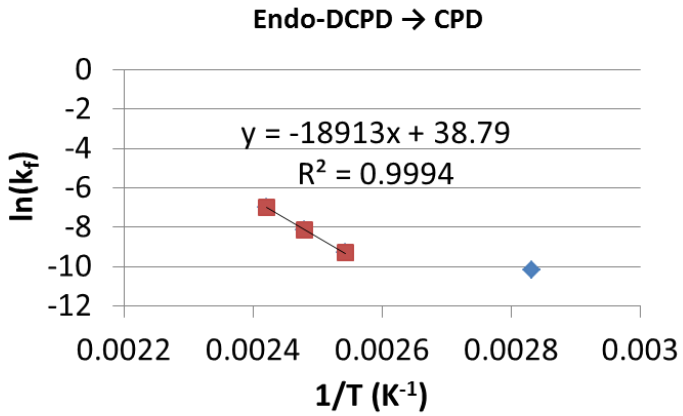

Figure 8: Arrhenius plot for the reverse dimerization of endo-DCPD to CPD.

The activation energy for CPD to exo-DCPD was calculated as 82.0 ± 3.4 kJ/mol. The pre-exponential factor is (5.08 ± 0.31) · 10^{7} 1/M·min. Krupka reported an activation energy of 82.0 kJ/mol for CPD to exo-DCPD in cyclohexane.[2]

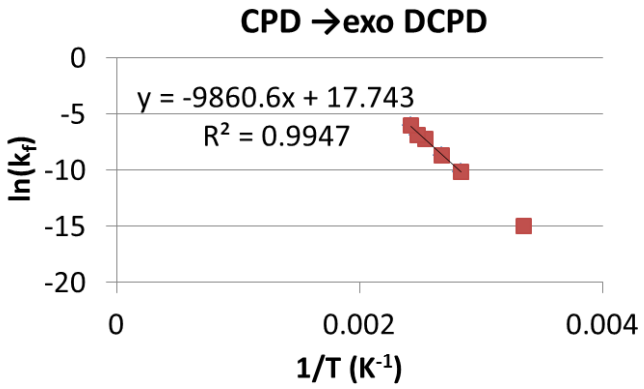

Figure 9: Arrhenius plot for CPD to exo-DCPD.

Lastly, the equilibrium between CPD and endo-DCPD was considered. Initially Density Functional Theory was used to calculate ΔH°, ΔS°, and ΔG° values, based on a system in vacuum and using B3LYP 6-311+G(2df,2p). The resulting ΔH°, ΔS°, and ΔG° values were -18.4 kcal/mol, -35 cal/K·mol, -8.3 kcal/mol respectively. These values were then used to determine the equilibrium between CPD and endo-DCPD in both neat CPD and a 0.571 CPD in toluene solution at temperatures between 0 and 300 °C. The results are shown in Figure 10.

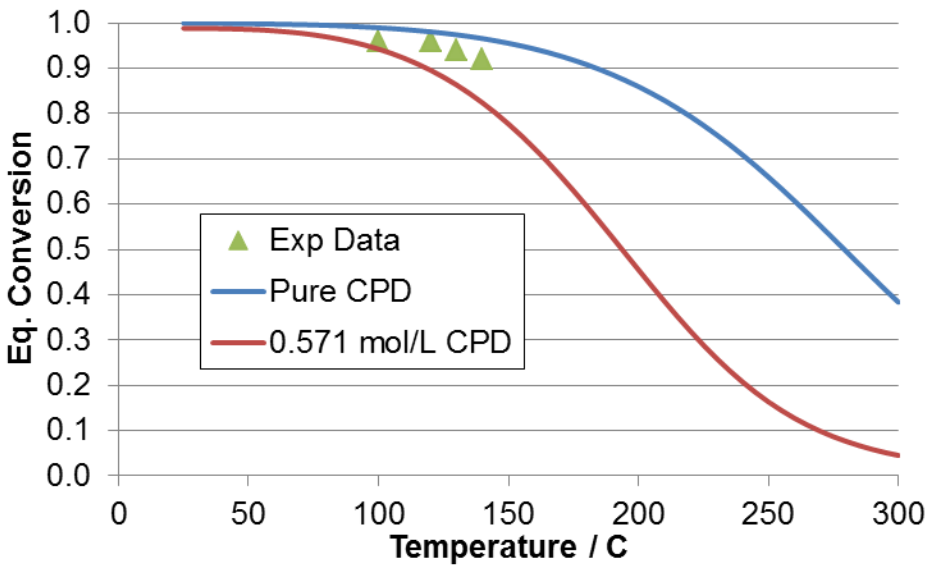

Figure 10: Equilibrium conversion between CPD and endo-DCPD based on DFT calculated values.

The experimental data matches the trend of the equilibrium conversion from DFT calculated values. However, the differences can be explained by the DFT system being calculated for a system in vacuum, rather than in toluene as the solvent, and that the DFT calculations do not consider trimer formation, which influences the equilibrium conversion at higher temperatures.

3.1.4 Long-term Equilibration Studies

Two long-term reactions at 140 °C and 160 °C were performed over 14 and 12 days, respectively. The starting mixture was toluene and CPD in a 9:1 molar ratio, resulting in a 1.32 M solution. Samples were examined after 5 minutes, considered time required for the heating block and the reaction vessels to reach a stable temperature, and then every 2 days for a total of 14 days. These initial experiments were analyzed by GC-MS to determine what products were produced over a long period and to determine

equilibrium concentrations. However, GC-MS is a more qualitative technique than quantitative.

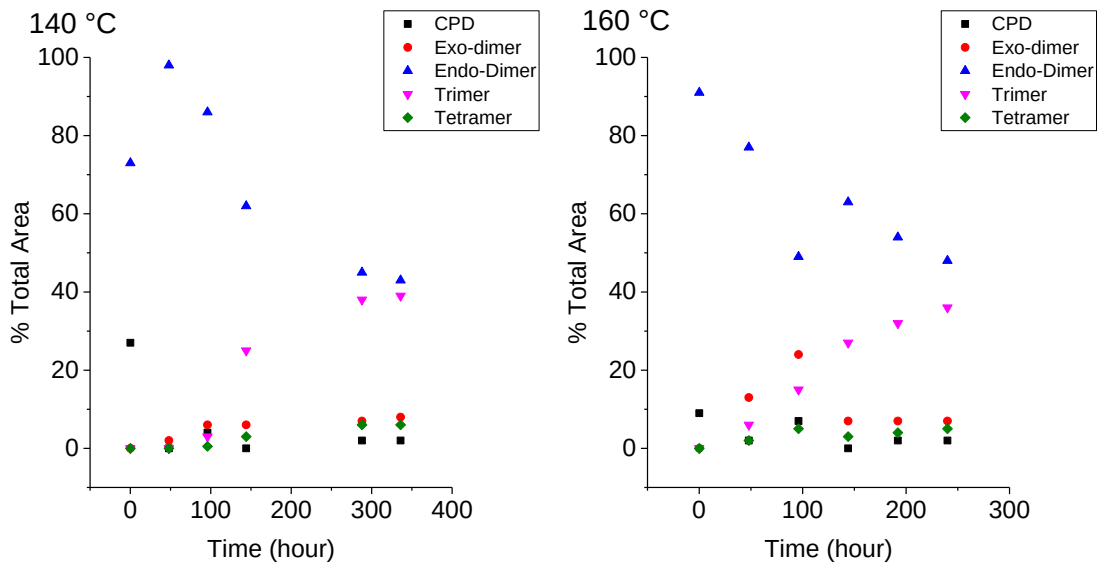

Figure 11: Composition based on percentage of GC-MS total area for CPD in toluene at 140 °C and 160 °C.

For both these experiments, the first samples were taken within 5 minutes, but at the high temperatures and initial concentrations used, much of the cyclopentadiene was converted into endo-dicyclopentadiene. In the case of 140 °C, over 70% was converted; for 160 °C, over 90% was converted. At longer time scales, endo-dicyclopentadiene was converted to exo-dicyclopentadiene, and trimers and tetramers were formed. The more rapid formation of trimers compared to tetramers indicates that tetramers preferentially form by a trimer + monomer, as opposed to two dimers reacting.

3.1.5 CPD Trimerization

At 160 °C, trimerization of CPD becomes significant, as trimer formation increases above a 1% value observed in lower temperatures. Figure 12 below shows the formation of trimer as a function of time. For this temperature, k_f is $3.22 \cdot 10^{-1}$ 1/M·min. k_r is $6.84 \cdot 10^{-3}$ 1/min. k_2 is $5.84 \cdot 10^{-4}$ 1/M·min. k_{trimer} is $9.55 \cdot 10^{-4}$ 1/M·min. Trimers are primarily formed as a reaction between endo-DCPD and a CPD monomer, as determined in section 3.1.4.

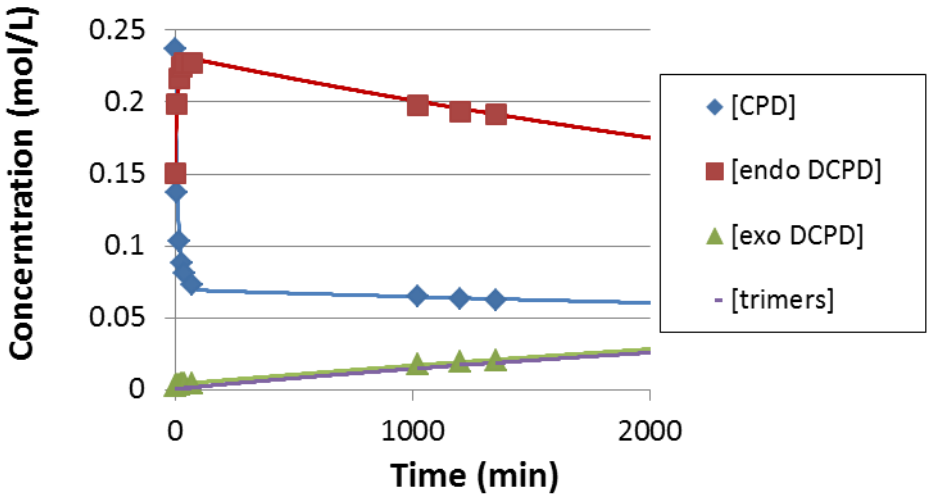

Figure 12: Formation of CPD trimers at 160 °C.

3.1.6 Effect of Solvent on CPD Dimerization

Since I compared my initial results to data collected by Krupka, the difference in activation energies resulting from cyclohexane – used as a solvent by Krupka – and toluene – used in most of my experiments – was examined.[2] The use of a different solvent was expected to have a negligible effect on the rate data. Decreased solvent

polarity increases relative reactivity – where cyclohexane (0.006) has a lower polarity than toluene (0.099).[12] However, solvents with higher boiling points increase the reaction rate – where toluene (110.6 °C) has a higher boiling point than cyclohexane (80.7 °C). These two effects appear to cancel out, resulting in minimal difference of the CPD dimerization reaction in toluene and in cyclohexane.

The activation energy for CPD dimerization in cyclohexane is70.1 kJ/mol, as compared to 68.8 kJ/mol determined in section 3.1.3. This value for CPD dimerization in cyclohexane is within 0.5 kJ/mol of Krupka's reported activation energy.[2] The slight difference may be due to the different injector temperature that Krupka uses as detailed in section 3.1.2. Details of the data and comparison can be found in Appendix B.4.2.

3.1.7 Summary of CPD Self-Dimerization

Overall, the activation energies from my research are consistent with those calculated by Krupka in literature. However, my model is more detailed in considering both the reverse dimerization of endo-DCPD to CPD and the formation of trimers at higher temperatures.

Table 2. Comparison of Calculated Activation Energies for CPD Dimerization with Literature Values

Reaction	Activation Energy (kJ/mol)	Krupka's Value[2] (kJ/mol)
2 CPD → Endo-DCPD	68.8 ± 0.7	70.62
2 CPD → Exo-DCPD	82.0 ± 3.4	80.16
Endo-DCPD → 2 CPD	157.2 ± 3.9	N/A

3.2 Conversion of CPD with Model Impurities

Having obtained the activation energy and pre-exponential factor for cyclopentadiene by itself, the next step was to test individual impurities. The impurities studied were isoprene, trans-1,3-pentadiene, 1-pentene, and cyclopentene. These impurities were chosen as they are found in C_5 streams produced during stream cracking of petroleum.[13]

3.2.1 Initial Mixture of Impurities

Before preforming individual impurity studies, an experiment consisting of possible impurities was run to determine the priority of impurities to be studied. The only impurity excluded from this study was isoprene, as it was expected to be the most reactive due to its own polymerization activity. The results in Figure 13 show that trans-1,3-pentadiene was the most reactive in this experiment, followed by n-pentene and trans-2-pentene. Therefore, these were the impurities I focused on in the following experiments.

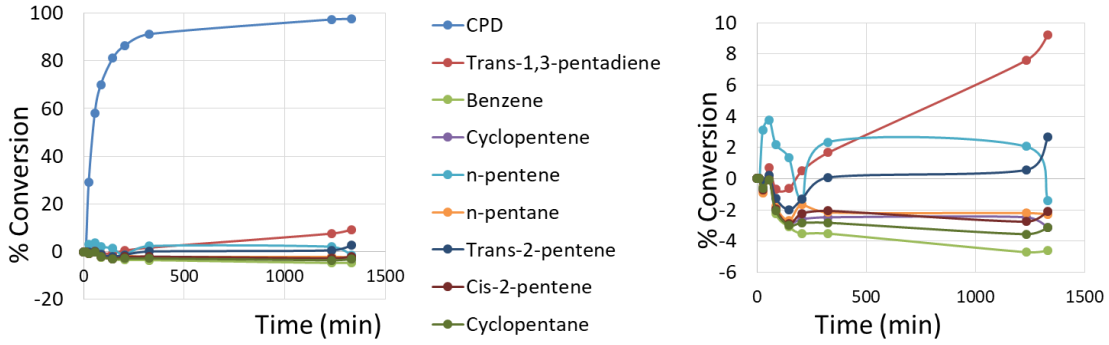

Figure 13: Conversion of various impurities at 100 °C (left) with CPD plotted and (right) without CPD plotted.

To affirm that these impurities were the most active, I also ran another experiment at 150 °C to increase the relative reaction rates. This experiment confirmed that besides isoprene, trans-1,3-pentadiene was the most reactive followed by n-pentene. The results are detailed in appendix B.6 Initial Mixture Results

3.2.2 Isoprene

Since isoprene was expected to be one of the more reactive compounds due the reactivity it has with other isoprene molecules, it was the first impurity to be studied in detail. As noted in section 2.5.2, isoprene rapidly polymerizes with itself. Commercial isoprene is thus sold with 5-tert-butylcatechol as a stabilizer to prevent polymerization. However, at higher temperatures, this stabilizer is no longer active and isoprene molecules react to form polymers.

3.2.2.1 Isoprene Self-dimerization

Just as cyclopentadiene was first studied alone, isoprene was also first studied to determine products from self-dimerization. As noted in section 2.5.2.1, six different

isoprene dimers were found. The calculated activation energies, pre-exponential factors, and a resulting rate constant (k) at 120 °C for the various isoprene dimers are listed in Table 3.

Table 3: Activation Energy and Pre-exponential Factors for Isoprene Dimers

Product	Activation Energy (kJ/mol)	Pre-exponential Factor (1/M·min)	k at 120 °C (1/M·min)
DISP 1	96.0 ± 1.9	$(1.75 \pm 0.06)\cdot 10^{7}$	$3.04\cdot 10^{-6}$
DISP 2	100.9 ± 2.8	$(1.32 \pm 0.05)\cdot 10^{8}$	$5.12\cdot 10^{-6}$
DISP 3	86.3 ± 3.6	$(6.60 \pm 0.45)\cdot 10^{6}$	$2.23\cdot 10^{-5}$
DISP 4	88.6 ± 0.7	$(8.44 \pm 0.11)\cdot 10^{6}$	$1.41\cdot 10^{-5}$
DISP 5&6	95.9 ± 3.5	$(1.42 \pm 0.09)\cdot 10^{7}$	$2.54\cdot 10^{-6}$

The activation energies for the dimerization reactions of isoprene are more than 20 kJ/mol greater than the activation energy for CPD self-dimerization. DISP 3 and DISP 4 are the most dominant dimers formed, which agrees with their lower activation energies and resulting higher k at 120 °C.

3.2.2.2 Effect of Air on Polymerization of Isoprene

Initial experiments on the self-dimerization of isoprene indicated that the presence of air affected the polymerization of isoprene. A decrease in the carbon balance was

observed for reactions that had some air in the vial compared to those reactor vials, which were prepared in a glovebox to avoid air contamination in the vial. The difference in the carbon balances can be seen in Figure 14**Error! Reference source not found.**. The decrease in the carbon balance for the reactions in the presence of air also mirrored the increase in conversion of isoprene. Therefore, I hypothesize that this decrease is due to the polymerization of isoprene to heavier polymers that were not detected by our GC-FID method. Visually, I observed particles in the solution after the reaction, which also suggests the formation of heavier isoprene polymers.

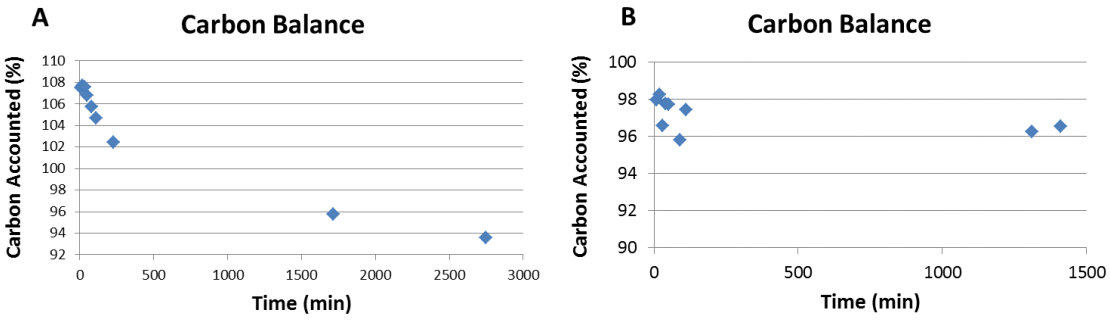

Figure 14: Carbon balance for reactions of isoprene and toluene at 120 °C, with feeds prepared in air (A) and prepared in a glove box with inert atmosphere (B).

In addition, air was found to affect the dimerization of isoprene to isoprene dimers 1 and 2 – as labeled in section 2.5.2.1.

3.2.2.3 Effect of Reactor Material

When the decreased carbon balance of isoprene mentioned above was observed, one theory was that the increase in polymerization was not due to the presence of air, but rather catalytically active material from the reactor vials. Leached metal from a reactor can catalyze a reaction.[9] For example, polymerization reactions can be catalyzed by

Ziegler-Natta catalysts, such as $TiCl_3$.[1] The reactor vials used initially were made from titanium, so I used stainless steel reactor vials to determine if the reactor vial material made a difference. The starting solution for both experiments was prepared in air. However, both experiments showed similar decreases in the carbon balance, indicating that polymerization was still occurring for both reactor vial materials.

3.2.2.4 Isoprene and CPD Co-dimerization

In the case of isoprene and CPD co-dimerization, six co-dimers were identified, as shown in section 2.5.2.2. However, the GC peak of CPD-ISP 4 overlaps with that of endo-DCPD, so only five co-dimer activation energies were determined. The calculated activation energies, pre-exponential factors, and a resulting rate constant (k) at 120 °C for the various isoprene dimers are listed in Table 4.

Table 4: Activation Energy and Pre-exponential Factors for Cyclopentadiene-Isoprene Co-dimers

Product	Activation Energy (kJ/mol)	Pre-exponential Factor (1/M·min)	k at 120 °C (1/M·min)
CPD-ISP 1	89.6 ± 2.1	$(6.13 \pm 0.21)\cdot 10^{7}$	$7.55\cdot 10^{-5}$
CPD-ISP 2	81.1 ± 1.5	$(6.57 \pm 0.16)\cdot 10^{7}$	$5.09\cdot 10^{-3}$
CPD-ISP 3	77.9 ± 2.0	$(5.08 \pm 0.19)\cdot 10^{6}$	$2.25\cdot 10^{-4}$
CPD-ISP 5	85.2 ± 2.3	$(9.26 \pm 0.39)\cdot 10^{6}$	$4.39\cdot 10^{-5}$

CPD-ISP 6	67.5 ± 9.4	$(2.30 \pm 0.65)\cdot 10^{4}$	$2.45\cdot 10^{-5}$
CPD-ISP 2 to 3	151.8 ± 5.2	$(1.05 \pm 0.04)\cdot 10^{16}$	$6.99\cdot 10^{-5}$

CPD-ISP 2 is produced with the highest concentration at the temperatures studied, which agrees with its high pre-exponential factor and activation energy that is within the middle range for all the possible co-dimers. The pre-exponential factor and activation energy results in a rate constant with one or two orders of magnitude greater than other co-dimers.

The rate constants for co-dimerization of CPD and isoprene are two to three orders of magnitude higher on average than the dimerization of isoprene, but the rate constant for the formation of CPD-ISP 2 is still one order of magnitude smaller than CPD dimerization to endo-DCPD.

3.2.3 Trans-1,3-pentadiene

When examining all possible impurities for a C5 stream, trans-1,3-pentadiene was the second most reactive after isoprene. Trans-1,3-pentadiene is also forms dimers with itself, so the self-dimerization react was studying before the dimerization of CPD with trans-1,3-pentadiene.

3.2.3.1 Trans-1,3-pentadiene Self-dimerization

Seven dimers were eluted with our GC method, as seen in Figure 15. The structures for Dtp 4 and Dtp 5 are indistinguishable so the labels are assigned arbitrarily to the two possible structures. A seventh peak is identified which most likely

corresponds to a product from a [4,4]-cycloaddition product – although the exact product is not identified.[10] The calculated activation energies, pre-exponential factors, and a resulting rate constant (k) at 120 °C for the various isoprene dimers are listed in Table 5.

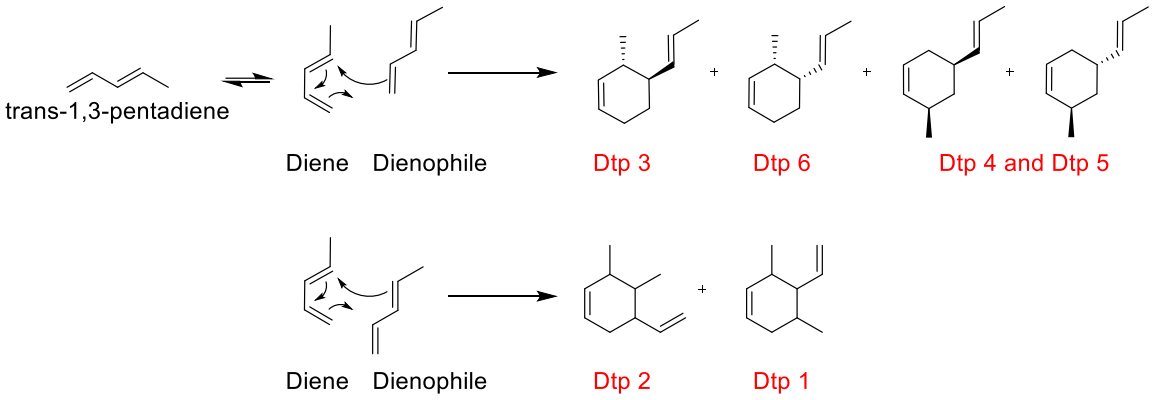

Figure 15: Dimers from trans-1,3-pentadiene self-dimerization.

Table 5: Activation Energy and Pre-exponential Factors for Trans-1,3-pentadiene Dimers

Product	Activation Energy (kJ/mol)	Pre-exponential Factor (1/M·min)	k at 120 °C (1/M·min)
Dtp 1	100.7 ± 2.5	$(3.88 \pm 0.16)\cdot 10^{7}$	$1.60\cdot 10^{-6}$
Dtp 2	108.2 ± 2.9	$(3.18 \pm 0.14)\cdot 10^{8}$	$1.32\cdot 10^{-6}$
Dtp 3	97.3 ± 0.6	$(5.79 \pm 0.06)\cdot 10^{7}$	$6.76\cdot 10^{-6}$

Dtp 4	97.5 ± 5.8	$(1.27 \pm 0.13)\cdot 10^{7}$	$1.39\cdot 10^{-6}$
Dtp 5	97.9 ± 4.8	$(1.04 \pm 0.09)\cdot 10^{7}$	$1.01\cdot 10^{-6}$
Dtp 6	89.6 ± 1.4	$(8.06 \pm 0.21)\cdot 10^{6}$	$9.93\cdot 10^{-6}$
Dtp 7	125.1 ± 2.5	$(1.33 \pm 0.04)\cdot 10^{10}$	$3.13\cdot 10^{-7}$

Trans-1,3-pentadiene self-dimerization is not very favorable at the temperatures studied. The activation energies are all more than 30 kJ/mol higher than the activation energy for CPD to endo-DCPD. The activation energies result in rate constants on the order of -7, up to 5 orders less than CPD dimerization.

3.2.3.2 Trans-1,3-pentadiene and CPD Co-dimerization

For the co-dimerization of trans-1,3-pentadiene and CPD, six co-dimers were identified, labelled CPD-tP 1 to 6, and as shown in Figure 16 below. Identifications were made based on peaks in my GC-FID chromatograms and previous identifications by Krupka et al.[6]

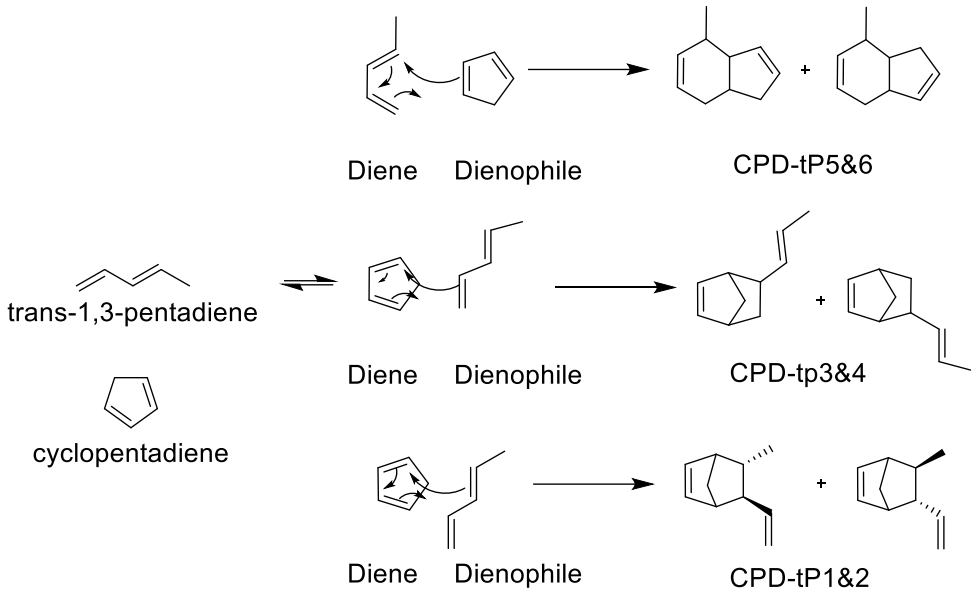

Figure 16: CPD and trans-1,3-pentadiene co-dimer structures.

Table 6: Activation Energy and Pre-exponential Factors for Cyclopentadiene-Trans-1,3-pentadiene Co-dimers

Product	Activation Energy (kJ/mol)	Pre-exponential Factor (1/M·min)	k at 120 °C (1/M·min)
CPD-tP 1	88.2 ± 3.5	$(9.62 \pm 0.64)\cdot 10^{6}$	$1.82\cdot 10^{-5}$
CPD-tP 2	96.7 ± 1.1	$(8.68 \pm 0.15)\cdot 10^{7}$	$1.22\cdot 10^{-5}$
CPD-tP 3	80.3 ± 1.6	$(1.76 \pm 0.05)\cdot 10^{7}$	$3.73\cdot 10^{-4}$
CPD-tP 4	85.8 ± 7.8	$(2.85 \pm 0.38)\cdot 10^{7}$	$1.12\cdot 10^{-4}$
CPD-tP 5	96.1 ± 5.9	$(4.58 \pm 0.47)\cdot 10^{7}$	$7.72\cdot 10^{-6}$
CPD-tP 6	93.3 ± 2.8	$(2.46 \pm 0.11)\cdot 10^{8}$	$9.77\cdot 10^{-5}$

Trans-1,3-pentadiene is slightly more reactive with CPD than it is with itself – as evidenced by rate constants being 1-2 orders of magnitude higher for co-dimers than just trans-1,3-pentadiene dimers. However, CPD still prefers to react with itself rather than trans-1,3-pentadiene, since CPD dimerization is still at least 2 orders of magnitude higher.

3.2.4 1-Pentene

1-pentene does not undergo any Diels-Alder reaction with itself or any other significant polymerization type reaction. Therefore, unlike the previous impurities, a detailed study on the self-dimerization is not required. The co-dimers produced from 1-pentene and CPD are studied. As seen in Figure 17, four possible co-dimers are identified. However, only two co-dimer peaks are identified. I hypothesize that first the exo-isomers will elude off the GC column, in the same that was exo-DCPD eludes before endo-DCPD. Furthermore, since only two peaks were identified, each peak represents a mixture of isomers: the first peak being both the exo-isomers and the second peak being both the endo-isomers.

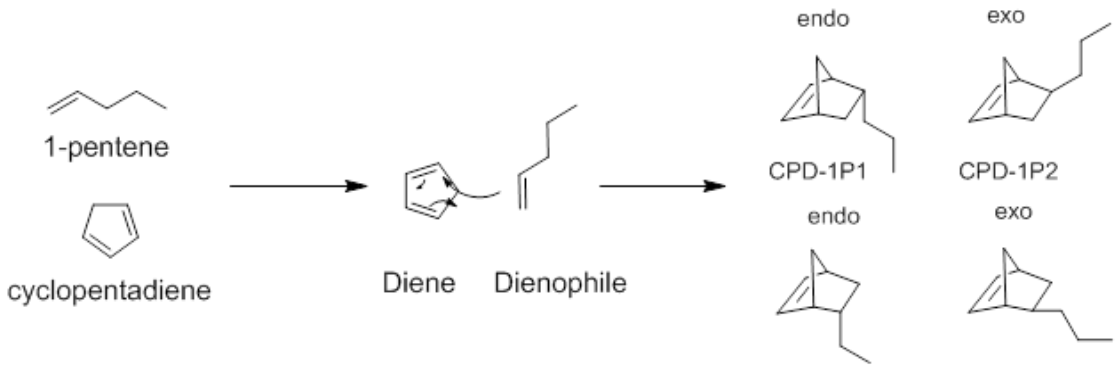

Figure 17: Co-dimers formed by 1-pentene and cyclopentadiene.

The calculated activation energy for the formation of CPD-1P 1 is 83.1 ± 1.8 kJ/mol. The pre-exponential factor is $(6.54 \pm 0.23) \cdot 10^6$ 1/M·min. The calculated activation energy for the formation of CPD-1P 2 is 78.6 ± 2.0 kJ/mol. The pre-exponential factor is $(5.63 \pm 0.25) \cdot 10^5$ 1/M·min.

Table 7: Activation Energy and Pre-exponential Factors for Cyclopentadiene-1-pentene Co-dimers

Product	Activation Energy (kJ/mol)	Pre-exponential Factor (1/M·min)	k at 120 °C (1/M·min)
CPD-1P 1	83.1 ± 1.8	$(6.54 \pm 0.23) \cdot 10^6$	$5.89 \cdot 10^{-5}$
CPD-1P 2	78.6 ± 2.0	$(5.63 \pm 0.25) \cdot 10^5$	$2.01 \cdot 10^{-5}$

The co-dimers are produced on a similar magnitude of order compared to other co-dimers.

3.2.5 Cyclopentene

I investigated the co-dimerization of cyclopentene with cyclopentadiene. The first experiment at 100 °C showed no reaction between cyclopentadiene and cyclopentene, as seen in Figure 18. Neither GC-MS analysis nor GC-FID analysis showed additional peaks which would indicated the co-dimer of cyclopentadiene and cyclopentene.

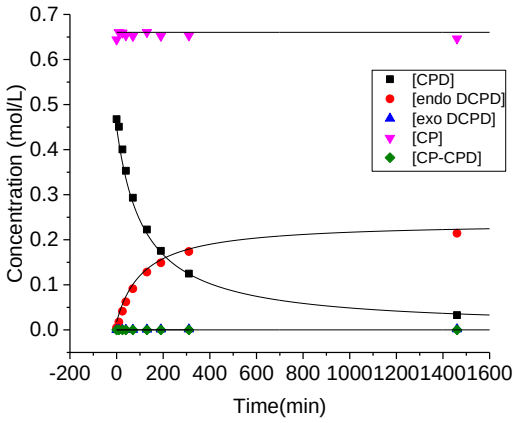

Figure 18: Co-dimerization of cyclopentadiene with cyclopentene at 100 °C and 1:1 vol. ratio.

For a model where only the dimerization of CPD by itself is considered, the calculated k_f rate constant is $1.87 \cdot 10^{-2}$ 1/M·min, which is within the 6% of the k_f at 100 °C for just cyclopentadiene in toluene $1.98 \cdot 10^{-2}$ 1/M·min. This indicates the rate constant is unaffected by the presence of cyclopentene at 100 °C.

Two additional experiments were performed to confirm that cyclopentadiene and cyclopentene do not react. I prepared a reaction solution with a 10:1 volume ratio of cyclopentene to cyclopentadiene. At 120 °C with this volume ratio, cyclopentene still reacts negligibly with cyclopentadiene such that no dimers are detected in the GC-FID chromatograph. The results are detailed in appendix B.

The second additional experiment was CPD with cyclopentene in toluene at 150 °C, with a 1:1 volume ratio. Even at an elevated temperature, no co-dimers were formed. The results are detailed in appendix B.

3.2.6 Summary of CPD with Model Impurities

For the impurities studied, cyclopentadiene was most reactive with isoprene. The CPD-ISP 3 and 4 co-dimers were most prominent. Trans-1,3-pentadiene had moderate reactivity compared to isoprene. 1-pentene had very small reactivity and cyclopentadiene did not react at all. In order to accurately use this model, the reaction must take place without the presence of air – as the isoprene dimerization is dependent on an inert atmosphere.

CHAPTER 4. CONCLUSIONS AND FURTHER RECOMMENDATIONS

In this thesis, I have presented a comprehensive kinetic model of cyclopentadiene dimerization with feed impurities. The model is accurate for temperature ranges of 80 °C to 160 °C. The model consists of cyclopentadiene as the primary reactant, toluene as the solvent, and isoprene, trans-1,3-pentadiene, trans-2-pentene, and cyclopentene as impurities. Figure 19 shows the reaction map for those impurities studied. The most reactive impurity is isoprene, with CPD-ISP 2 being produced at the highest rate. However, CPD self-dimerization is still the dominant reaction for all the temperatures studied. Generally, co-dimerization for an impurity with CPD occurs more readily than self-dimerization of the impurities studied.

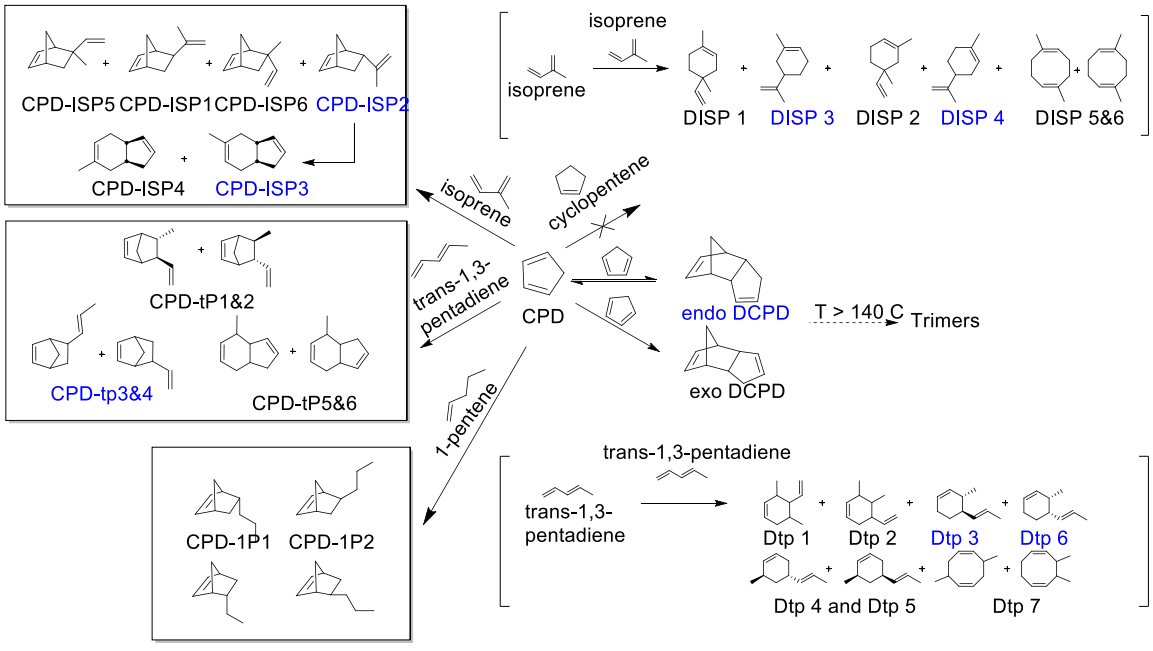

Figure 19: Reaction map of CPD with feed impurities.

Next steps for this reaction would be to further examine the effect of a Lewis acid on the reaction and determine if this reaction could be run catalytically at a lower temperature, reducing the energy burden industrially and preventing undesired side reactions. Alternatively to adding a Lewis acid catalyst intentionally, such research could shed light if industrial reaction rates are higher than a model such as the one I developed. Leeched metals from an industrial reactor could unintentionally act as a catalyst for either a desired or undesired reaction. Therefore, understanding how Lewis acids catalyze these reactions is beneficial both industrially and as novel information for the scientific field – as there is no literature on Lewis acid catalyzed CPD dimerization with feed impurities.

An additional step is to examine any other impurities that might be present in the C5 stream, including higher weight polymers from CPD and feed impurities. My study does not include rates of formation for tetramers or higher level molecular weights, nor does it include trimer formation for lower temperatures. The influence of trimers in the reaction mixture could be studied.

APPENDIX A. GC METHODS

A.1 GC-MS Method Conditions

The equipment used was a Shimadzu GC-2010 with GCMS-QP2010S detector.

GC Conditions	
Column	DB 18
Inlet Temperature	200 °C
Injection Mode	Split (150:1)
Injection Volume	1 μL
Carrier Gas, Inlet Pressure	He (12.4 psi)
Oven Program	40 °C (3 min) to 180 °C at 6 °C/min (Hold 1 min). Increase to 220 at 10 °C/min (Hold 15 min) for a total run time of 46.33 min.

MS Conditions (Full Scan Mode)	
Ion Source Temperature	200 °C
Interface Temperature	250 °C
Solvent Cut Time	0.3 min
Scan Range	50 – 6000 m/z
Scan Speed	1250
Event Time	0.5 sec

A.2 GC-FID Method Conditions

The equipment used was a Shimadzu GC-2010 equipped with an FID detector.

GC Conditions	
Column	HP-PONA (50 m x 0.20 mm id x 0.50 μm d_f)
Oven Program	40 °C (2 min) to 250 °C at 7 °C/min (Hold 5 min) for a total run time of 37 min.
Detector Temperature	340 °C
Injector Temperature	200 °C
Carrier Gas, Inlet Pressure	He (323.9 kPa)
Split Ratio	80
Injection Volume	1.0 μL

APPENDIX B. EXPERIMENTAL DATA

B.1 GC-MS Peak Identification

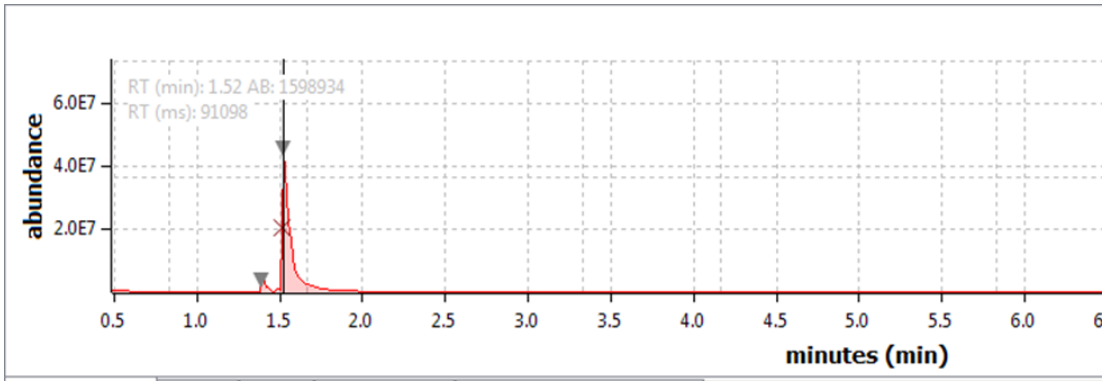

Figure 20: Chromatogram of pure CPD.

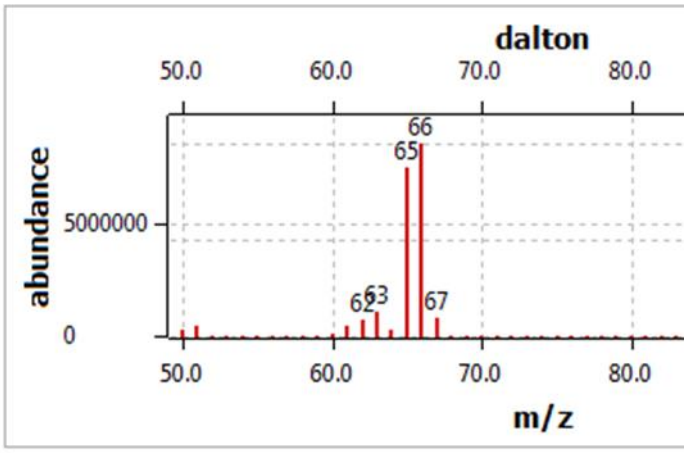

Figure 21: Mass spectrum of pure CPD.

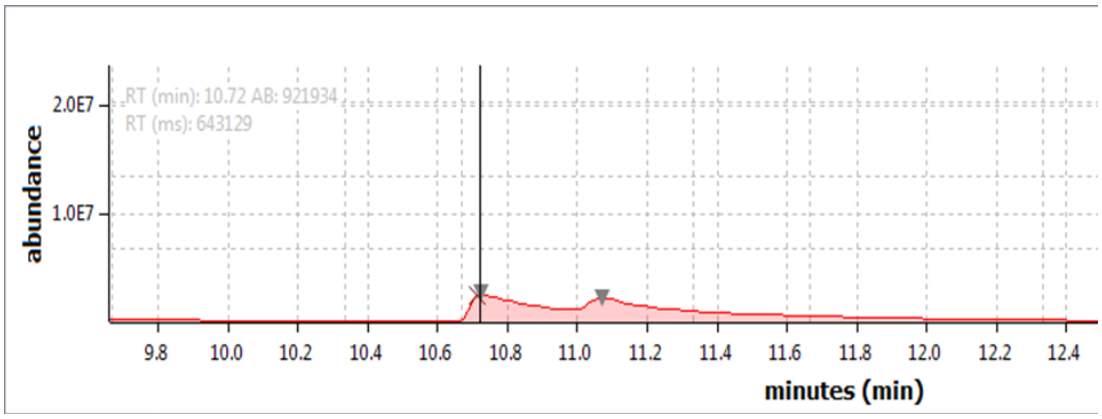

Figure 22: Chromatogram of DCPD isomers.

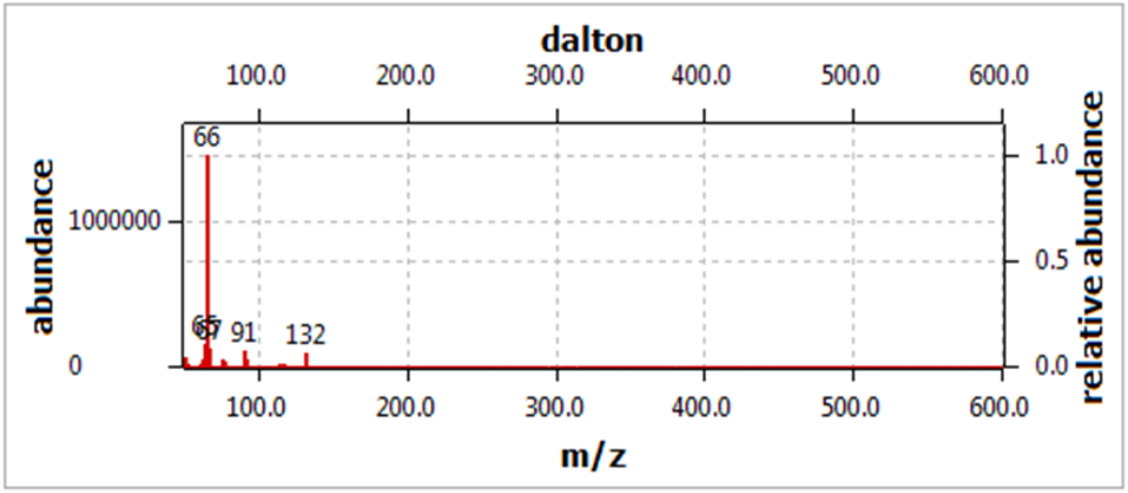

Figure 23: Mass spectrum of DCPD.

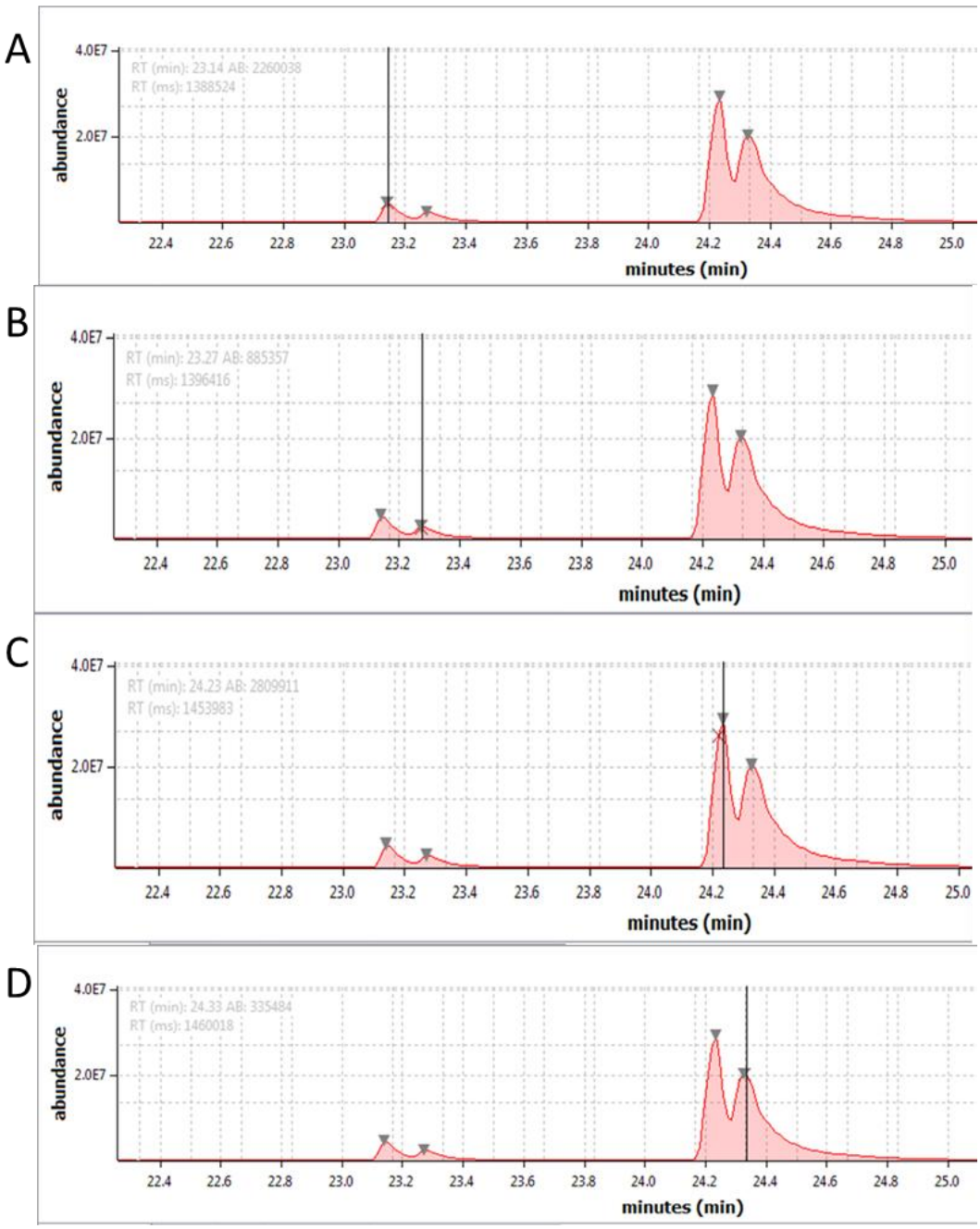

Figure 24: Chromatogram of CPD trimers.

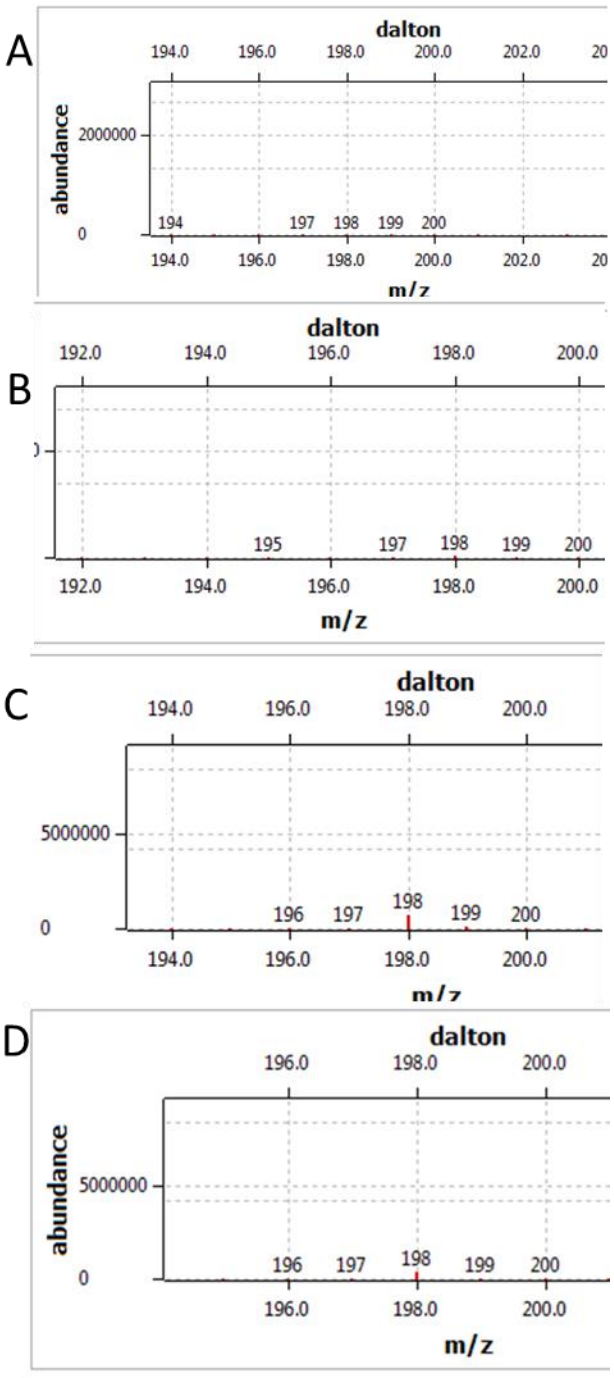

Figure 25: Corresponding mass spectrum for CPD tetramers.

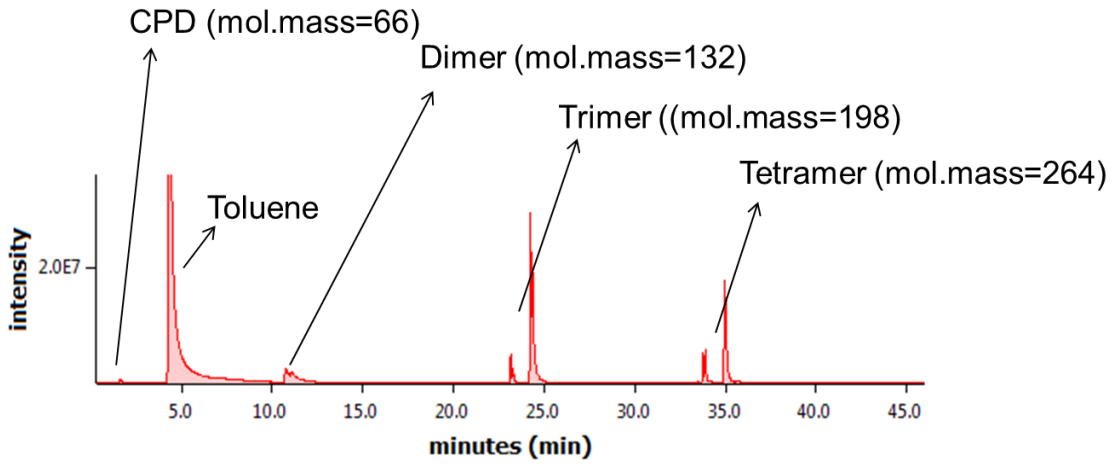

Figure 26: Summary GC-MS spectrum with peak indentifications.

B.2 Long-term CPD Dimerization with GC-MS Results

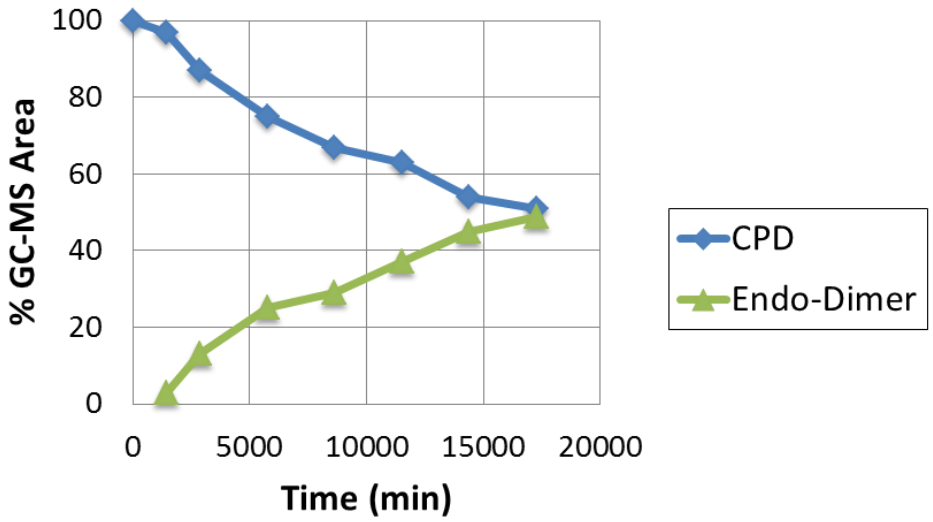

Figure 27: 1.32 M CPD in toluene at room temperature.

In Figure 27, conversion of the Exo-isomer is excluded due to the limited sensitivity of the MS towards small concentrations. Additionally, the y-axis unit is % of the total area (minus toluene as the solvent) as integrated from the GC-MS spectrum.

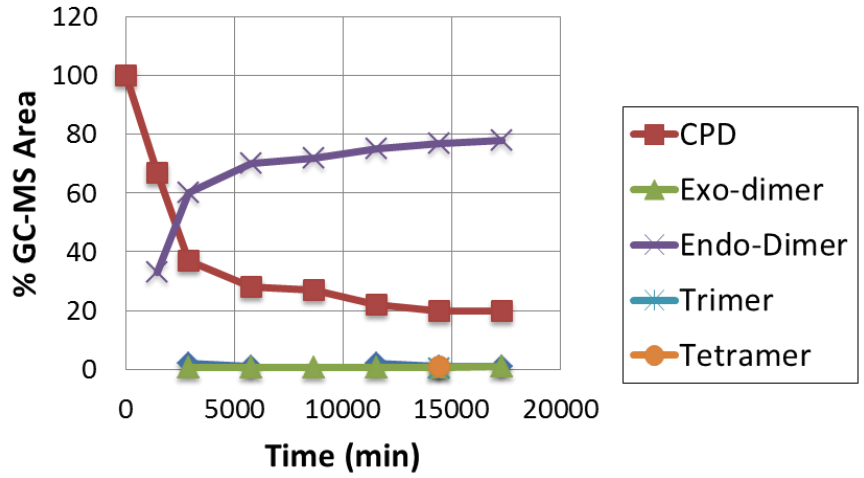

Figure 28: NEAT CPD at room temperature

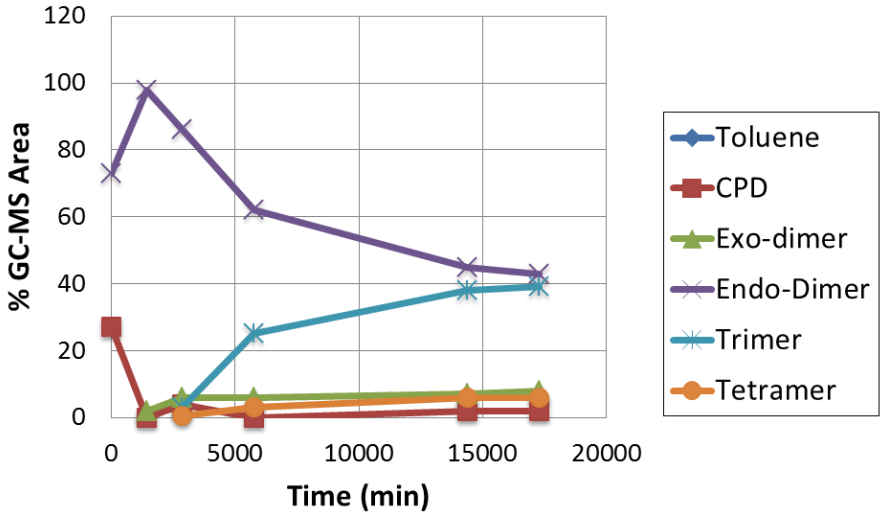

Figure 29: 1.32 M CPD in toluene at 140 °C.

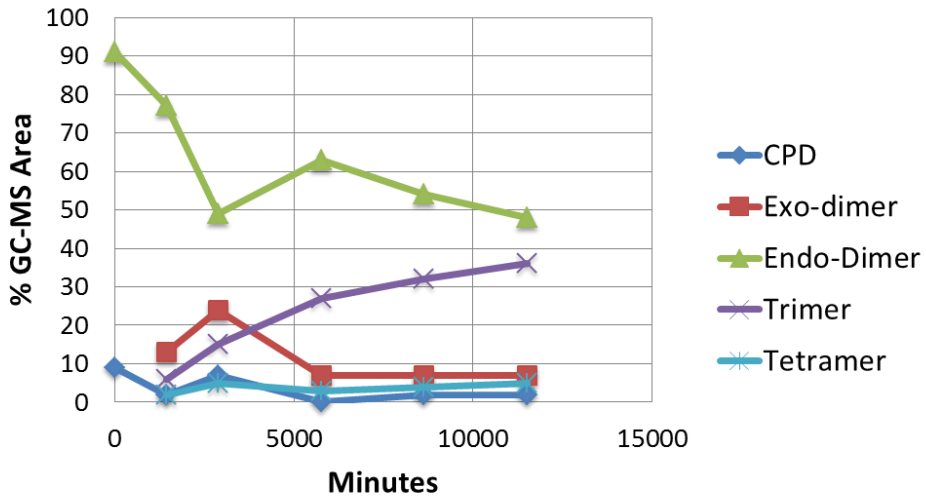

Figure 30: 1.32 M CPD in toluene at 160 °C

B.3 Experiments with Injector at 300 °C

B.3.1 CPD in Toluene - 80 °C Experiments

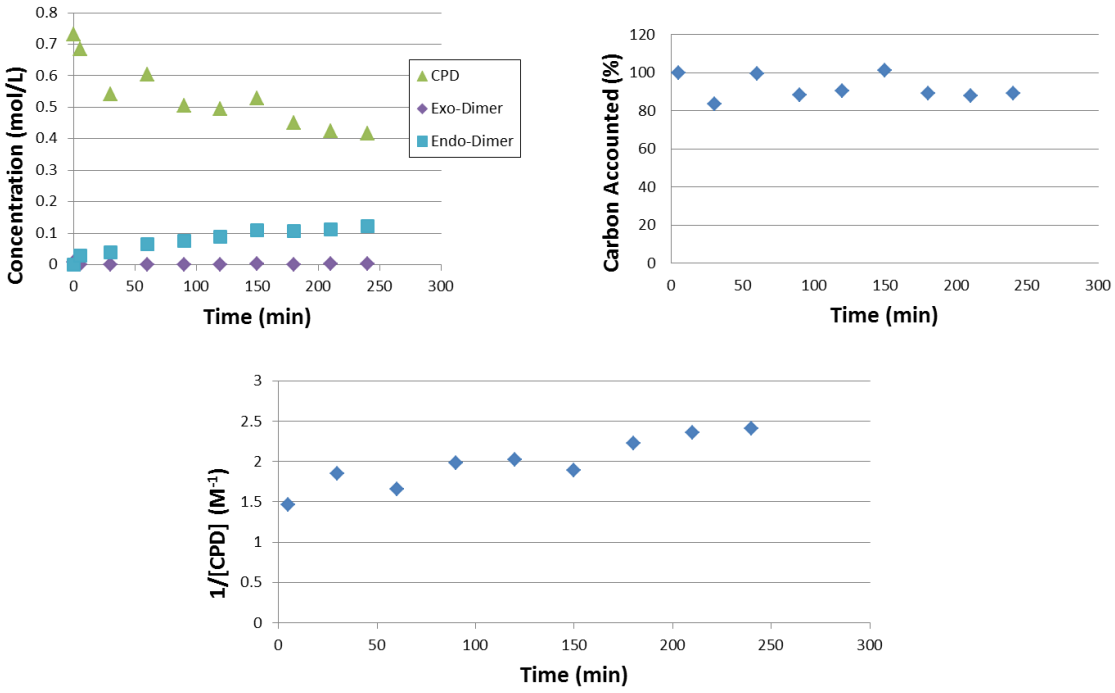

Figure 31: CPD in toluene at 80 °C – Run 1 with 300 °C injector temperature.

For this run, the calculated k_f is 0.0035 1/M·min. k_r is 0.0015 1/min.

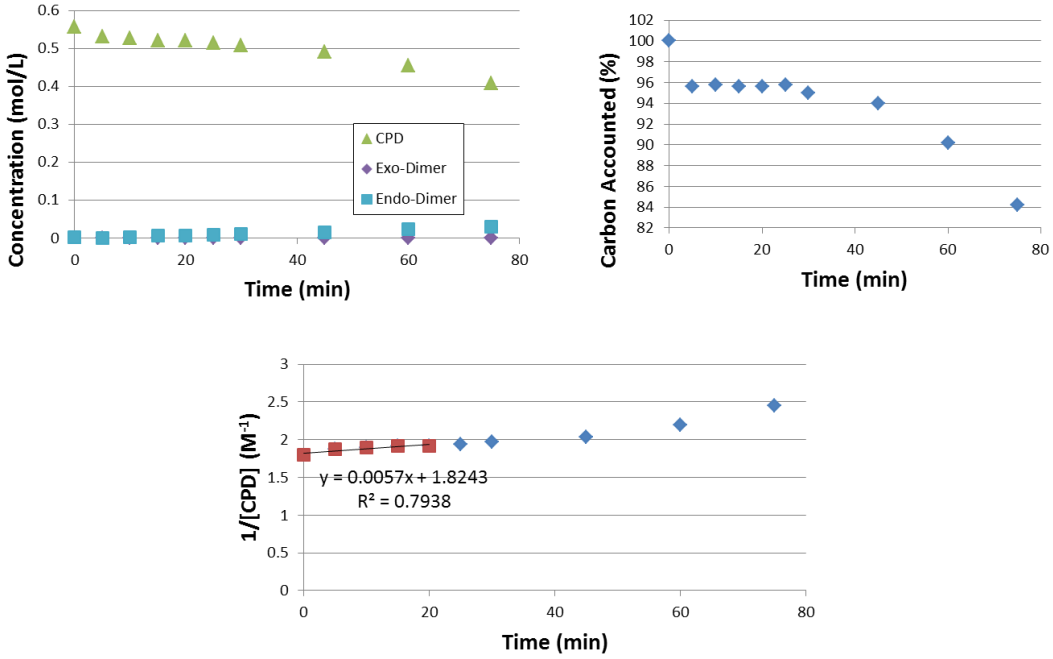

Figure 32: CPD in toluene at 80 °C – Run 2 with 300 °C injector temperature.

For this run, the calculated k_f is 0.0050 1/M·min. k_r was not reliably calculated for this run.

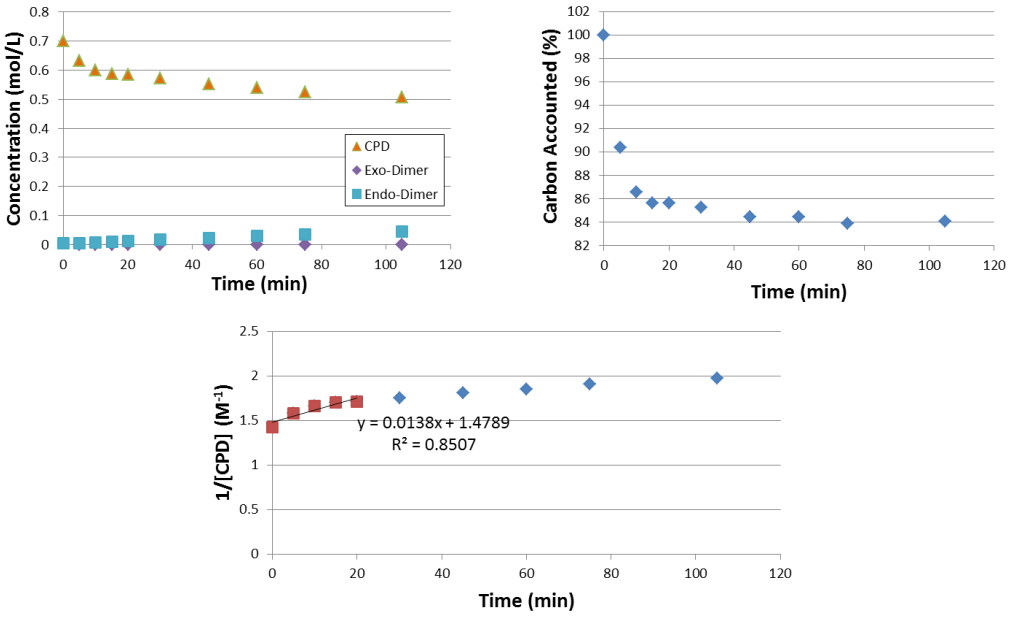

Figure 33: CPD in toluene at 80 °C – Run 3 with 300 °C injector temperature.

For this run, the calculated k_f is 0.0045 1/M·min. k_r was not reliably calculated.

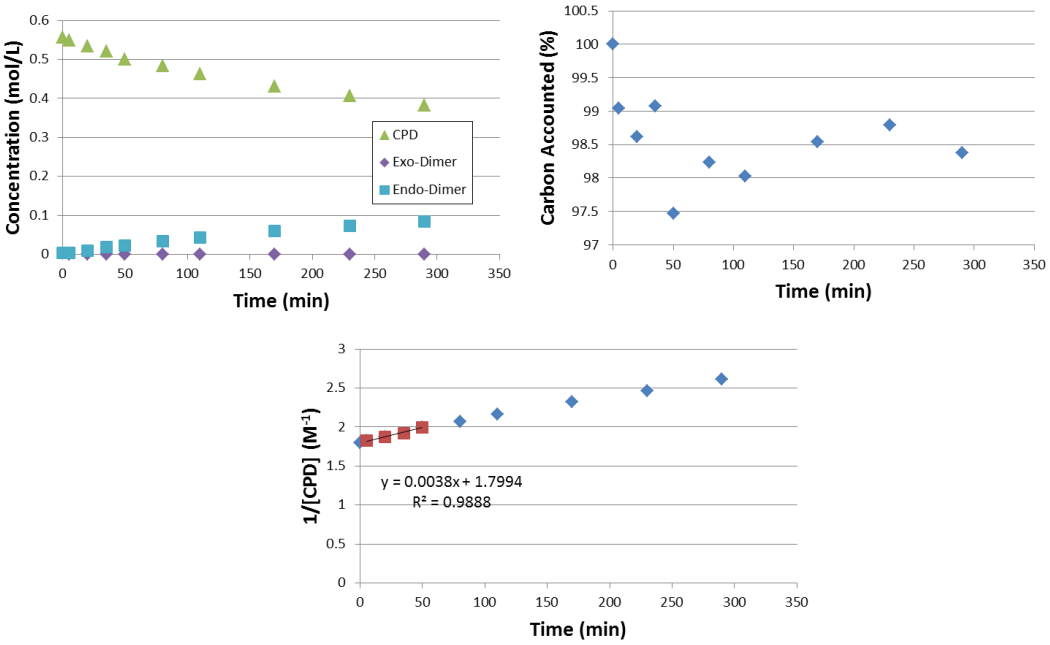

Figure 34: CPD in toluene at 80 °C – Run 4 with 300 °C injector temperature.

For this run, the calculated k_f is 0.0034 1/M·min. k_r is 0.0026 1/min.

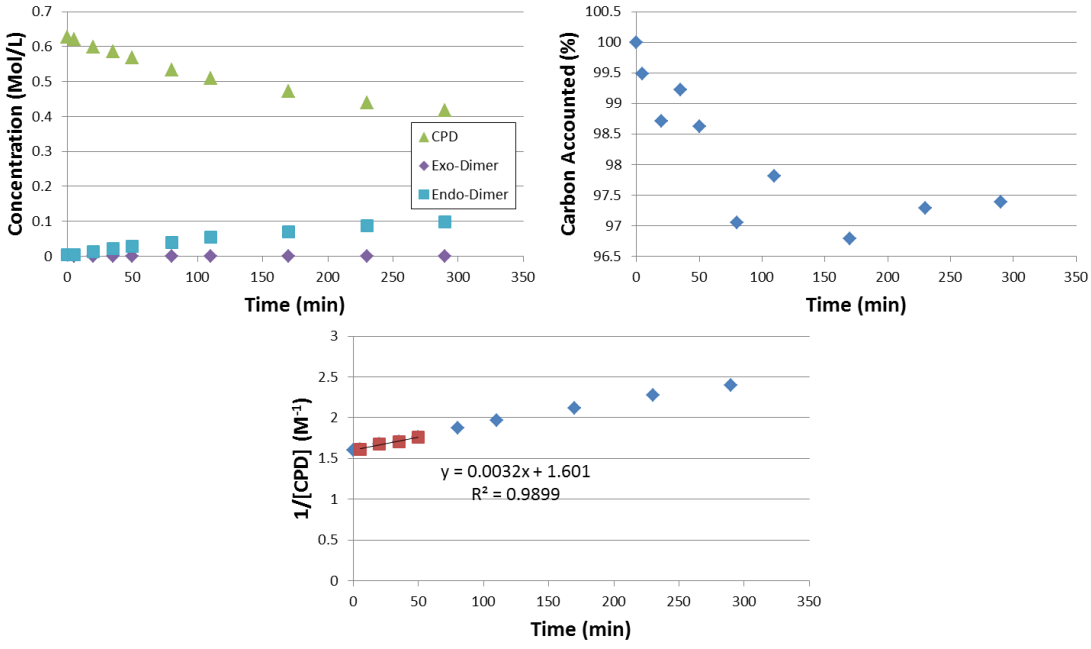

Figure 35: CPD in toluene at 80 °C – Run 5 with 300 °C injector temperature.

For this run, the calculated k_f is 0.0033 1/M·min. k_r is 0.0029 1/min.

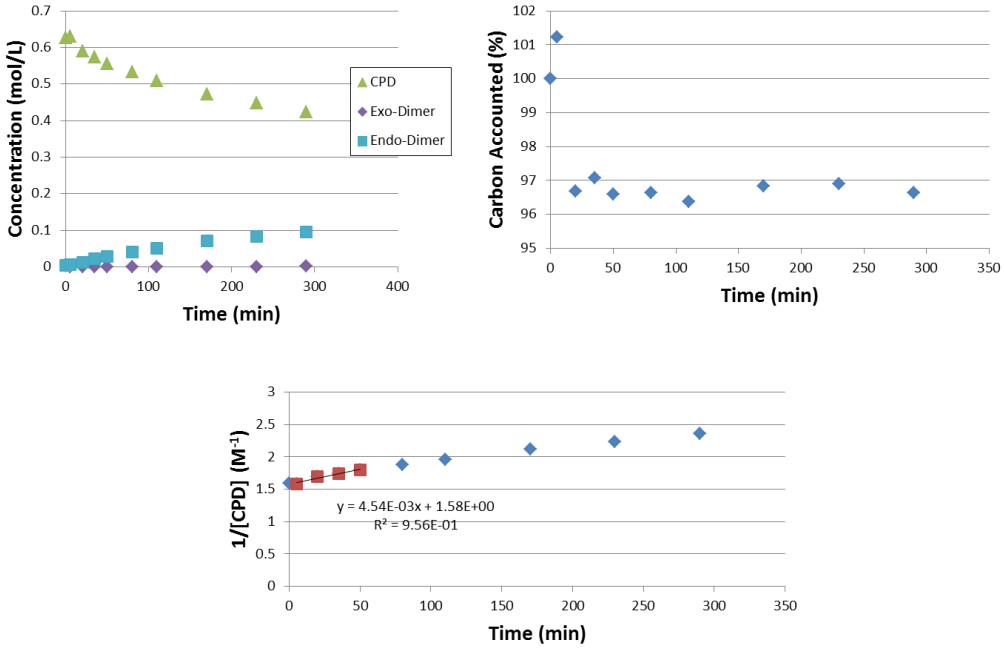

Figure 36: CPD in toluene at 80 °C – Run 6 with 300 °C injector temperature.

For this run, the calculated k_f is 0.0037 1/M·min. k_r is 0.0058 1/min.

B.3.2 CPD in Toluene – 100 °C Experiments

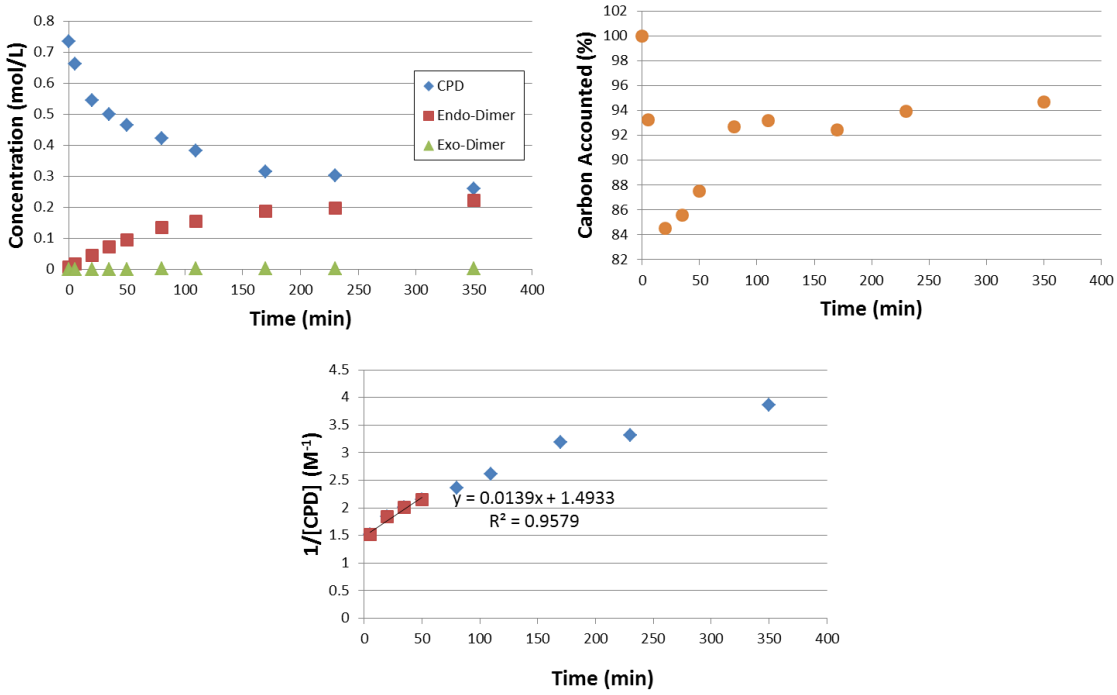

Figure 37: CPD in toluene at 100 °C – Run 1 with 300 °C injector temperature.

For this run, the calculated k_f is 0.0143 1/M·min. k_r is 0.0067 1/min.

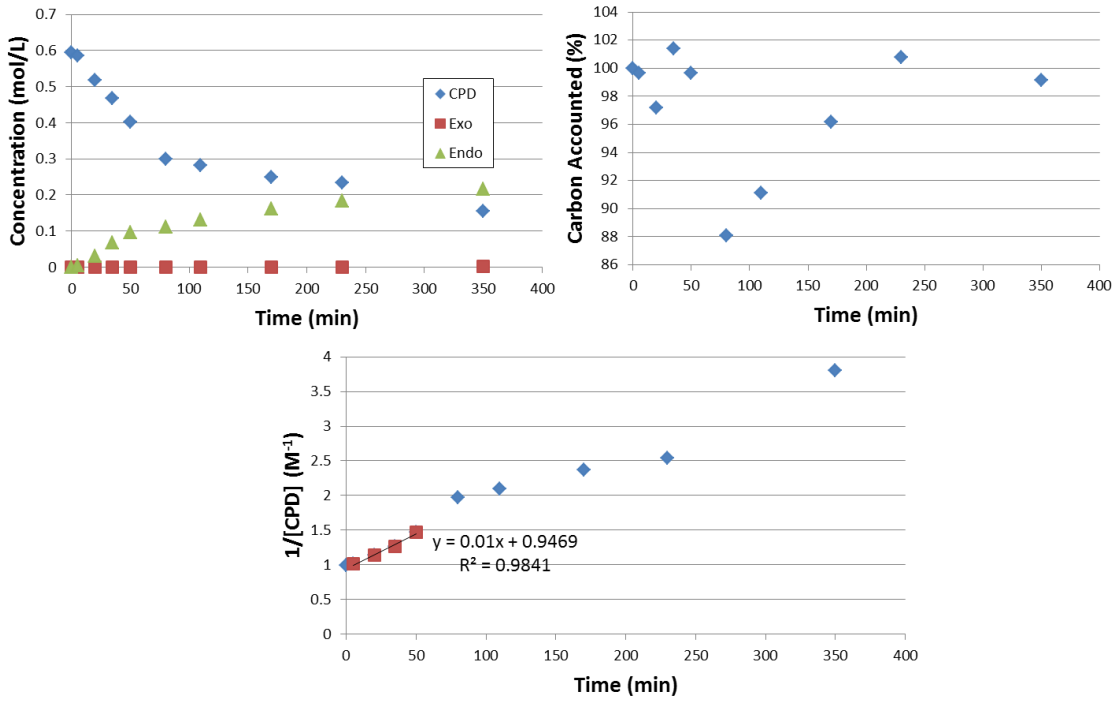

Figure 38: CPD in toluene at 100 °C – Run 2 with 300 °C injector temperature.

For this run, the calculated k_f is 0.0080 1/M·min. k_r is 0.0027 1/min. This run was analyzed from GC-MS data

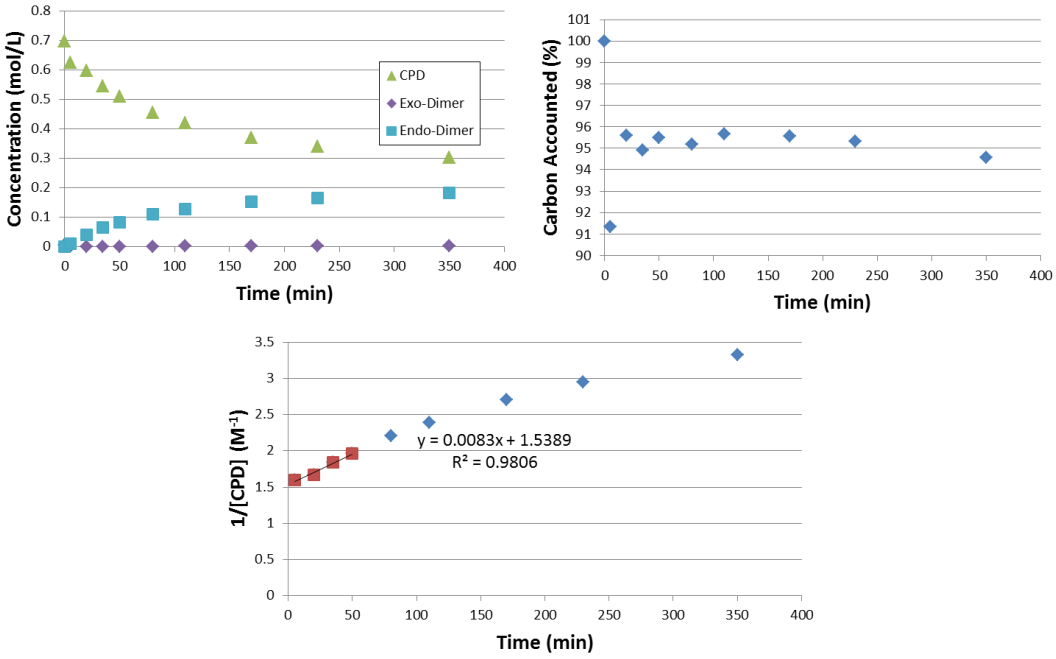

Figure 39: CPD in toluene at 100 °C – Run 3 with 300 °C injector temperature.

For this run, the calculated k_f is 0.0079 1/M·min. k_r is 0.0083 1/min.

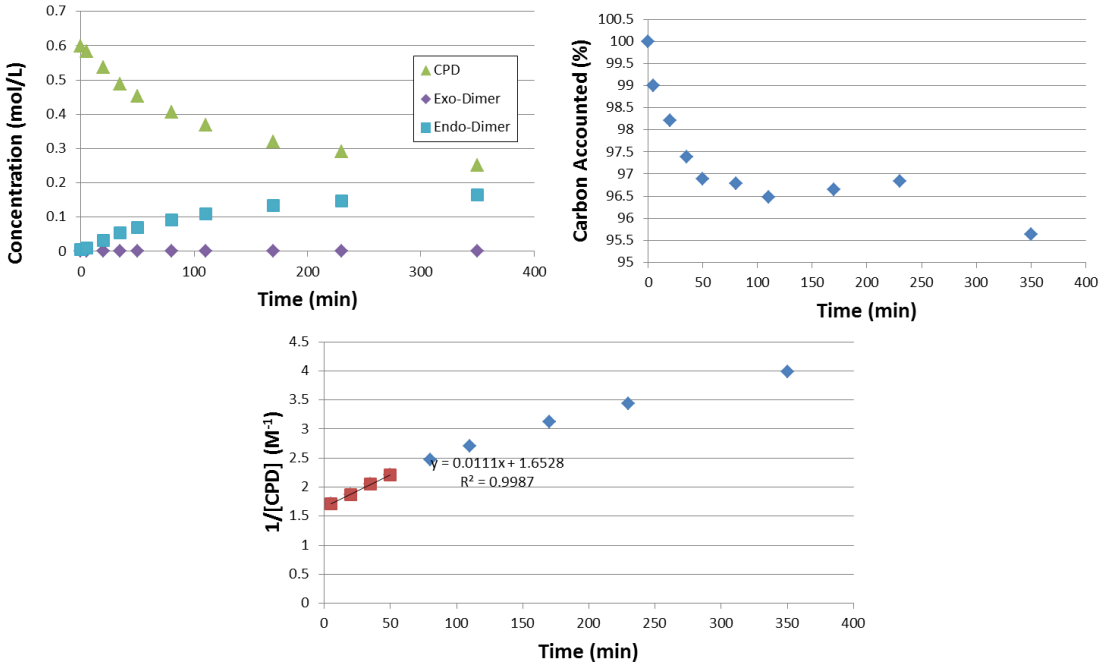

Figure 40: CPD in toluene at 100 °C – Run 4 with 300 °C injector temperature.

For this run, the calculated k_f is 0.0107 1/M·min. k_r is 0.0042 1/min.

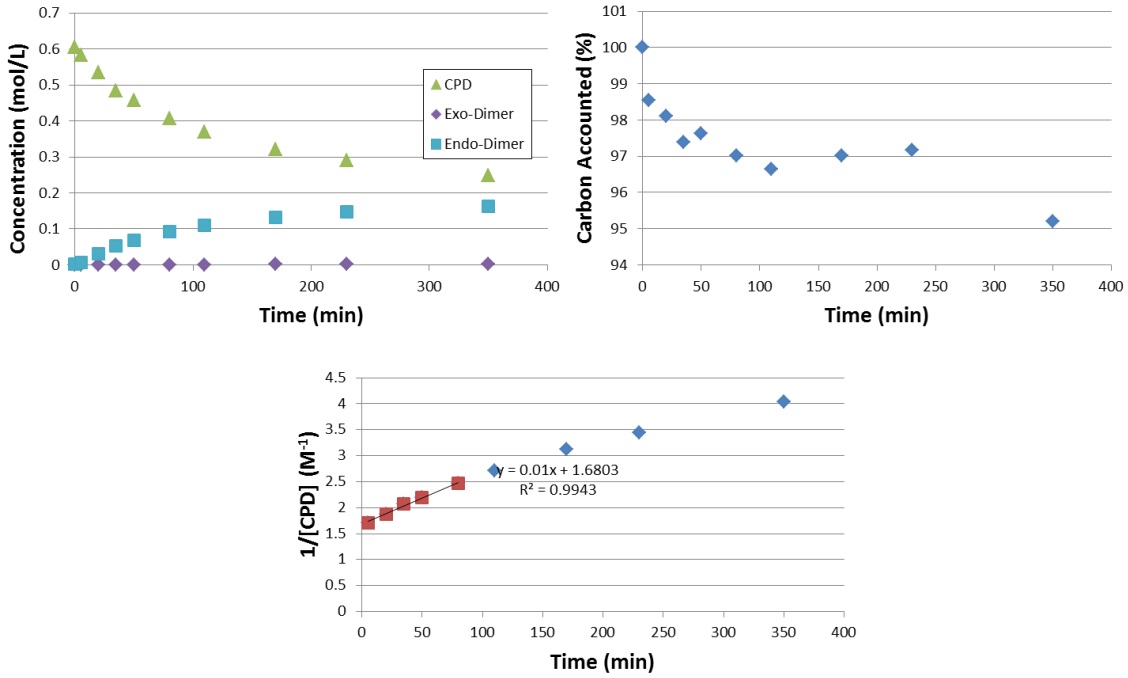

Figure 41: CPD in toluene at 100 °C – Run 5 with 300 °C injector temperature.

For this run, the calculated k_f is 0.0105 1/M·min. k_r is 0.0037 1/min.

Run 6 is not included because the solution was not properly mixed before being placed into reactor vials resulting in varying starting concentrations.

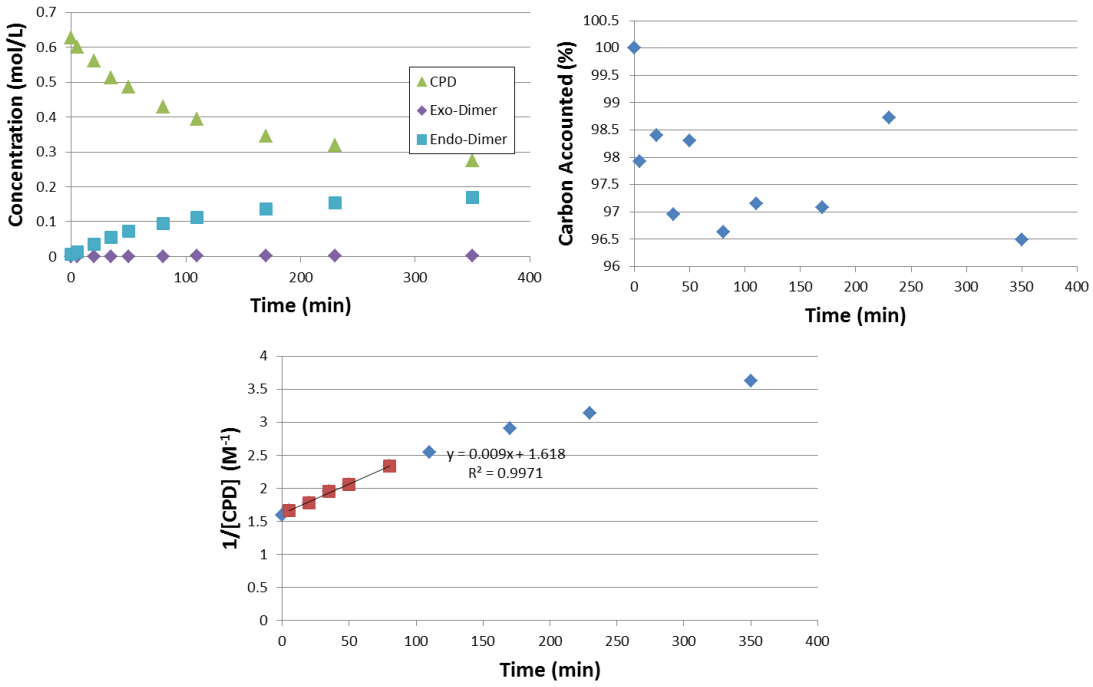

Figure 42: CPD in toluene at 100 °C – Run 7 with 300 °C injector temperature.

For this run, the calculated k_f is 0.0091 1/M·min. k_r is 0.0034 1/min.

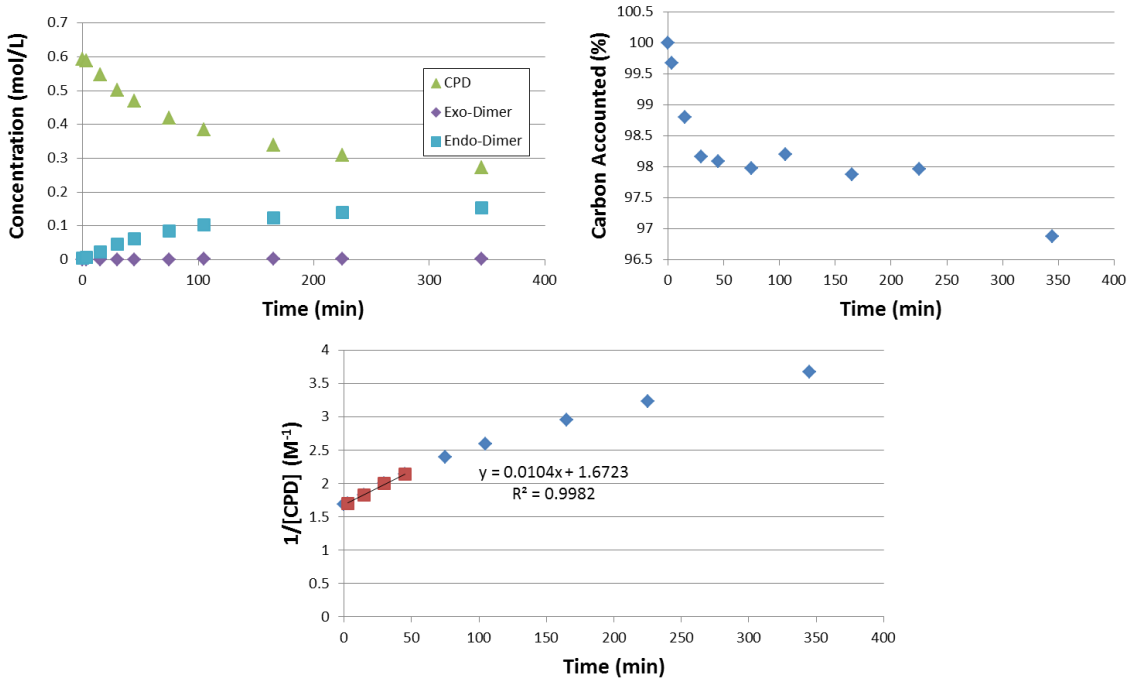

Figure 43: CPD in toluene at 100 °C – Run 8 with 300 °C injector temperature.

For this run, the calculated k_f is 0.0102 1/M·min. k_r is 0.0050 1/min.

B.3.3. CPD in Toluene – 120 °C Experiments

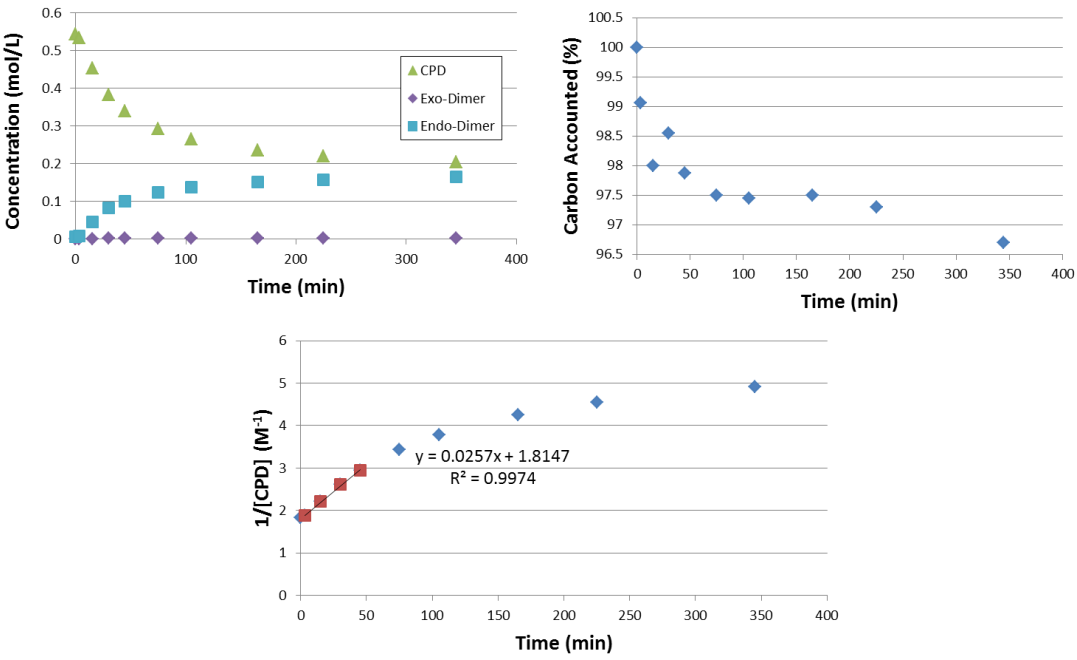

Figure 44: CPD in toluene at 120 °C – Run 2 with 300 °C injector temperature.

For this run, the calculated k_f is 0.0264 1/M·min. k_r is 0.0083 1/min.

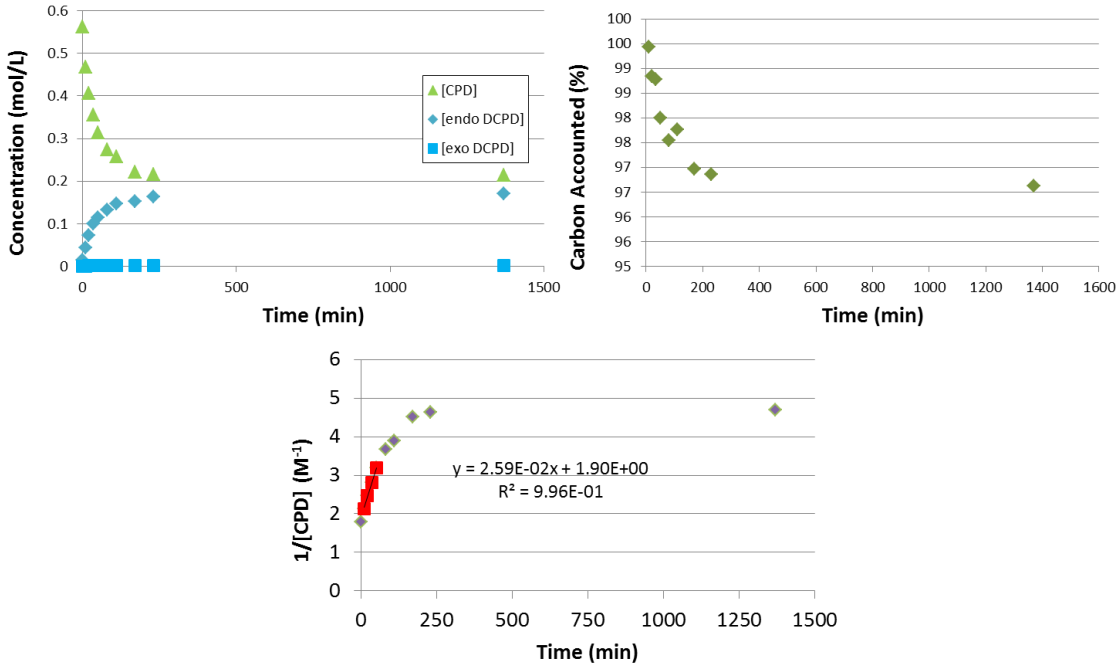

Figure 45: CPD in toluene at 120 °C – Run 4 with 300 °C injector temperature.

For this run, the calculated k_f is 0.0299 1/M·min. k_r is 0.0083 1/min.

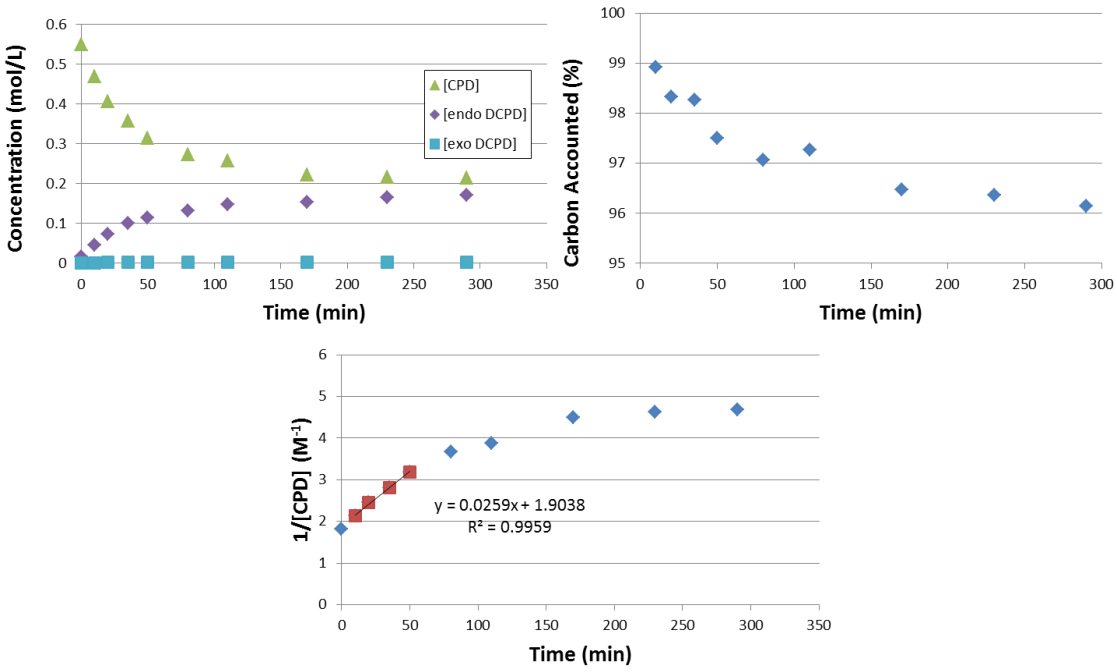

Figure 46: CPD in toluene at 120 °C – Run 5 with 300 °C injector temperature.

For this run, the calculated k_f is 0.0295 1/M·min. k_r is 0.0083 1/min.

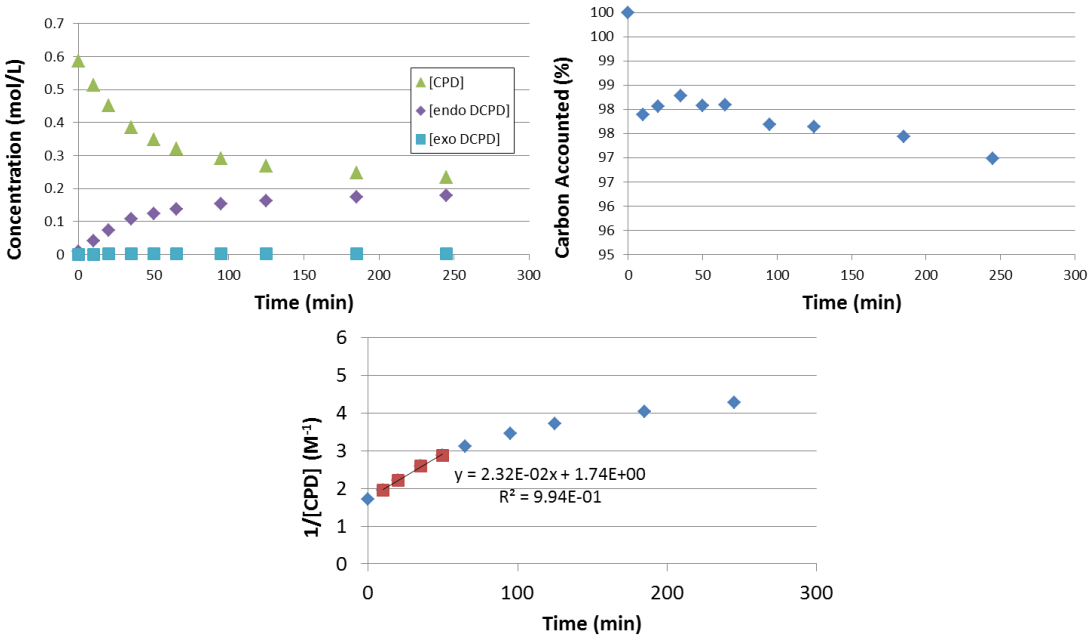

Figure 47: CPD in toluene at 120 °C – Run 6 with 300 °C injector temperature.

For this run, the calculated k_f is 0.0273 1/M·min. k_r is 0.0087 1/min.

B.3.4 CPD in Cyclohexane Experiments at 80 °C

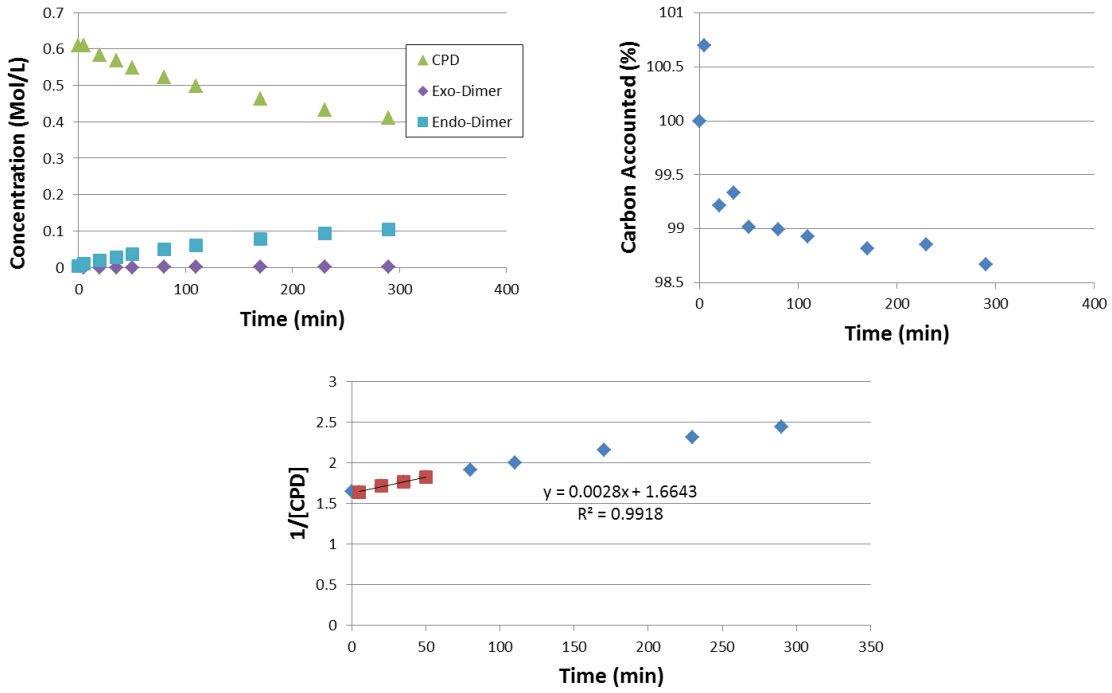

Figure 48: CPD in cyclohexane at 80 °C – Run 1 with 300 °C injector temperature.

For this run, the calculated k_f is 0.0039 1/M·min. k_r is 0.0041 1/min.

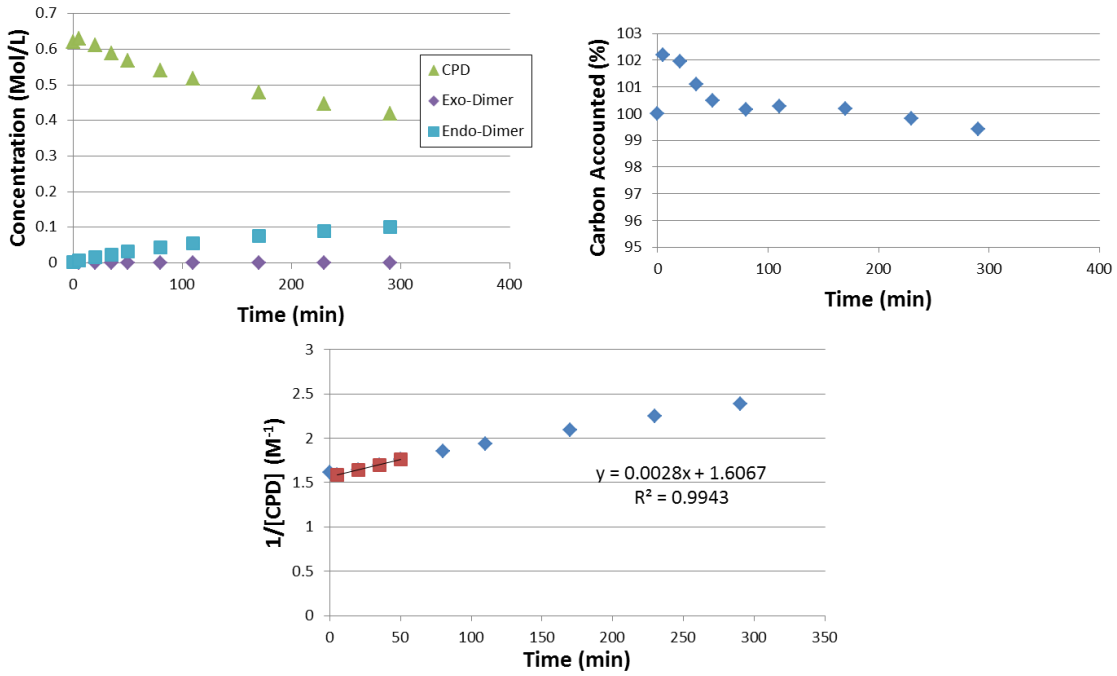

Figure 49: CPD in cyclohexane at 80 °C – Run 2 with 300 °C injector temperature.

For this run, the calculated k_f is 0.0036 1/M·min. k_r is 0.0037 1/min.

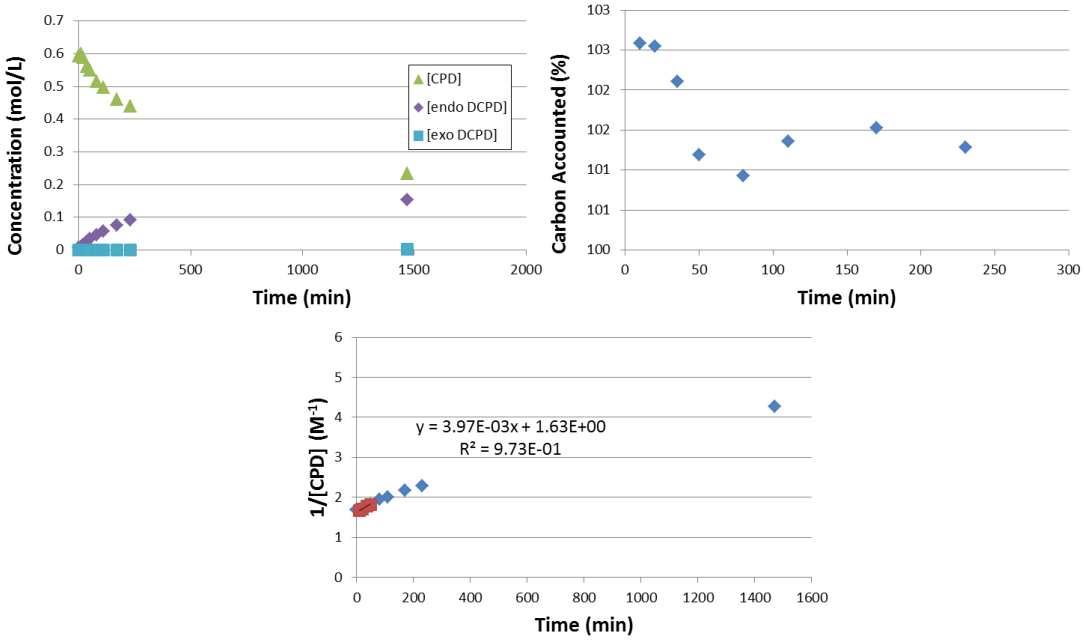

Figure 50: CPD in cyclohexane at 80 °C – Run 3 with 300 °C injector temperature.

For this run, the calculated k_f is 0.0032 1/M·min. k_r is 0.0010 1/min.

B.3.5 Cyclopentene Impurity Experiments

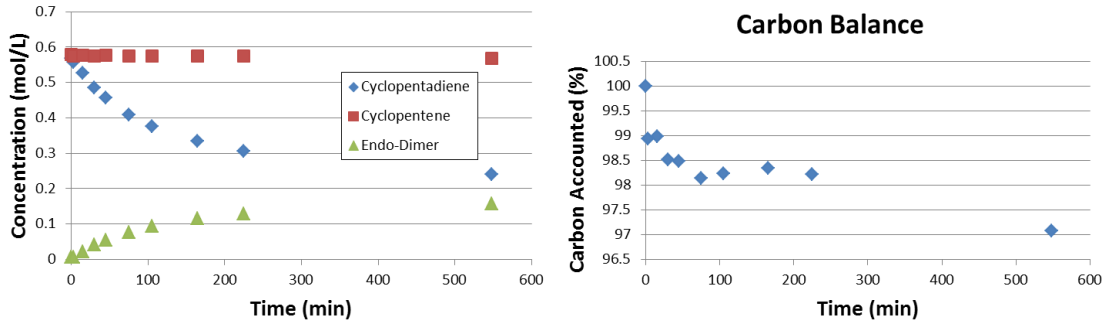

Figure 51: 1:1 volume ratio of CPD to cyclopentene at 100 °C

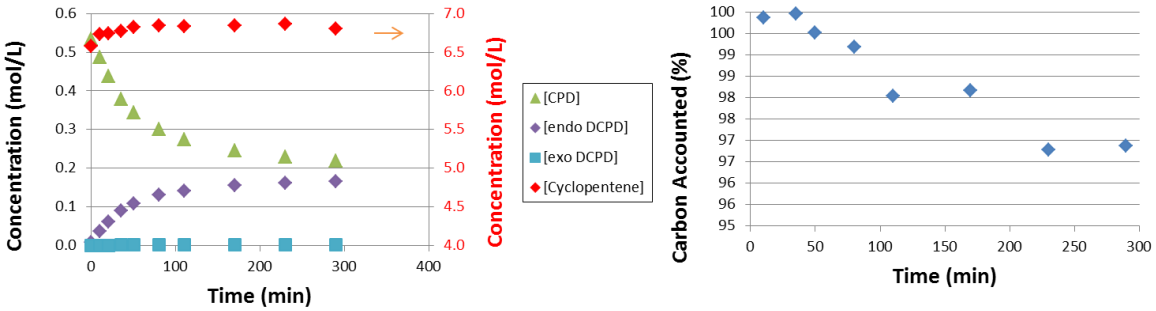

Figure 52: 10:1 volume ratio of cyclopentene to CPD at 120 °C

B.4 Calibration Curves

B.4.1 Cyclooctane Calibration

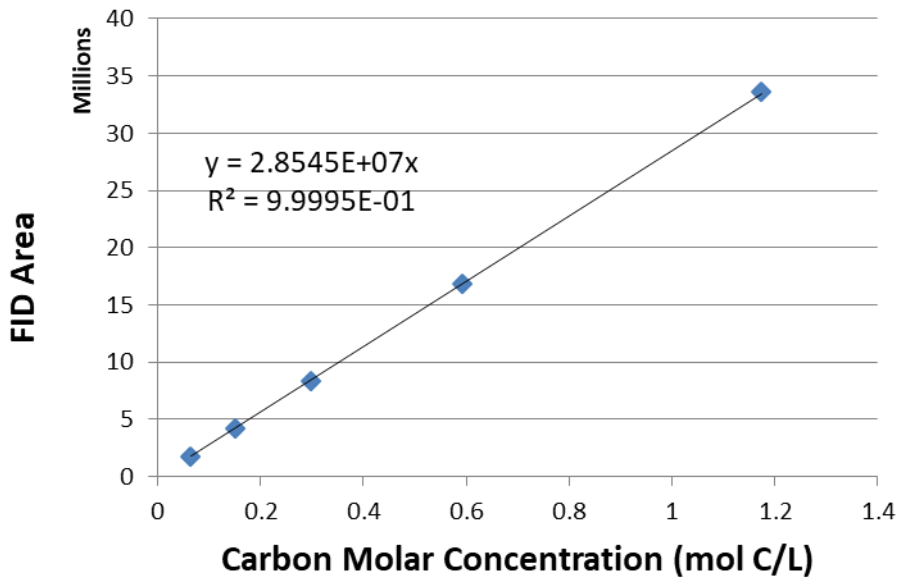

Figure 53: Cyclooctane GC-FID calibration curve.

B.4.2 Cyclopentadiene Calibration curve

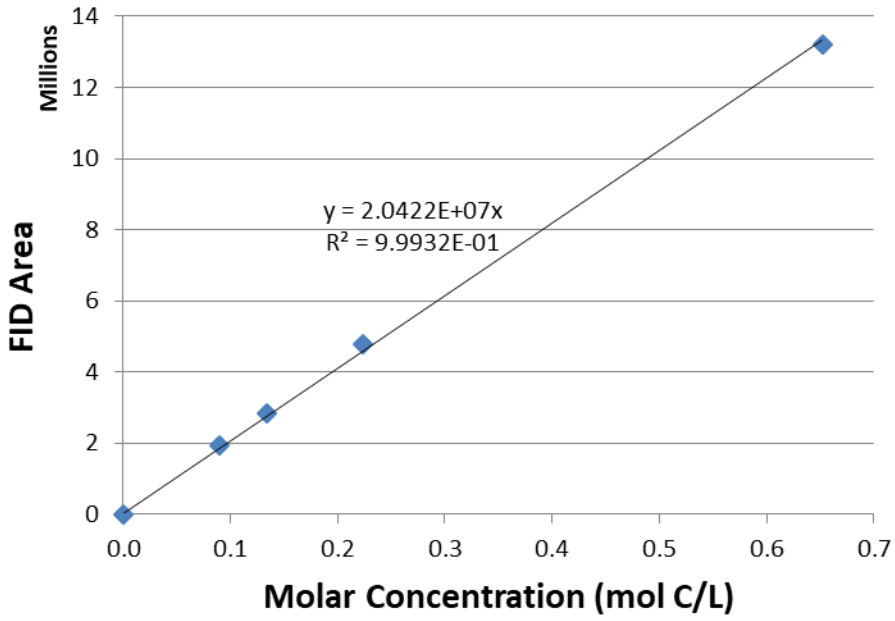

Figure 54: Cyclopentadiene GC-FID calibration curve.

B.4.3 Cyclopentene Calibration Curve

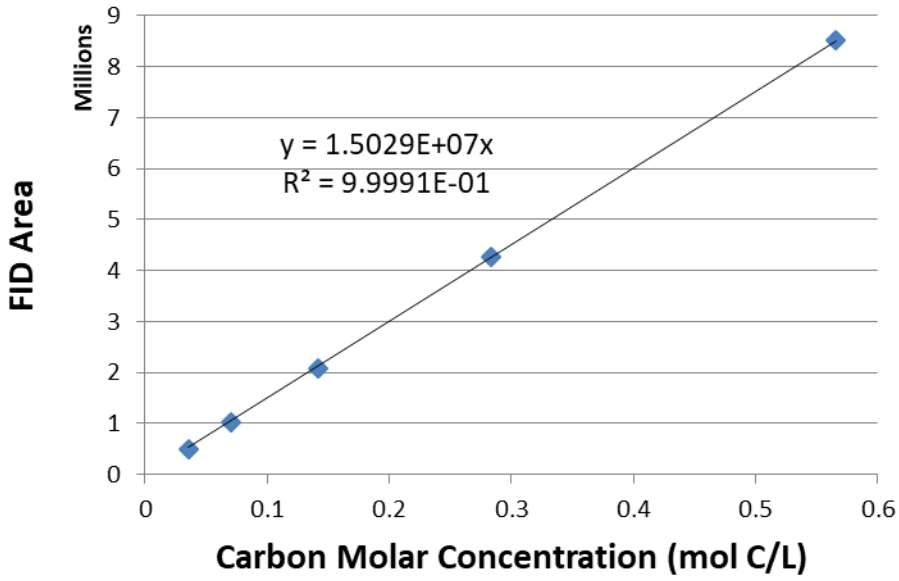

Figure 55: Cyclopentene GC-FID calibration curve.

B.4.4 Trans-1,3-pentadiene

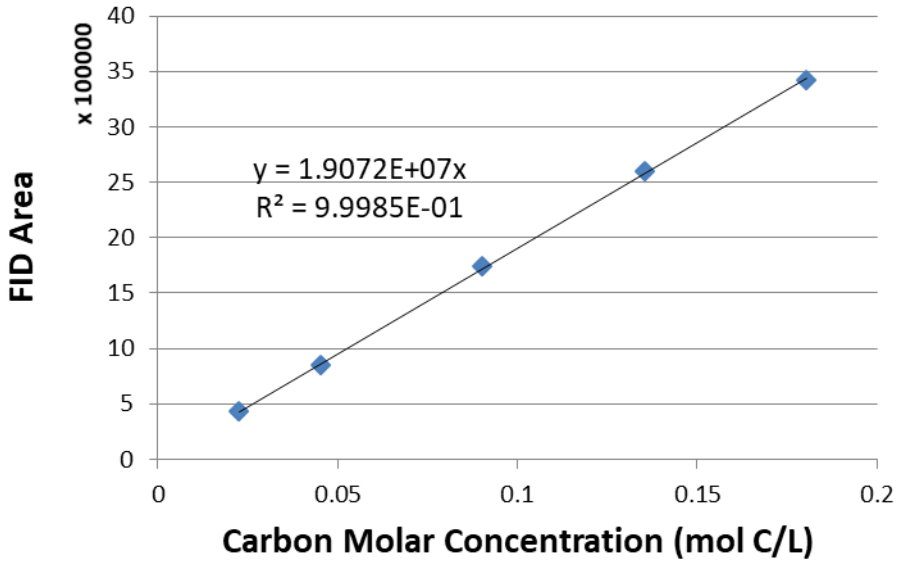

Figure 56: Trans-1,3-pentadiene GC-FID Calibration Curve.

B.5 CPD Dimerization Data with 200 °C Injector Data

B.5.1 CPD in Toluene

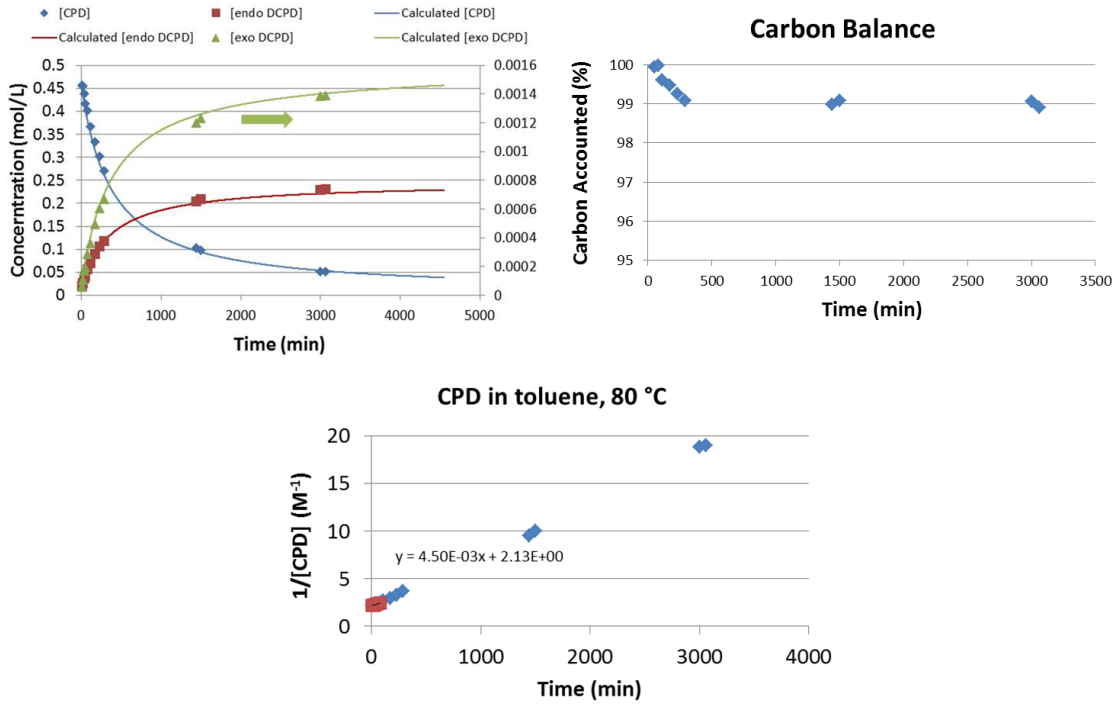

Figure 57: CPD in toluene at 80 °C – Run N1.

For this run, the calculated k_f is $5.69 \cdot 10^{-3}$ 1/M·min. k_r and k_2 are not reliably calculated due to the low temperature.

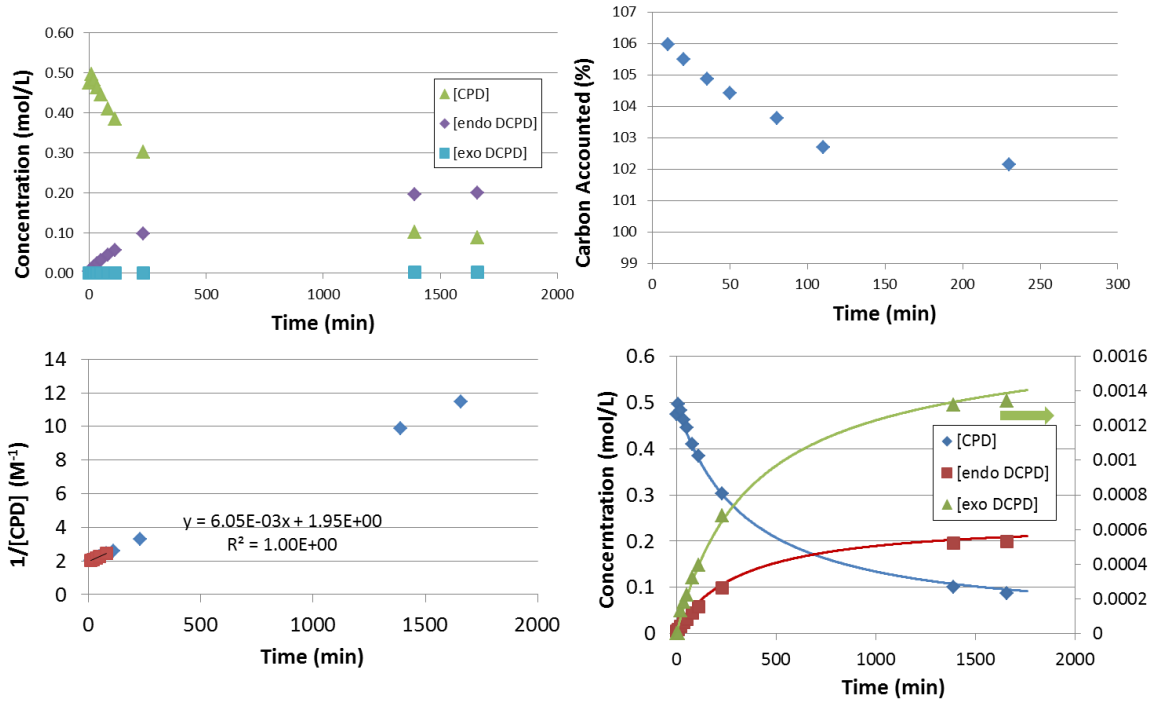

Figure 58: CPD in toluene at 80 °C – Run N2.

For this run, the calculated k_f is $5.67 \cdot 10^{-3}$ 1/M·min. k_r and k_2 are not reliably calculated due to the low temperature.

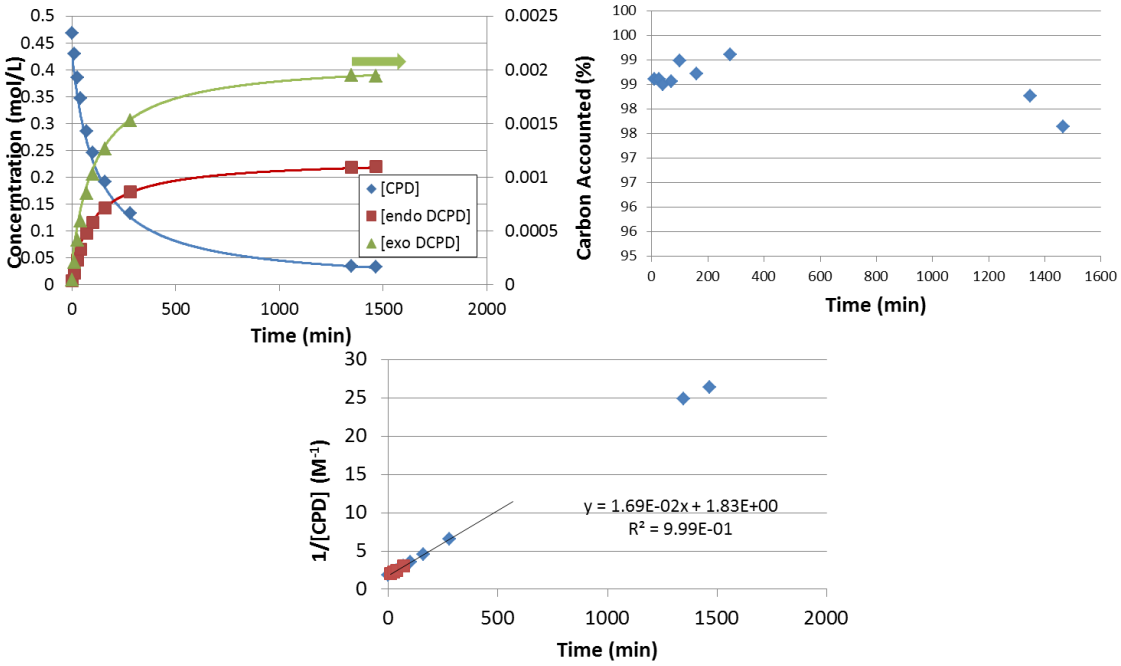

Figure 59: CPD in toluene at 100 °C – Run N1.

For this run, the calculated k_f is $1.98 \cdot 10^{-2}$ 1/M·min. k_r and k_2 are not reliably calculated due to the low temperature.

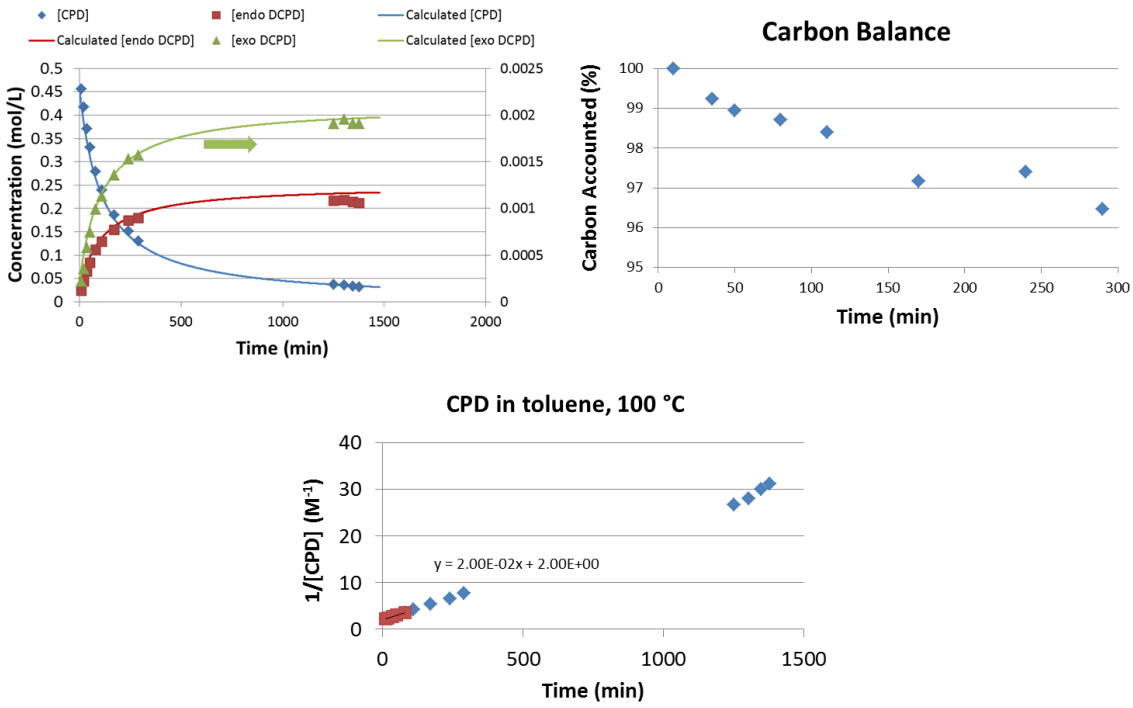

Figure 60: CPD in toluene at 100 °C – Run N2.

For this run, the calculated k_f is $1.98 \cdot 10^{-2}$ 1/M·min. k_r and k_2 are not reliably calculated due to the low temperature.

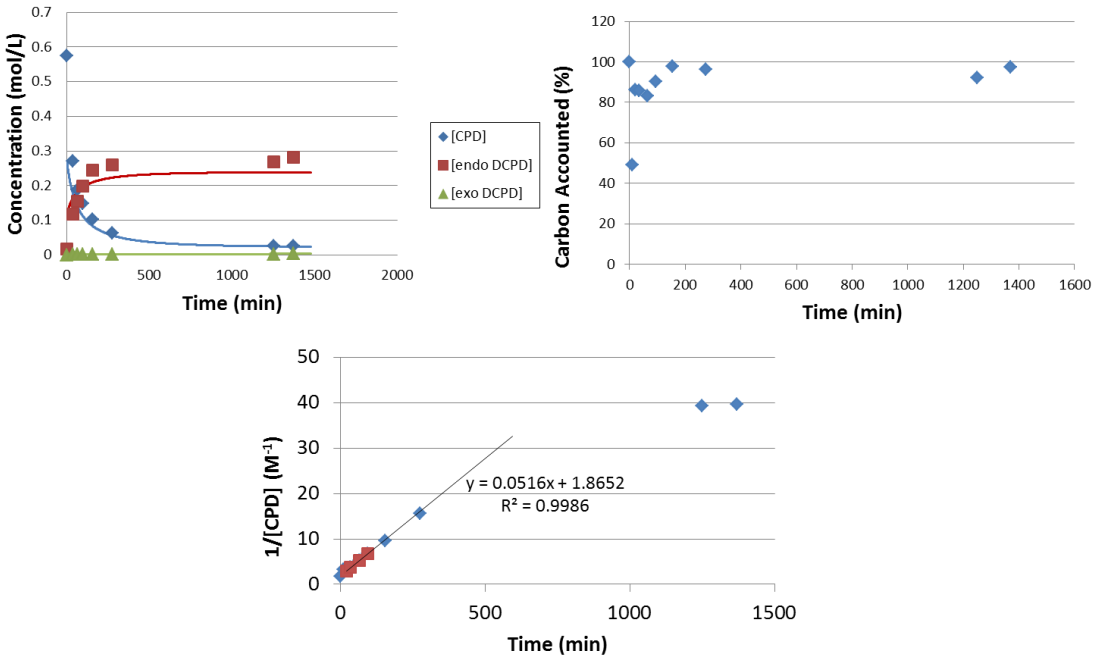

Figure 61: CPD in toluene at 120 °C – Run N1.

This data was not used in calculating the rate constants for this temperature due to discrepancies in the initial concentration.

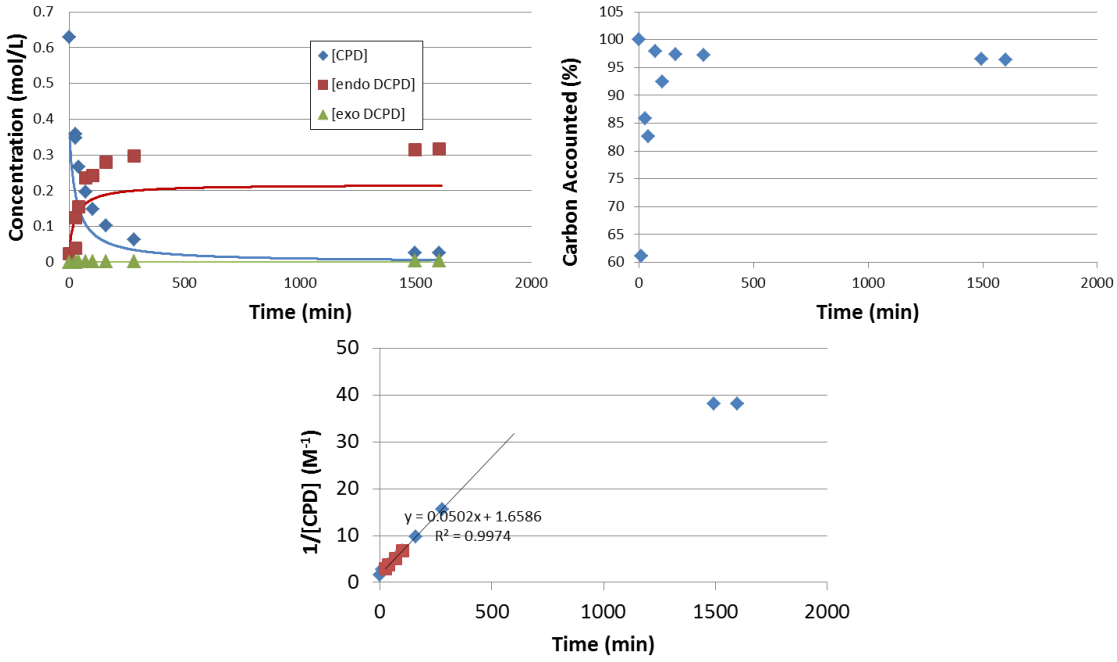

Figure 62: CPD in toluene at 120 °C – Run N2.

This data was not used in calculating the rate constants for this temperature due to discrepancies in the initial concentration.

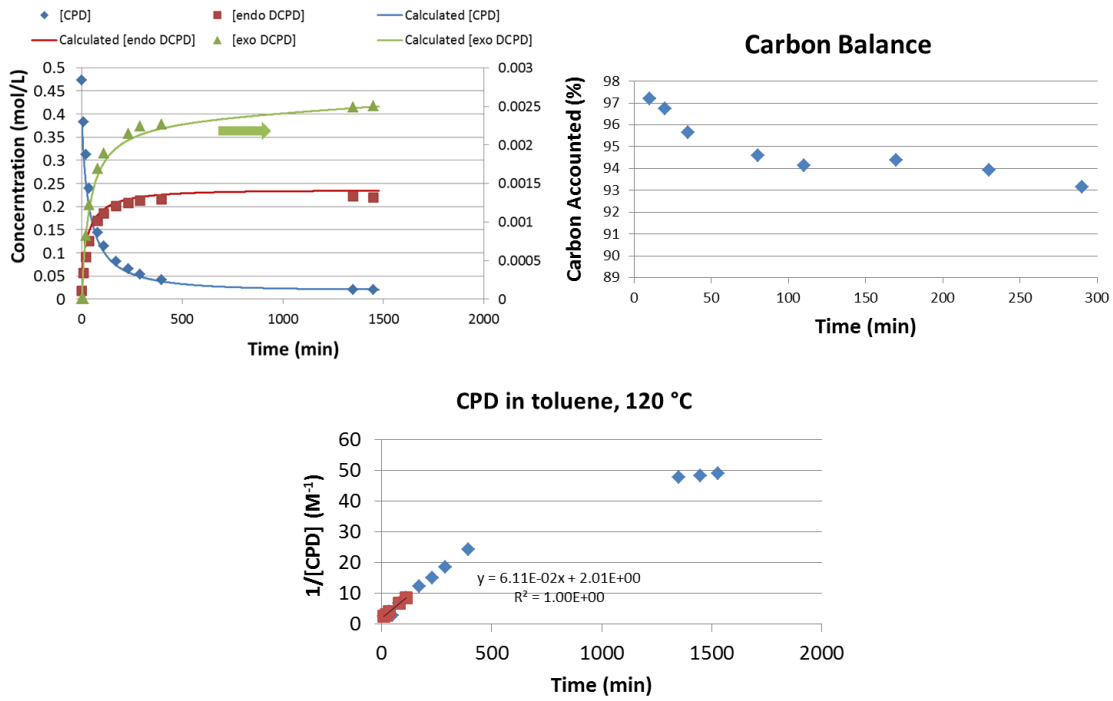

Figure 63: CPD in toluene at 120 °C – Run N3.

For this run, the calculated k_f is $5.94 \cdot 10^{-2}$ 1/M·min. k_r is $9.77 \cdot 10^{-5}$ 1/min. k_2 is $8.07 \cdot 10^{-4}$ 1/M·min. The equilibrium constant as calculated by the ratio of k_f to k_r is 608. The equilibrium constant as calculated by the approximately equilibrium concentration is 513.

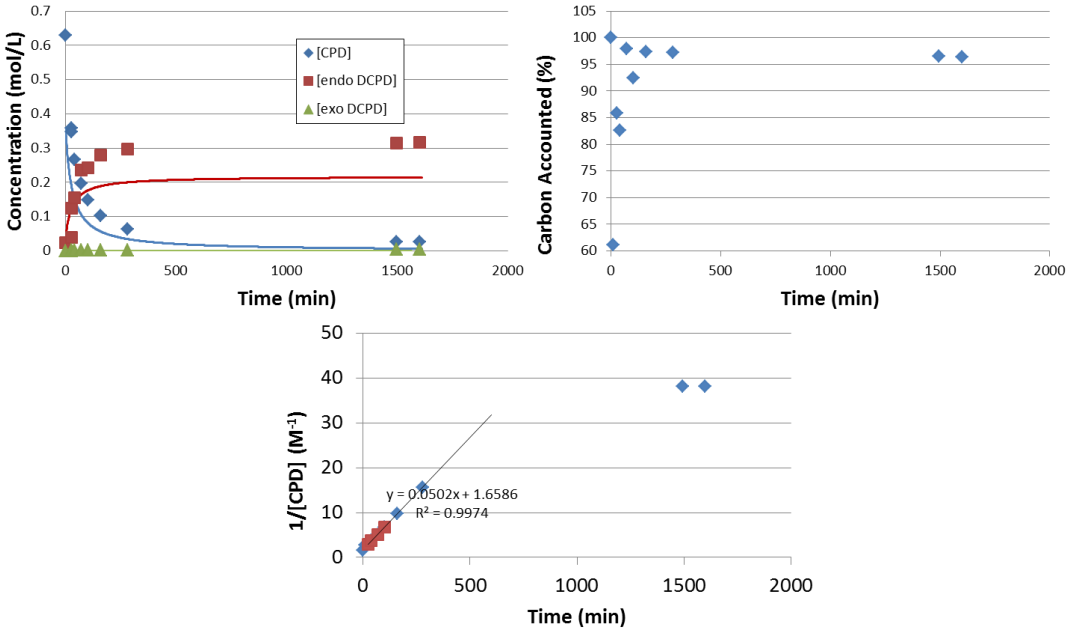

Figure 64: CPD in toluene at 120 °C – Run N4.

For this run, the calculated k_f is $5.81 \cdot 10^{-2}$ 1/M·min. k_r is $8.51 \cdot 10^{-5}$ 1/min. k_2 is $6.53 \cdot 10^{-4}$ 1/M·min. The equilibrium constant as calculated by the ratio of k_f to k_r is 608. The equilibrium constant as calculated by the approximately equilibrium concentration is 516.

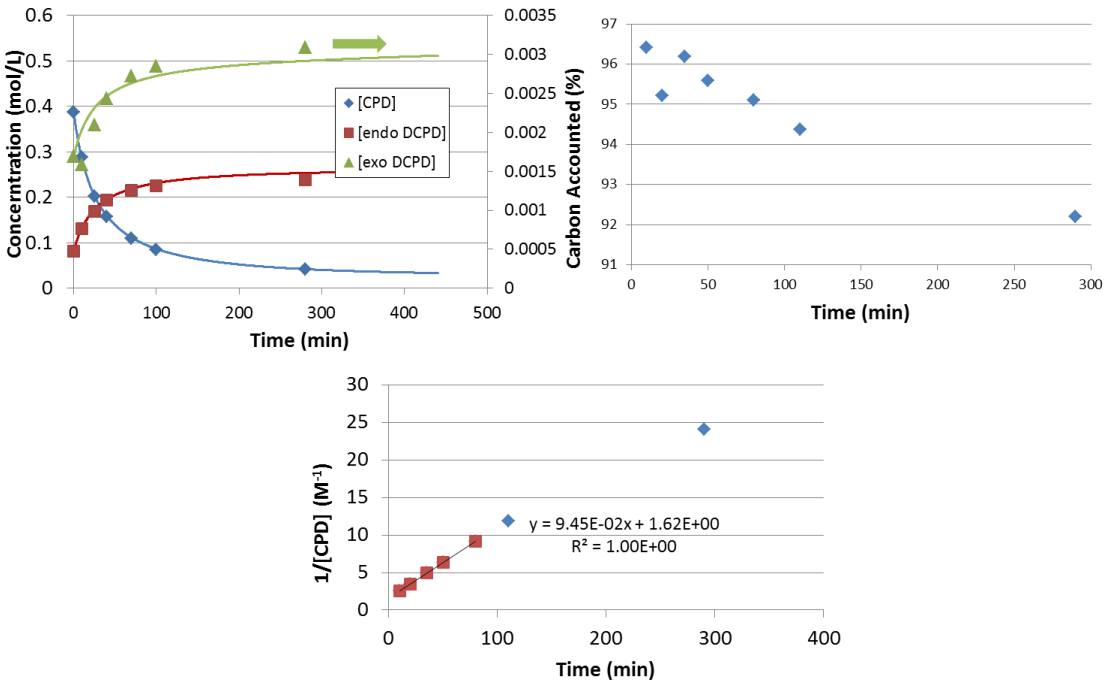

Figure 65: CPD in toluene at 130 °C – Run N1.

For this run, the calculated k_f is $9.24 \cdot 10^{-2}$ 1/M·min. k_r is $2.87 \cdot 10^{-4}$ 1/min. k_2 is $6.27 \cdot 10^{-4}$ 1/M·min. The equilibrium constant as calculated by the ratio of k_f to k_r is 322. The equilibrium constant as calculated by the approximately equilibrium concentration is 138.

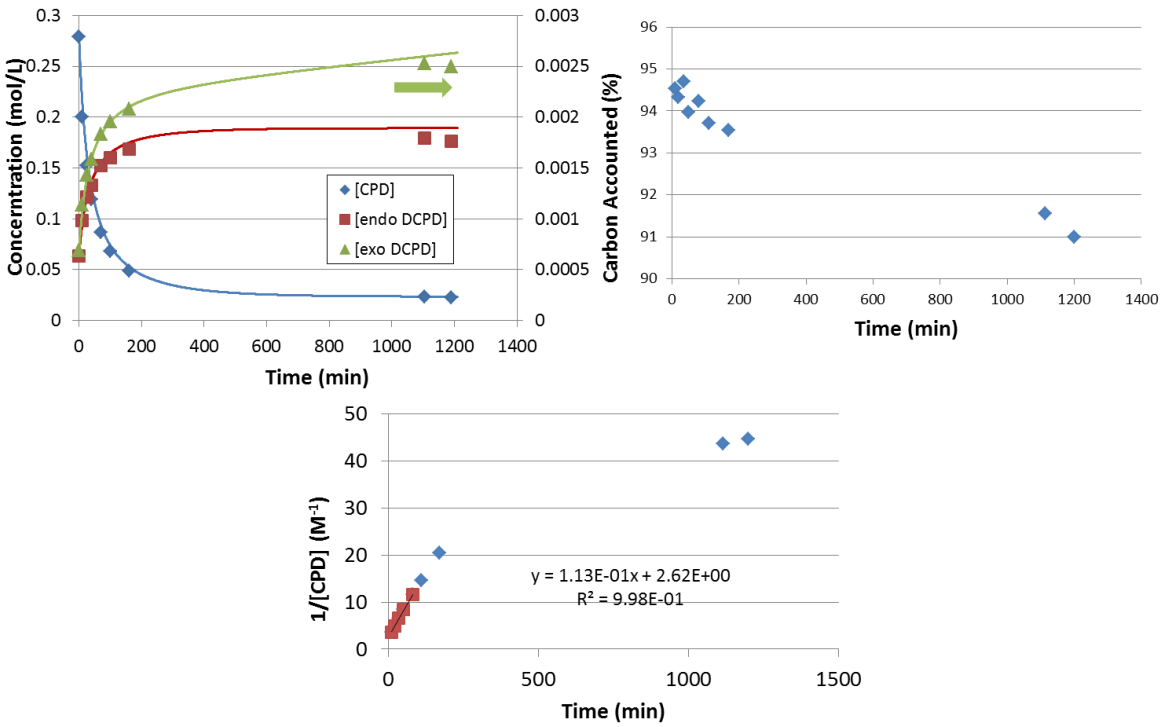

Figure 66: CPD in toluene at 130 °C – Run N2.

For this run, the calculated k_f is $1.02 \cdot 10^{-1}$ 1/M·min. k_r is $2.99 \cdot 10^{-4}$ 1/min. k_2 is $1.25 \cdot 10^{-3}$ 1/M·min. The equilibrium constant as calculated by the ratio of k_f to k_r is 340. The equilibrium constant as calculated by the approximately equilibrium concentration is 340.

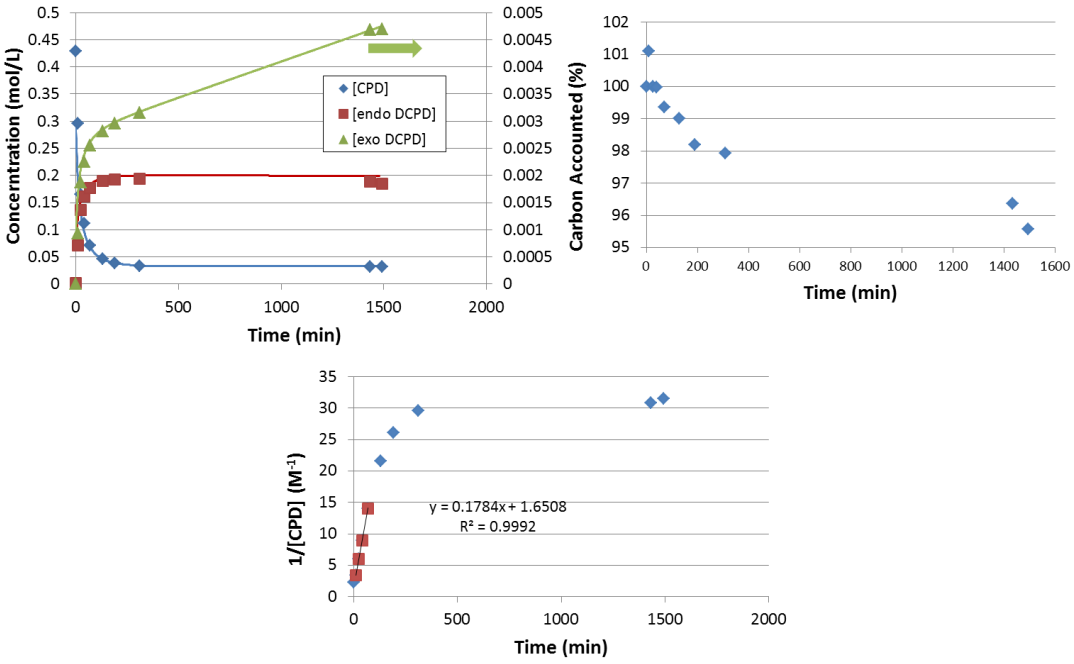

Figure 67: CPD in toluene at 140 °C – Run N1.

For this run, the calculated k_f is $1.72 \cdot 10^{-1}$ 1/M·min. k_r is $9.37 \cdot 10^{-4}$ 1/min. k_2 is $2.48 \cdot 10^{-3}$ 1/M·min. The equilibrium constant as calculated by the ratio of k_f to k_r is 184. The equilibrium constant as calculated by the approximately equilibrium concentration is 184.

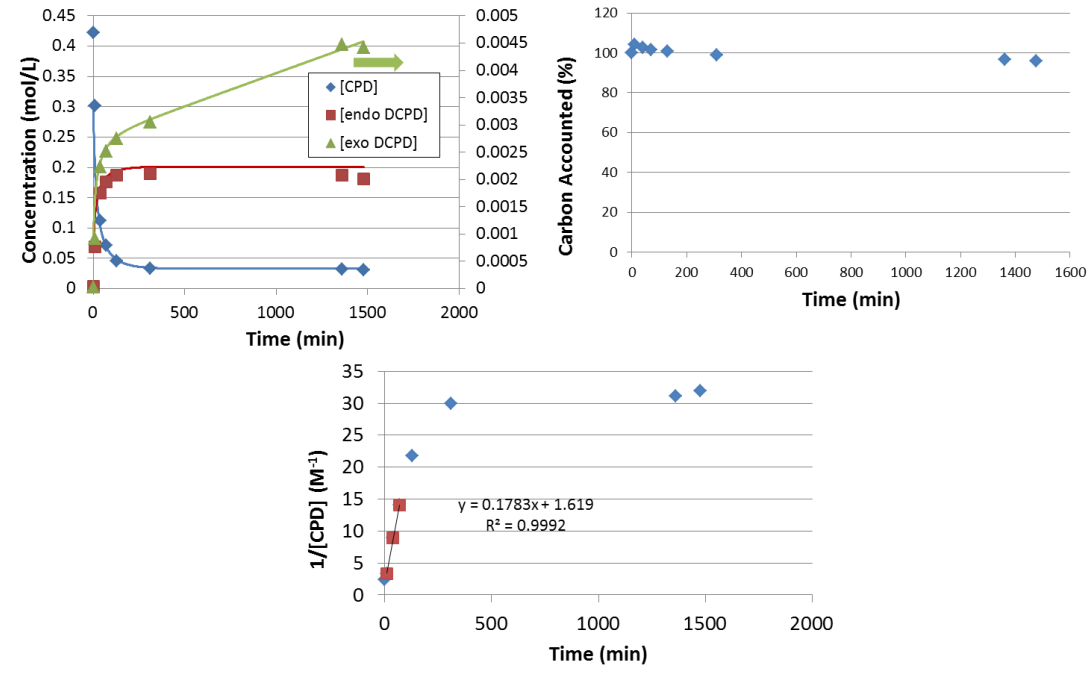

.

Figure 68: CPD in toluene at 140 °C – Run N2.

For this run, the calculated k_f is $1.64 \cdot 10^{-1}$ 1/M·min. k_r is $8.85 \cdot 10^{-4}$ 1/min. k_2 is $2.27 \cdot 10^{-3}$ 1/M·min. The equilibrium constant as calculated by the ratio of k_f to k_r is 185. The equilibrium constant as calculated by the approximately equilibrium concentration is 185.

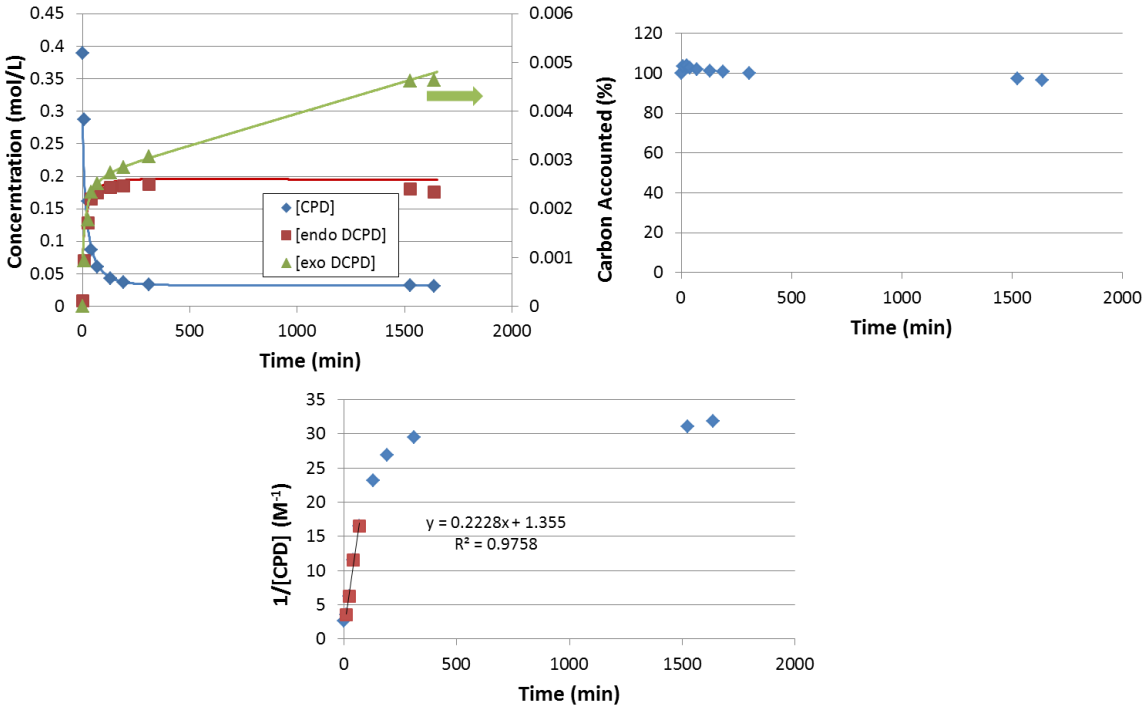

Figure 69: CPD in toluene at 140 °C – Run N3.

For this run, the calculated k_f is $1.83 \cdot 10^{-1}$ 1/M·min. k_r is $9.95 \cdot 10^{-4}$ 1/min. k_2 is $2.51 \cdot 10^{-3}$ 1/M·min. The equilibrium constant as calculated by the ratio of k_f to k_r is 184. The equilibrium constant as calculated by the approximately equilibrium concentration is 178.

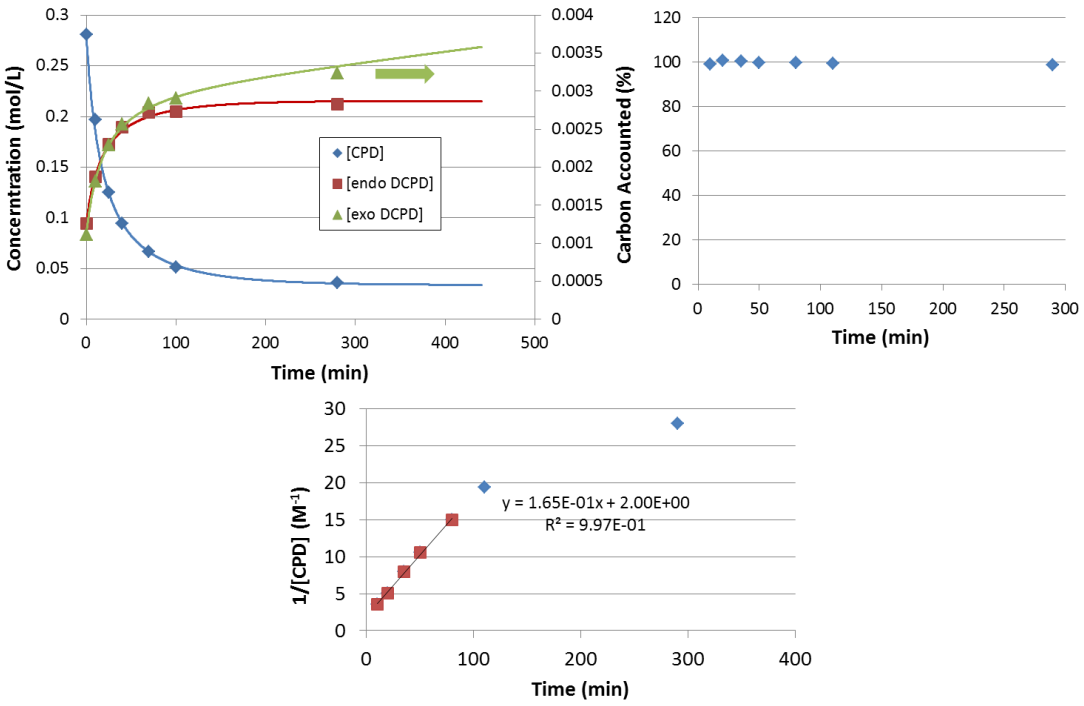

Figure 70: CPD in toluene at 140 °C – Run N4.

For this run, the calculated k_f is $1.83 \cdot 10^{-1}$ 1/M·min. k_r is $9.95 \cdot 10^{-4}$ 1/min. k_2 is $2.51 \cdot 10^{-3}$ 1/M·min. The equilibrium constant as calculated by the ratio of k_f to k_r is 184. The equilibrium constant as calculated by the approximately equilibrium concentration is 178.

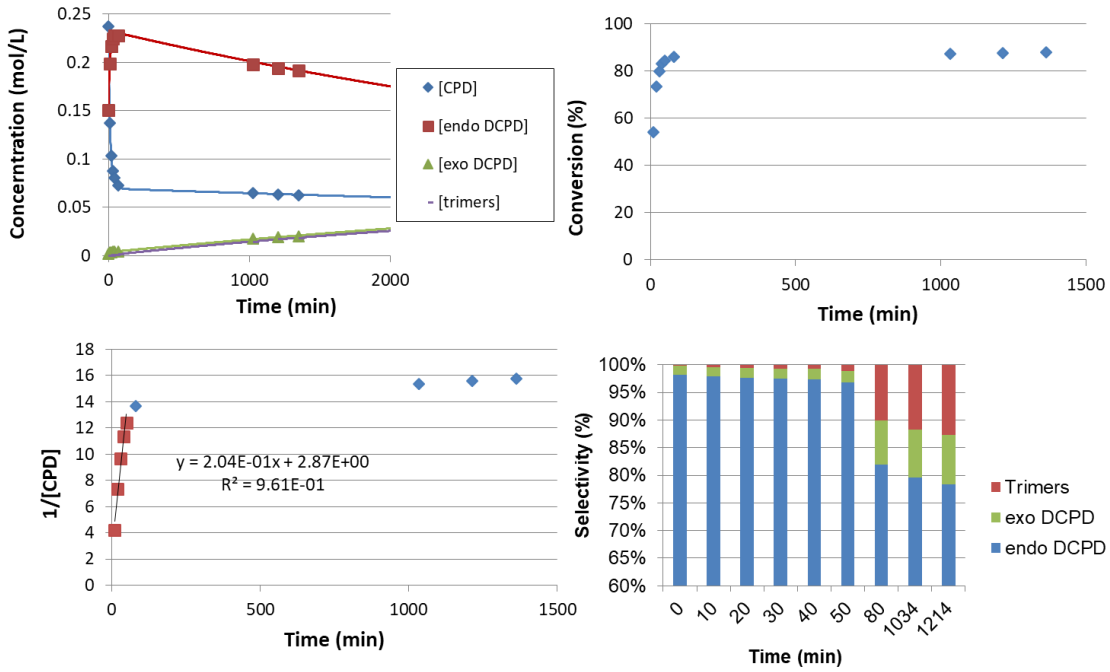

Figure 71: CPD in toluene at 160 °C – Run 1.

For this run, the calculated k_f is $3.22 \cdot 10^{-1}$ 1/M·min. k_r is $6.84 \cdot 10^{-3}$ 1/min. k_2 is $5.84 \cdot 10^{-3}$ 1/M·min. k_{trimer} is $9.55 \cdot 10^{-4}$ 1/M·min. The equilibrium constant as calculated by the ratio of k_f to k_r is 47. The equilibrium constant as calculated by the approximately equilibrium concentration is 49.

B.5.2 CPD in Cyclohexane

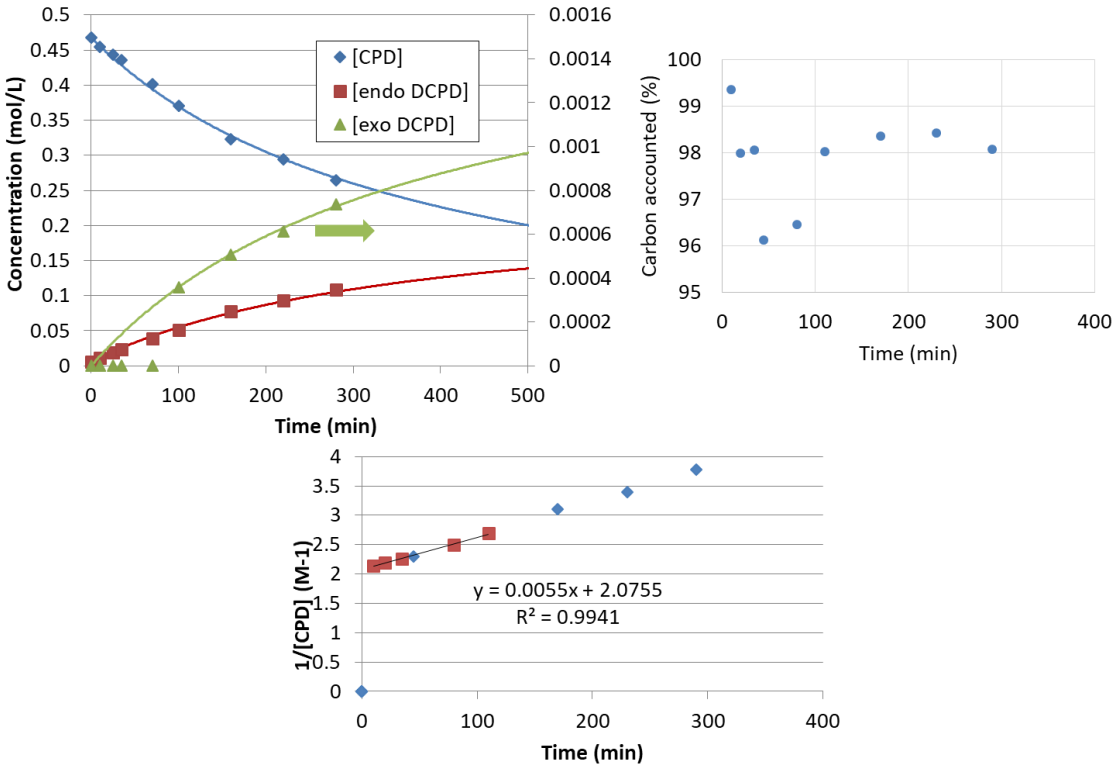

Figure 72: CPD in cyclohexane at 80 °C – Run N1.

For this run, the calculated k_f is $5.66 \cdot 10^{-3}$ 1/M·min. k_r and k_2 are not reliably calculated due to the low temperature.

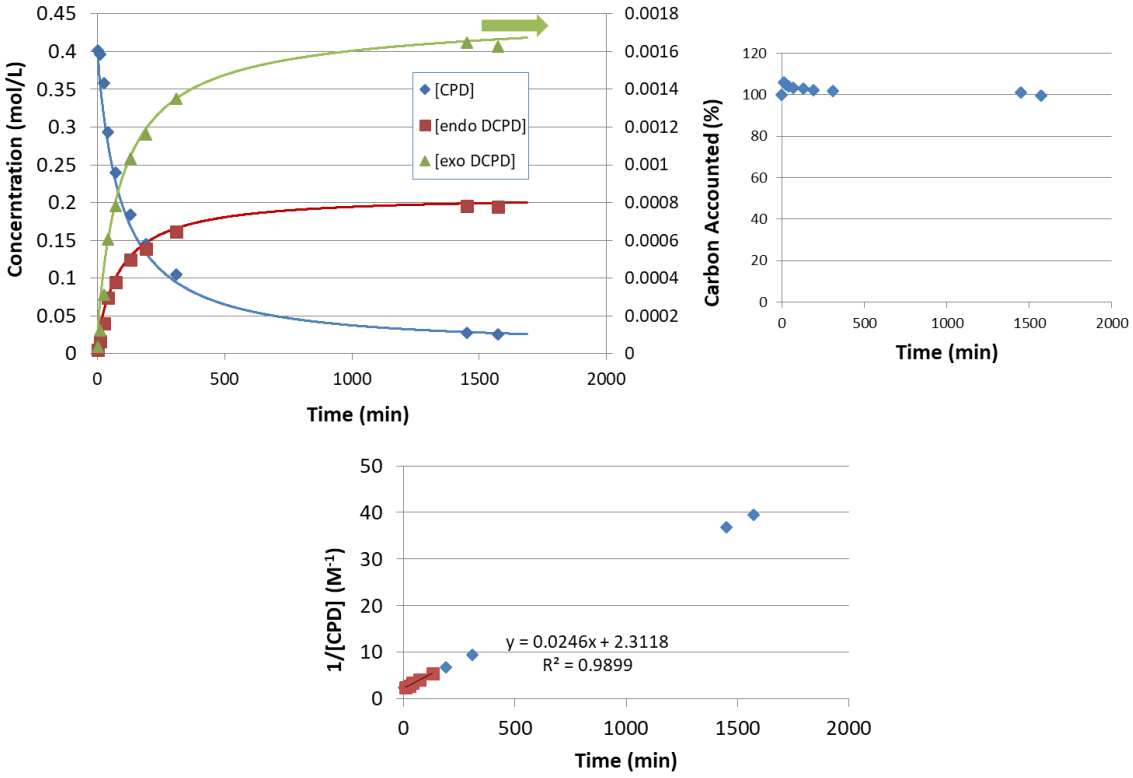

Figure 73: CPD in cyclohexane at 100 °C – Run 1.

For this run, the calculated k_f is $2.60 \cdot 10^{-2}$ 1/M·min. k_r is $4.02 \cdot 10^{-5}$ 1/min. k_2 is $2.12 \cdot 10^{-4}$ 1/M·min. The equilibrium constant as calculated by the ratio of k_f to k_r is 646. The equilibrium constant as calculated by the approximately equilibrium concentration is 304.

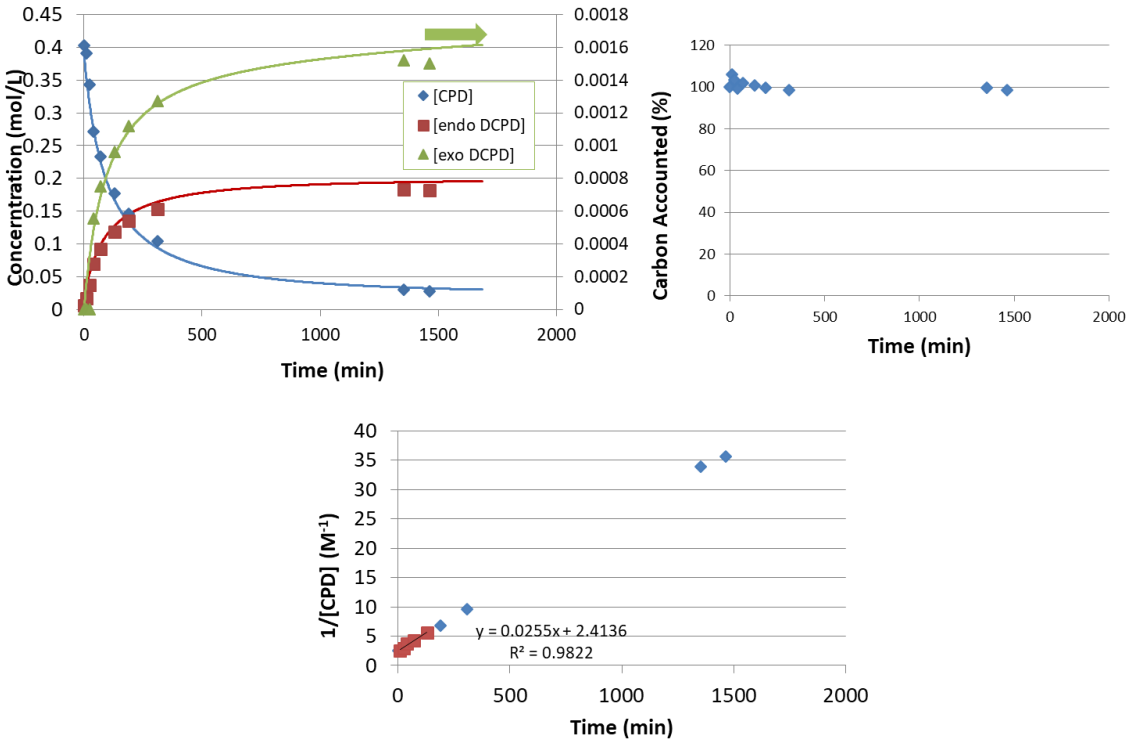

Figure 74: CPD in cyclohexane at 100 °C – Run 2.

For this run, the calculated k_f is $2.62 \cdot 10^{-2}$ 1/M·min. k_r is $8.50 \cdot 10^{-5}$ 1/min. k_2 is $2.22 \cdot 10^{-4}$ 1/M·min. The equilibrium constant as calculated by the ratio of k_f to k_r is 309. The equilibrium constant as calculated by the approximately equilibrium concentration is 230.

B.6 Initial Mixture Results

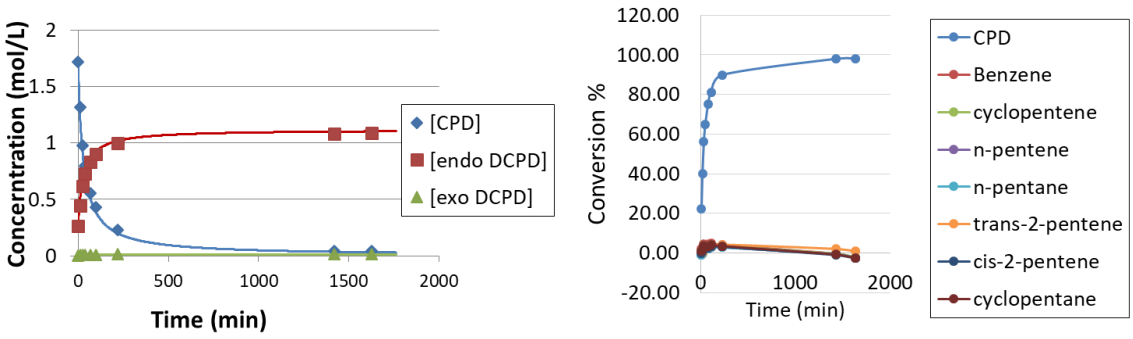

Figure 75: Initial mixture of CPD with impurities at 100 °C – Run 1, comparing the expected model of CPD alone to experimental CPD in mixture and conversion of impurities.

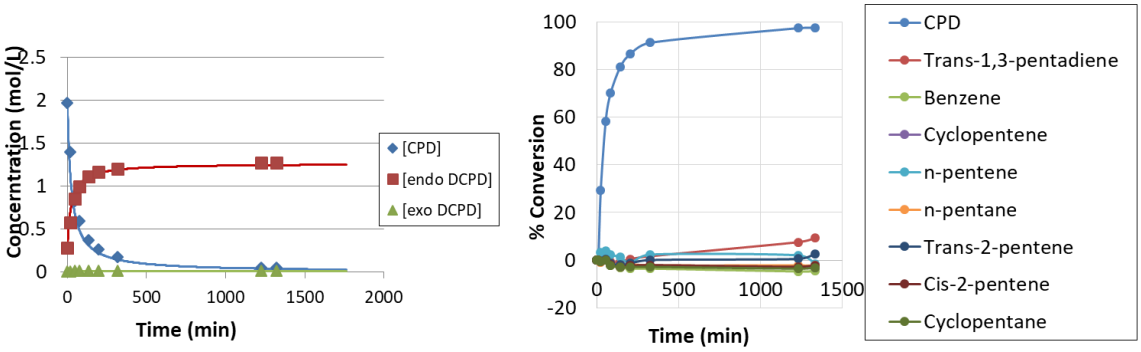

Figure 76: Initial mixture of CPD with impurities at 100 °C – Run 2, comparing the expected model of CPD alone to experimental CPD in mixture and conversion of impurities.

;

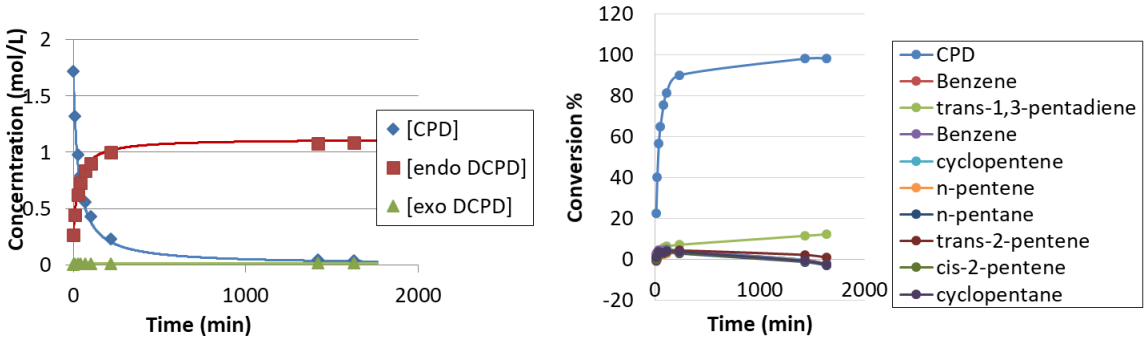

Figure 77: Initial mixture of CPD with impurities at 100 °C – Run 3, comparing the expected model of CPD alone to experimental CPD in mixture and conversion of impurities.

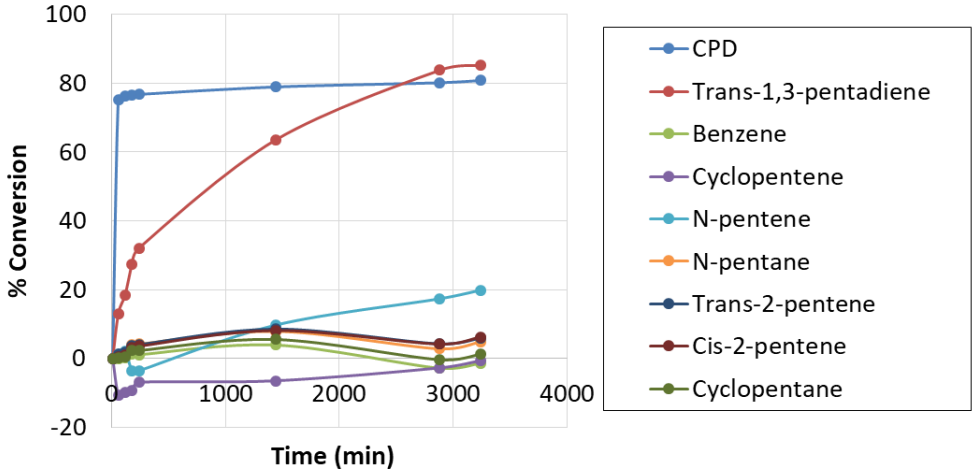

Figure 78: Initial mixture of CPD with impurities at 150 °C – conversion of impurities.

B.7 Isoprene Self-Dimerization Study

B.7.1 Isoprene Self-Dimerization Experiments in Air

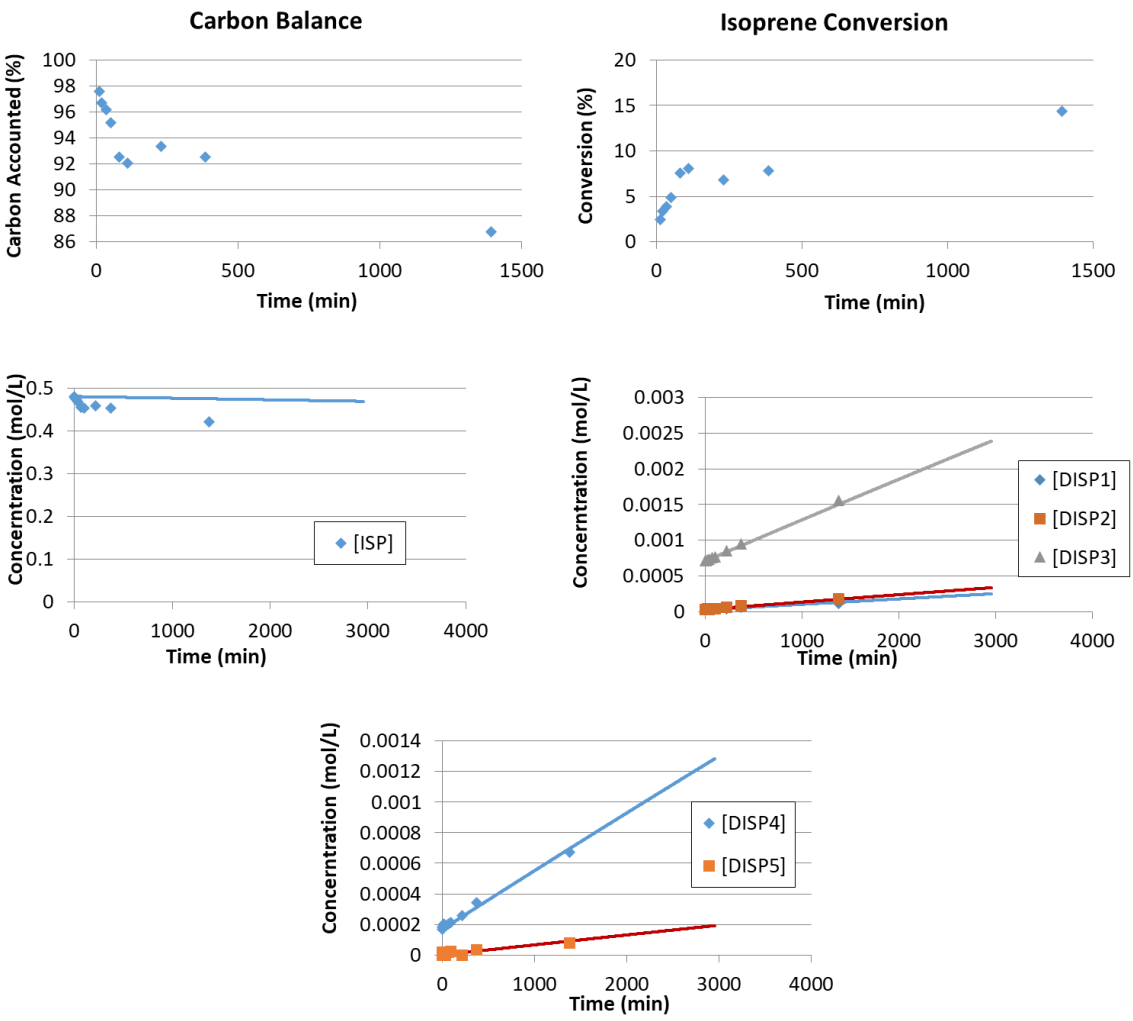

Figure 79: Isoprene in air dimerization at 100 °C – Run 1.

Table 8: Fitted Rate Constants for Isoprene in Air Dimerization at 100 °C – Run 1

k_{DISP1}	$6.71 \cdot 10^{-7}$ 1/M·min
k_{DISP2}	$9.19 \cdot 10^{-7}$ 1/M·min
k_{DISP3}	$5.05 \cdot 10^{-6}$ 1/M·min
k_{DISP4}	$3.36 \cdot 10^{-6}$ 1/M·min
k_{DISP5}	$5.77 \cdot 10^{-7}$ 1/M·min

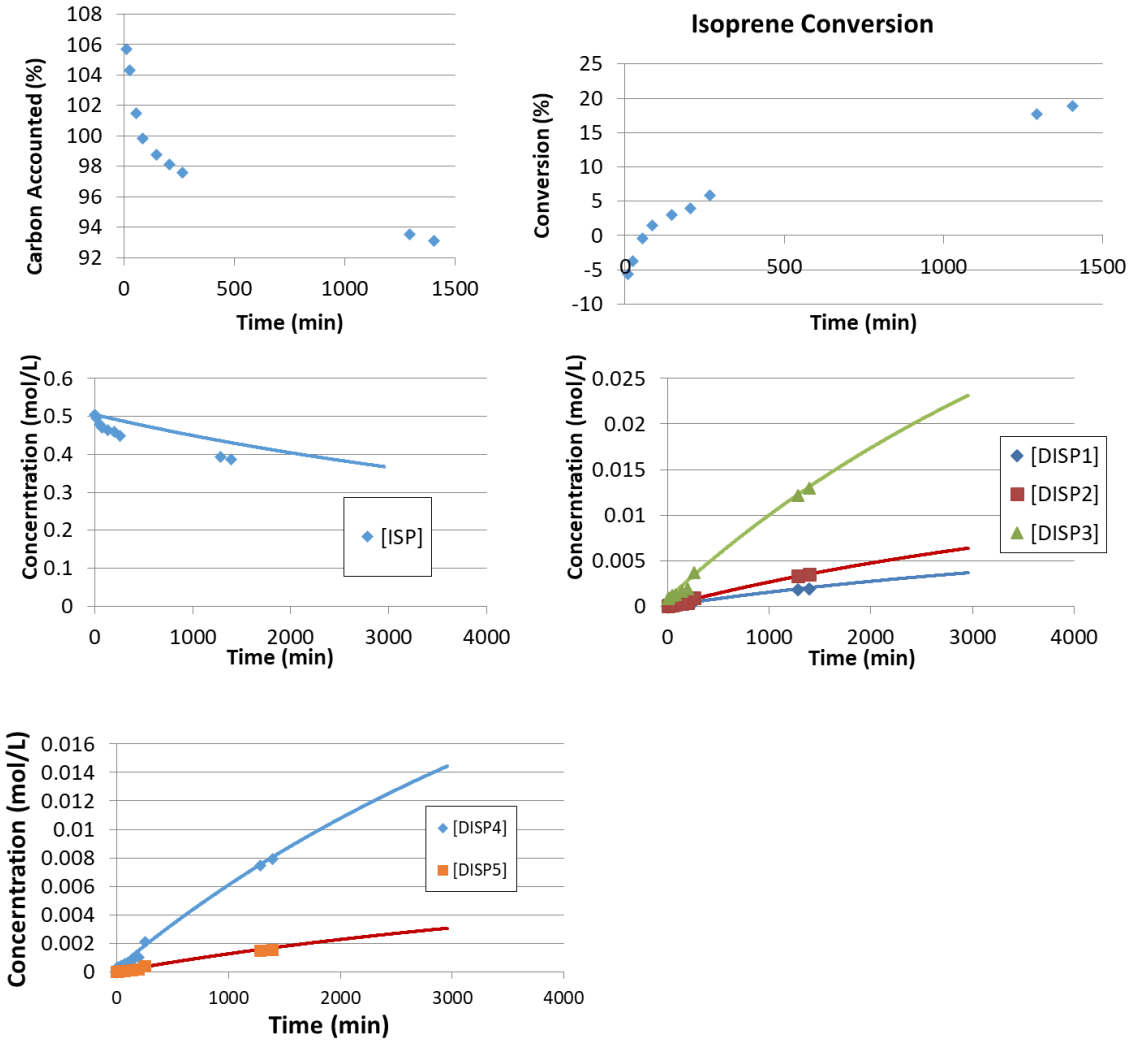

Figure 80: Isoprene in air dimerization at 120 °C – Run 1.

Table 9: Fitted Rate Constants for Isoprene in Air Dimerization at 120 °C – Run 1

k_{DISP1}	$1.32 \cdot 10^{-5}$ 1/M·min
k_{DISP2}	$2.29 \cdot 10^{-5}$ 1/M·min
k_{DISP3}	$8.10 \cdot 10^{-5}$ 1/M·min
k_{DISP4}	$5.16 \cdot 10^{-5}$ 1/M·min
k_{DISP5}	$1.11 \cdot 10^{-5}$ 1/M·min

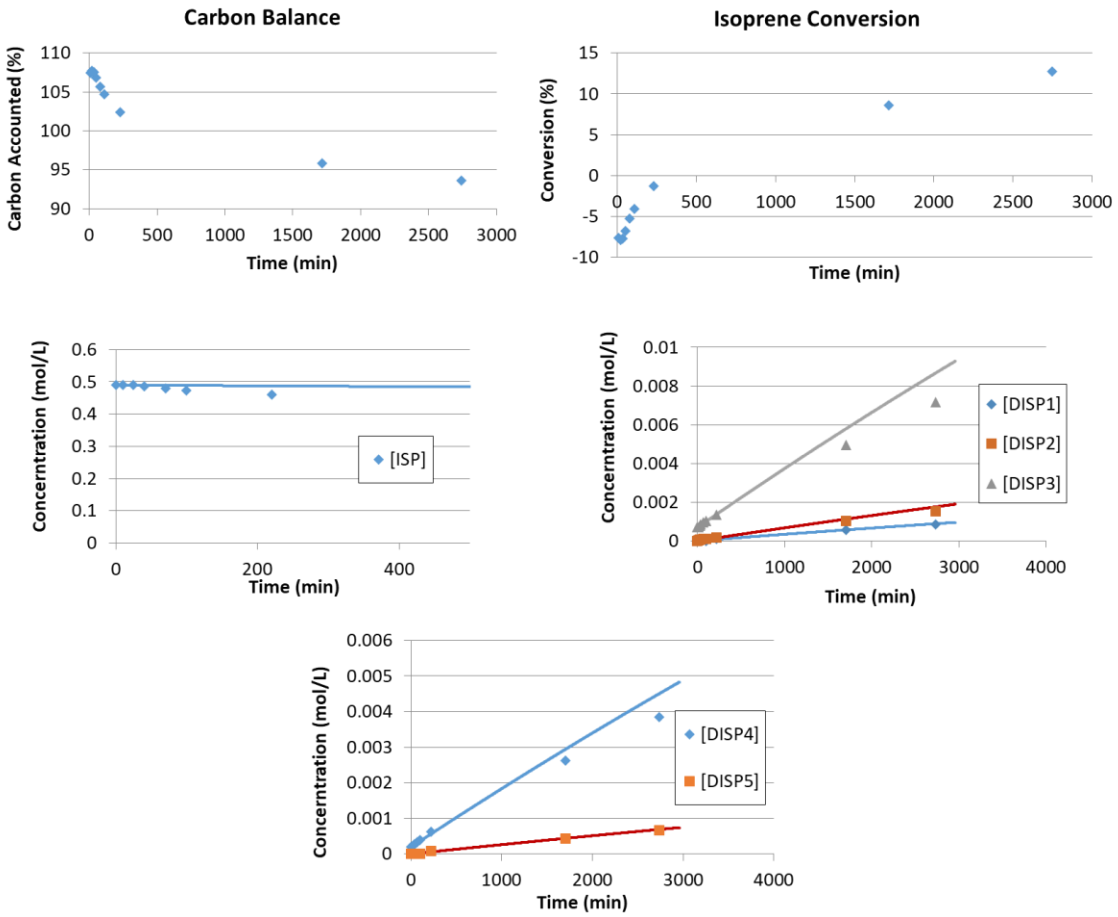

Figure 81: Isoprene in air dimerization at 120 °C – Run 2.

Table 10: Fitted Rate Constants for Isoprene in Air Dimerization at 120 °C – Run 2

k_{DISP1}	$2.88 \cdot 10^{-6}$ 1/M·min
k_{DISP2}	$5.71 \cdot 10^{-6}$ 1/M·min
k_{DISP3}	$2.60 \cdot 10^{-5}$ 1/M·min
k_{DISP4}	$1.40 \cdot 10^{-5}$ 1/M·min
k_{DISP5}	$2.24 \cdot 10^{-6}$ 1/M·min

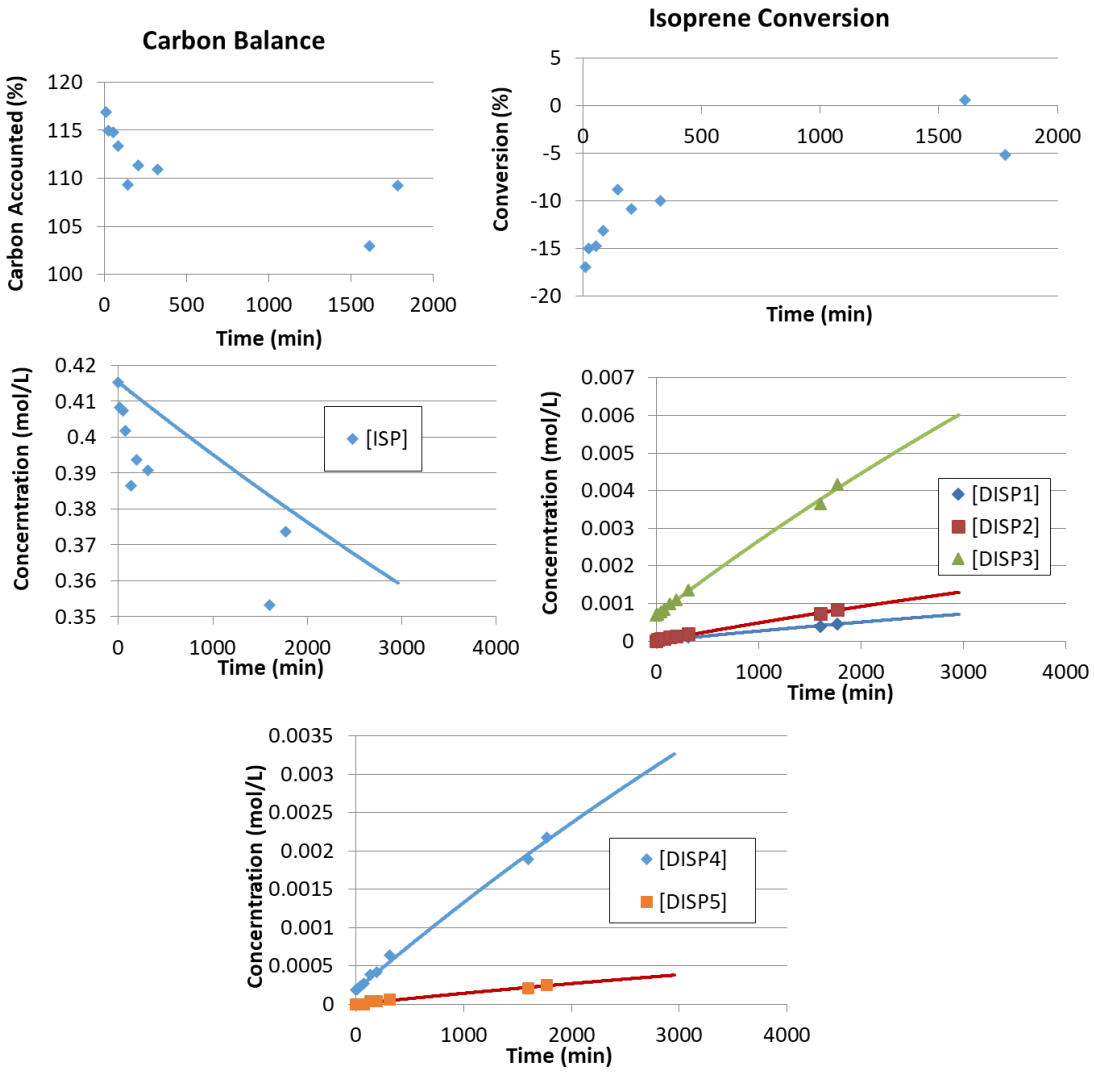

Figure 82: Isoprene in air dimerization using stainless steel reactors at 120 °C.

Table 11: Fitted Rate Constants for Isoprene in Air Dimerization Using Stainless Steel Reactors at 120 °C

k_{DISP1}	$3.21 \cdot 10^{-6}$ 1/M·min
k_{DISP2}	$5.86 \cdot 10^{-6}$ 1/M·min
k_{DISP3}	$2.41 \cdot 10^{-5}$ 1/M·min
k_{DISP4}	$1.39 \cdot 10^{-5}$ 1/M·min
k_{DISP5}	$1.71 \cdot 10^{-6}$ 1/M·min

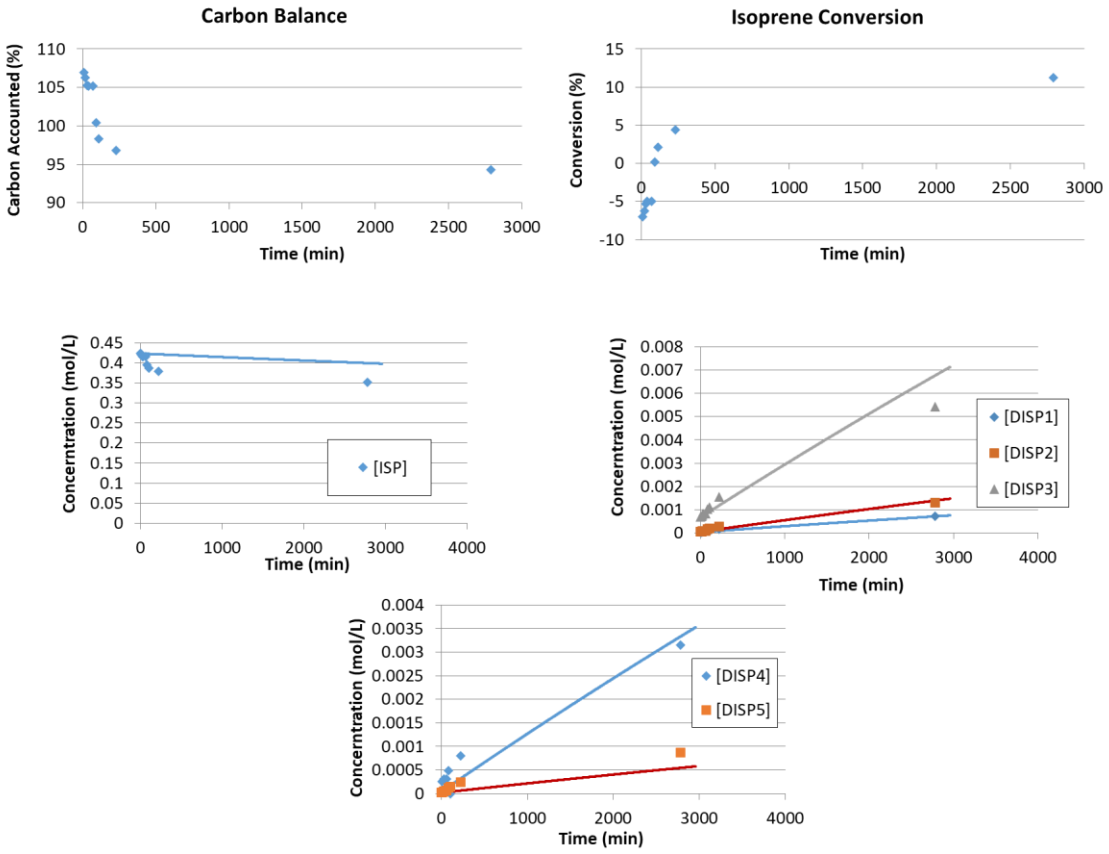

Figure 83: Isoprene in air dimerization at 130 °C – Run 1.

Table 12: Fitted Rate Constants for Isoprene in Air Dimerization at 130 °C – Run 1

k_{DISP1}	$2.88 \cdot 10^{-6}$ 1/M·min
k_{DISP2}	$5.71 \cdot 10^{-6}$ 1/M·min
k_{DISP3}	$2.60 \cdot 10^{-5}$ 1/M·min
k_{DISP4}	$1.40 \cdot 10^{-5}$ 1/M·min
k_{DISP5}	$2.24 \cdot 10^{-6}$ 1/M·min

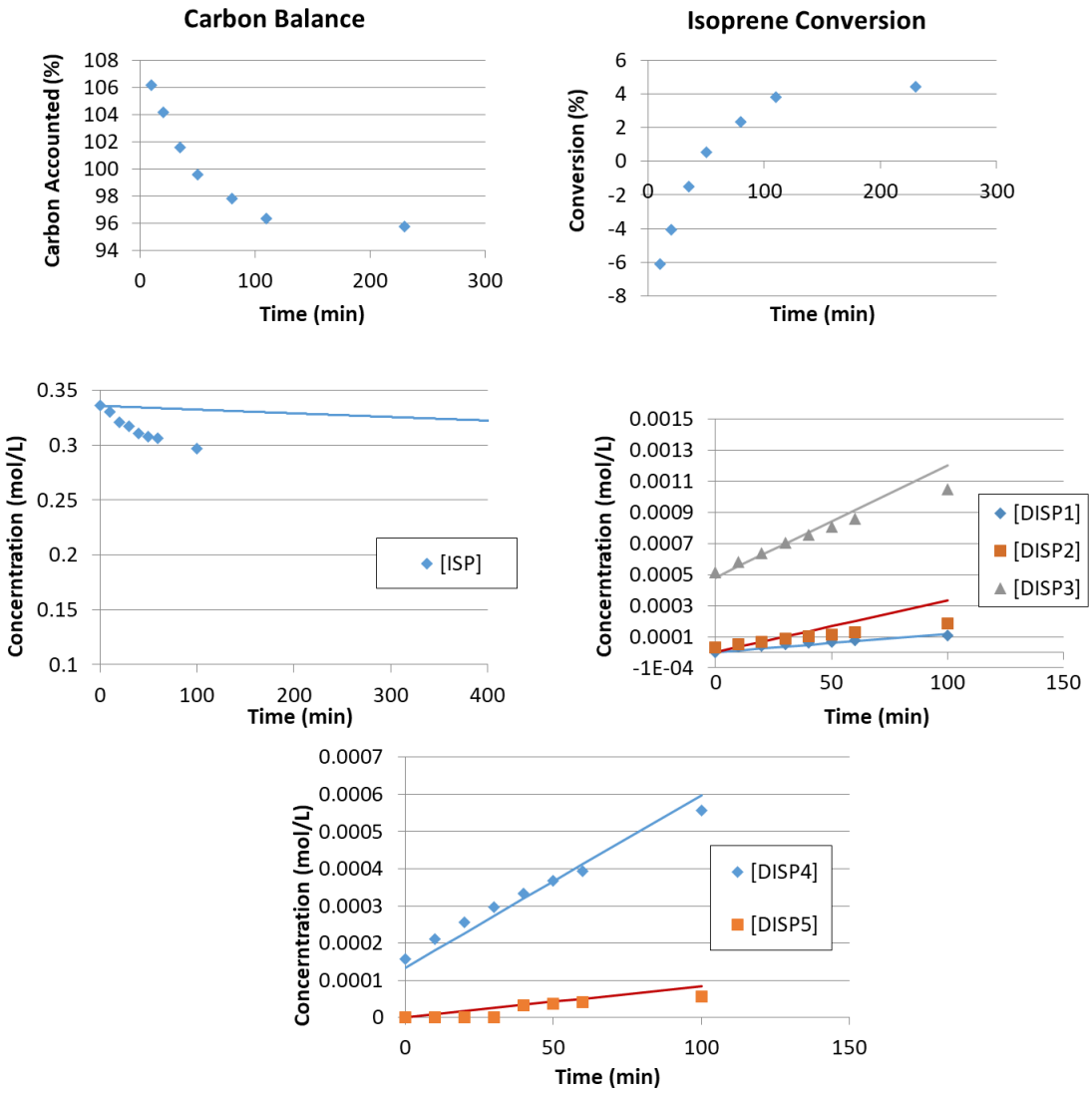

Figure 84: Isoprene in air dimerization at 140 °C – Run 1.

Table 13: Fitted Rate Constants for Isoprene in Air Dimerization at 140 °C – Run 1

k_{DISP1}	$2.14 \cdot 10^{-5}$ 1/M·min
k_{DISP2}	$6.00 \cdot 10^{-5}$ 1/M·min
k_{DISP3}	$1.30 \cdot 10^{-4}$ 1/M·min
k_{DISP4}	$8.32 \cdot 10^{-5}$ 1/M·min
k_{DISP5}	$1.51 \cdot 10^{-5}$ 1/M·min

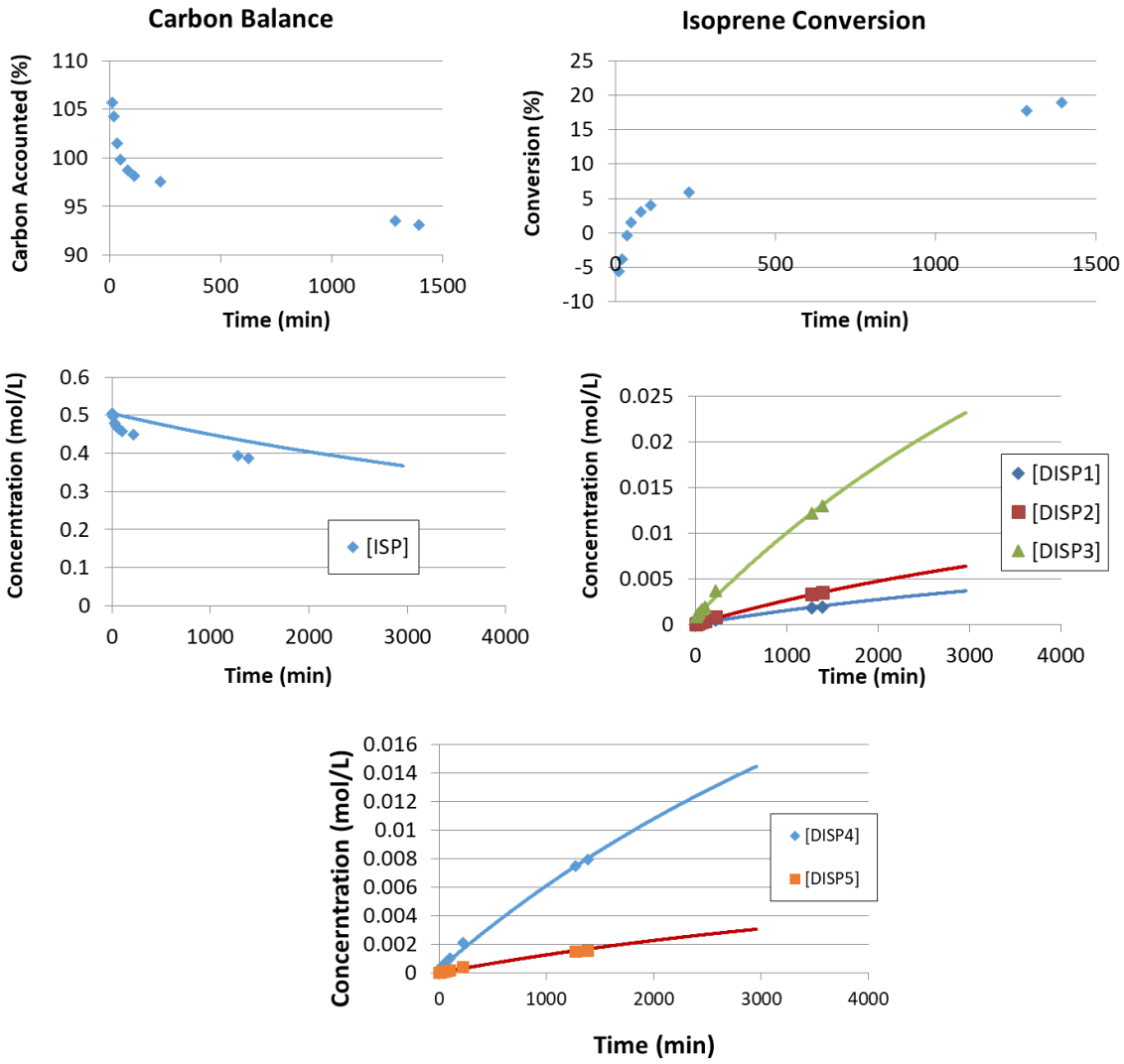

Figure 85: Isoprene in air dimerization at 140 °C – Run 2.

Table 14: Fitted Rate Constants for Isoprene in Air Dimerization at 140 °C – Run 2

k_{DISP1}	$1.32 \cdot 10^{-5}$ 1/M·min
k_{DISP2}	$2.29 \cdot 10^{-5}$ 1/M·min
k_{DISP3}	$8.10 \cdot 10^{-5}$ 1/M·min
k_{DISP4}	$5.16 \cdot 10^{-5}$ 1/M·min
k_{DISP5}	$1.11 \cdot 10^{-5}$ 1/M·min

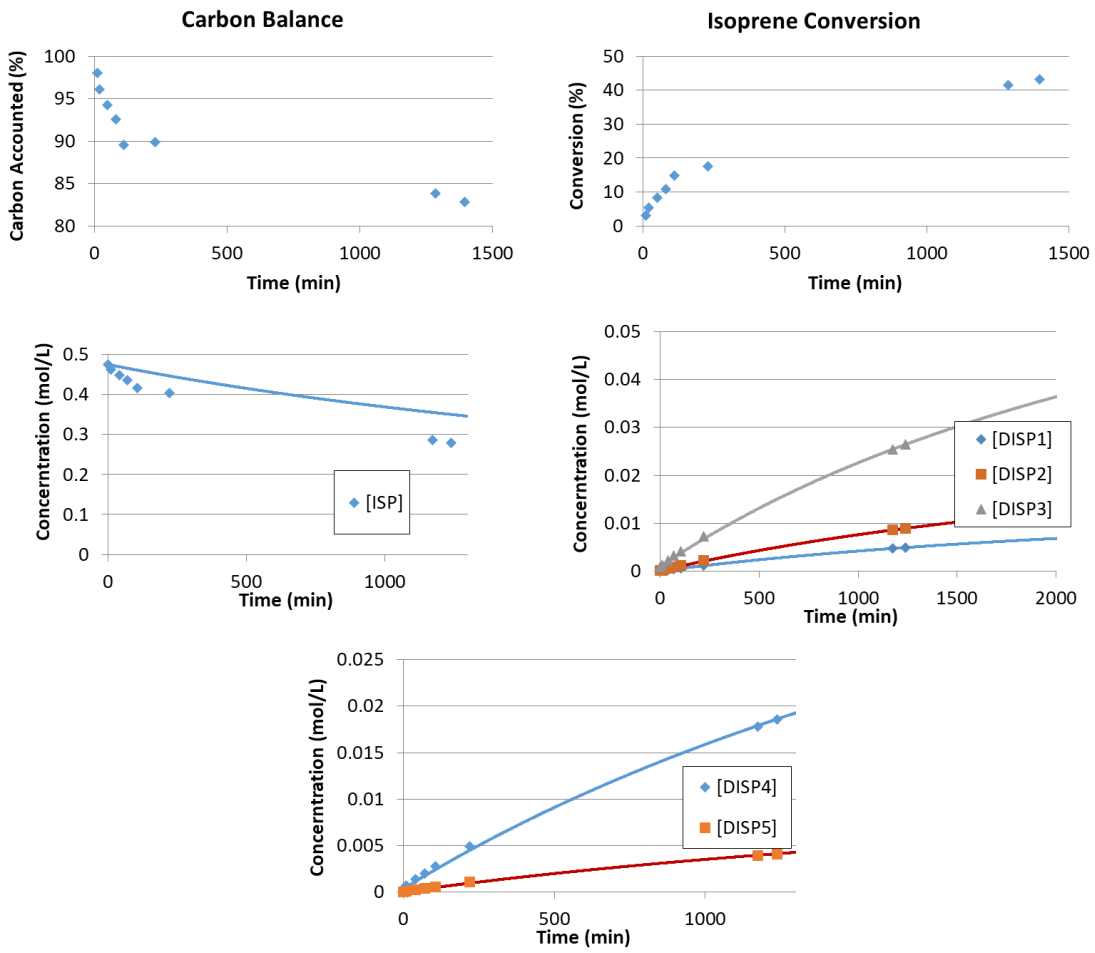

Figure 86: Isoprene in air dimerization at 160 °C – Run 1.

Table 15: Fitted Rate Constants for Isoprene in Air Dimerization at 160 °C – Run 1

k_{DISP1}	$4.73 \cdot 10^{-5}$ 1/M·min
k_{DISP2}	$8.57 \cdot 10^{-5}$ 1/M·min
k_{DISP3}	$2.47 \cdot 10^{-4}$ 1/M·min
k_{DISP4}	$1.77 \cdot 10^{-4}$ 1/M·min
k_{DISP5}	$3.96 \cdot 10^{-5}$ 1/M·min

B.7.2 Isoprene Self-Dimerization in the Absence of Air

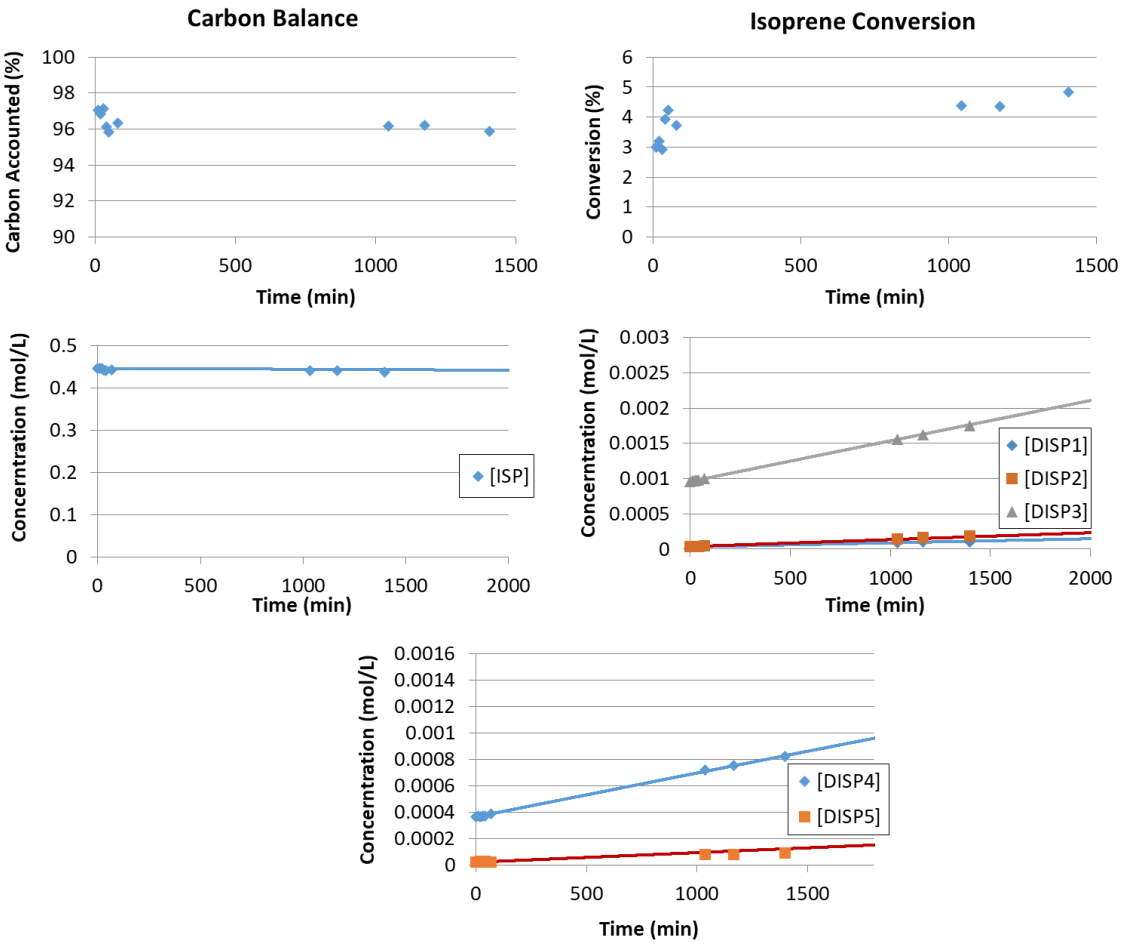

Figure 87: Isoprene dimerization in absence of air at 100 °C – Run 1.

Table 16: Fitted Rate Constants for Isoprene Dimerization in Absence of Air at 100 °C – Run 1

k_{DISP1}	$5.68 \cdot 10^{-7}$ 1/M·min
k_{DISP2}	$9.95 \cdot 10^{-7}$ 1/M·min
k_{DISP3}	$5.83 \cdot 10^{-6}$ 1/M·min
k_{DISP4}	$3.35 \cdot 10^{-6}$ 1/M·min
k_{DISP5}	$7.38 \cdot 10^{-7}$ 1/M·min

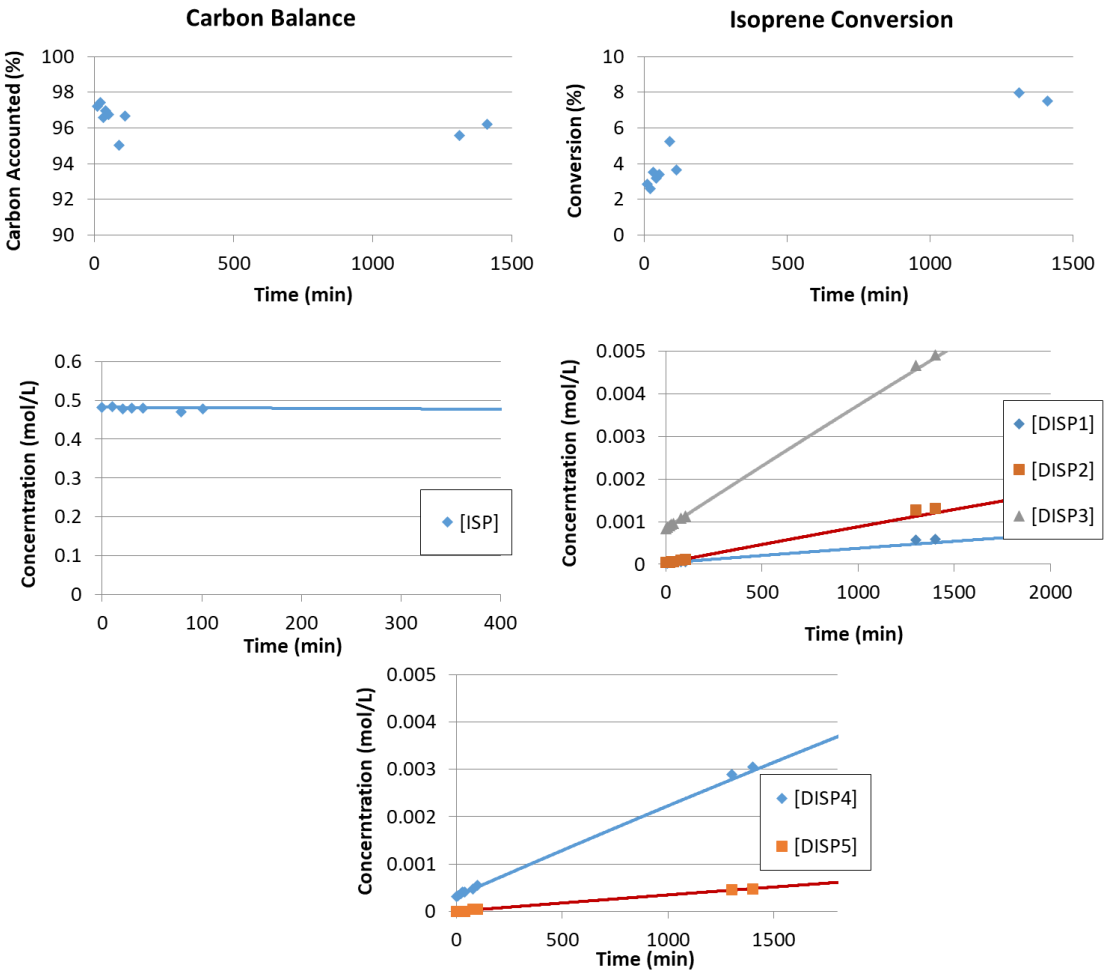

Figure 88: Isoprene dimerization in absence of air at 120 °C – Run 1.

Table 17: Fitted Rate Constants for Isoprene Dimerization in Absence of Air at 120 °C – Run 1

k_{DISP1}	$3.03 \cdot 10^{-6}$ 1/M·min
k_{DISP2}	$7.46 \cdot 10^{-6}$ 1/M·min
k_{DISP3}	$2.55 \cdot 10^{-5}$ 1/M·min
k_{DISP4}	$1.69 \cdot 10^{-5}$ 1/M·min
k_{DISP5}	$3.06 \cdot 10^{-6}$ 1/M·min

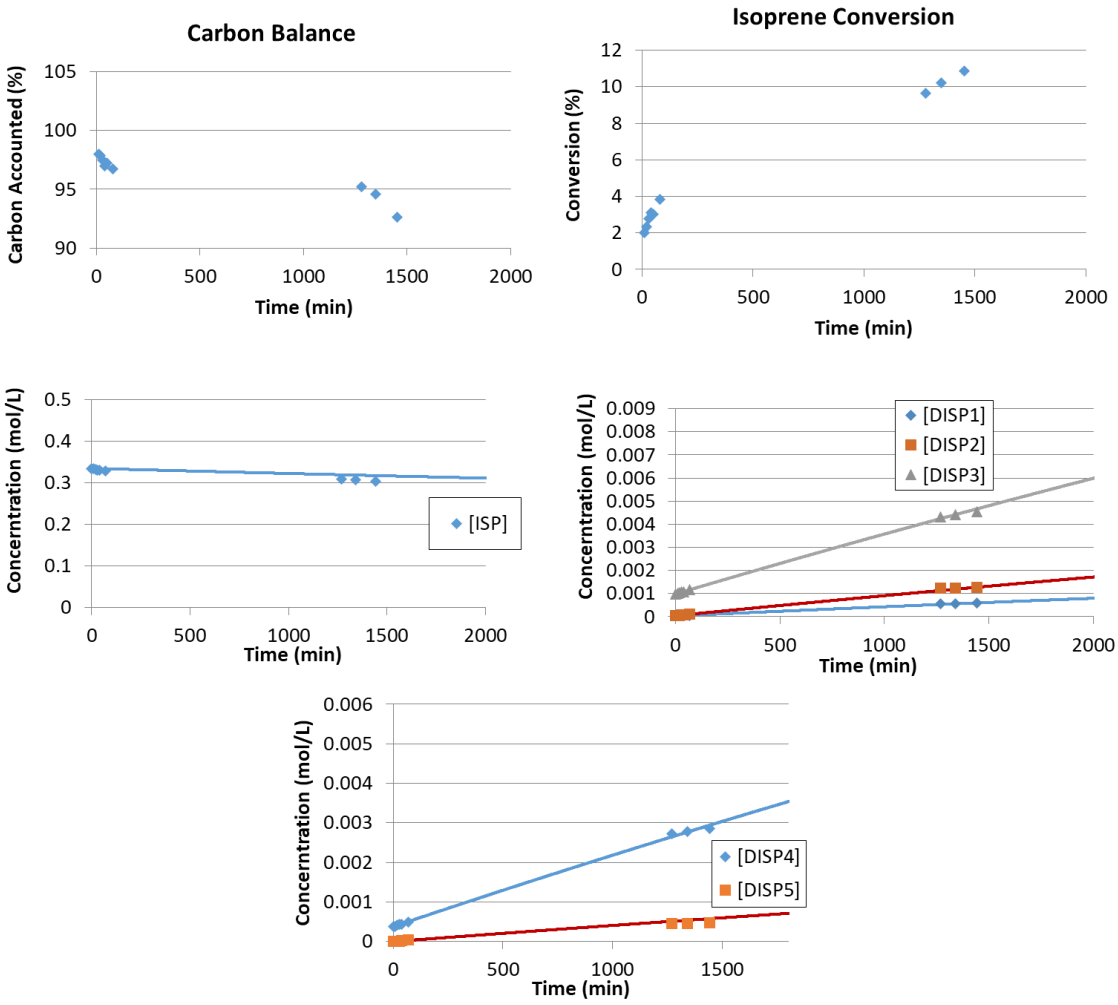

Figure 89: Isoprene dimerization in absence of air at 130 °C – Run 1.

Table 18: Fitted Rate Constants for Isoprene Dimerization in Absence of Air at 130 °C – Run 1

k_{DISP1}	$7.33 \cdot 10^{-6}$ 1/M·min
k_{DISP2}	$1.61 \cdot 10^{-5}$ 1/M·min
k_{DISP3}	$4.81 \cdot 10^{-5}$ 1/M·min
k_{DISP4}	$3.35 \cdot 10^{-5}$ 1/M·min
k_{DISP5}	$7.56 \cdot 10^{-6}$ 1/M·min

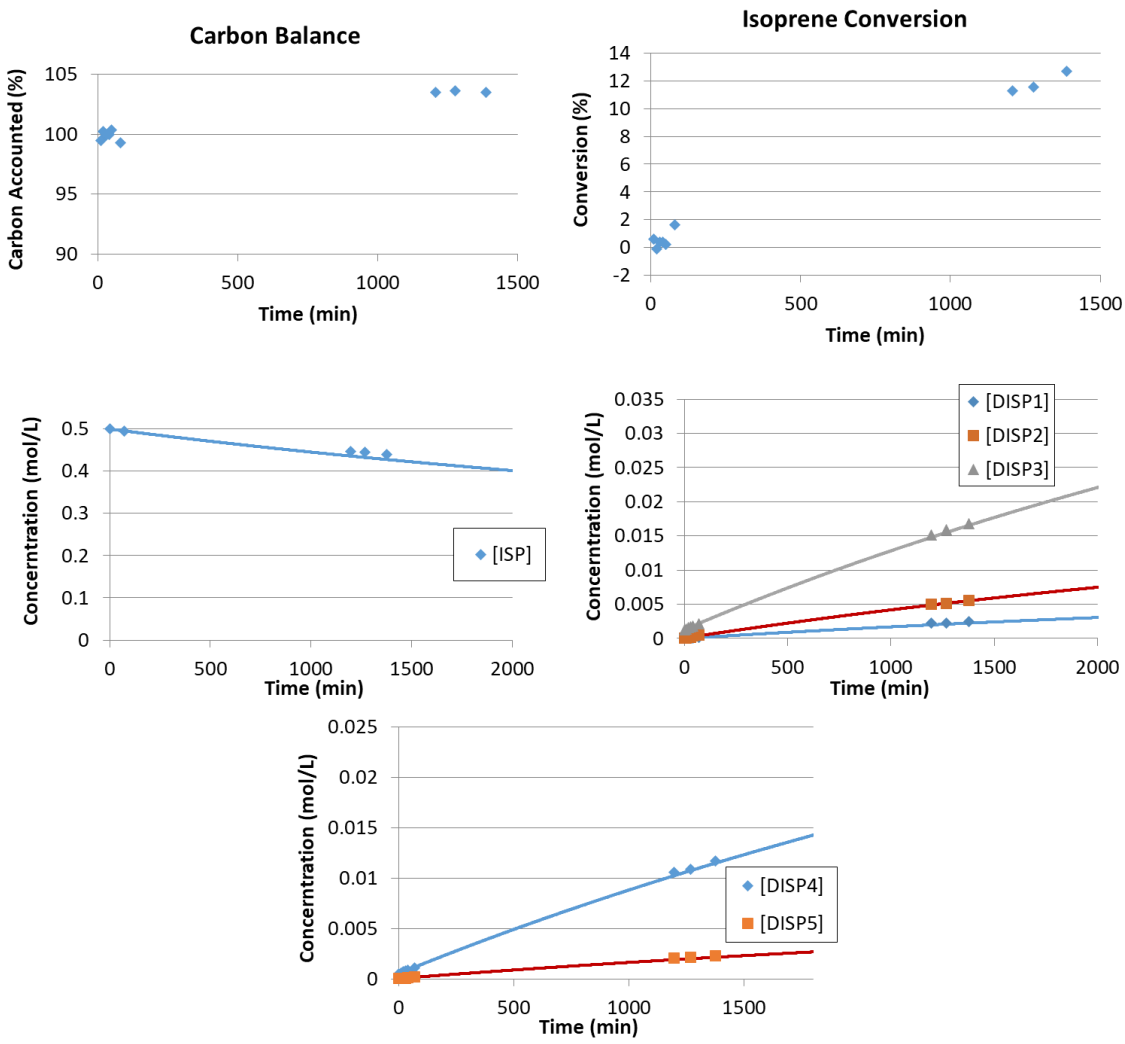

Figure 90: Isoprene dimerization in absence of air at 140 °C – Run 1.

Table 19: Fitted Rate Constants for Isoprene Dimerization in Absence of Air at 140 °C – Run 1

k_{DISP1}	$1.52 \cdot 10^{-5}$ 1/M·min
k_{DISP2}	$3.70 \cdot 10^{-5}$ 1/M·min
k_{DISP3}	$1.04 \cdot 10^{-4}$ 1/M·min
k_{DISP4}	$7.47 \cdot 10^{-5}$ 1/M·min
k_{DISP5}	$1.43 \cdot 10^{-5}$ 1/M·min

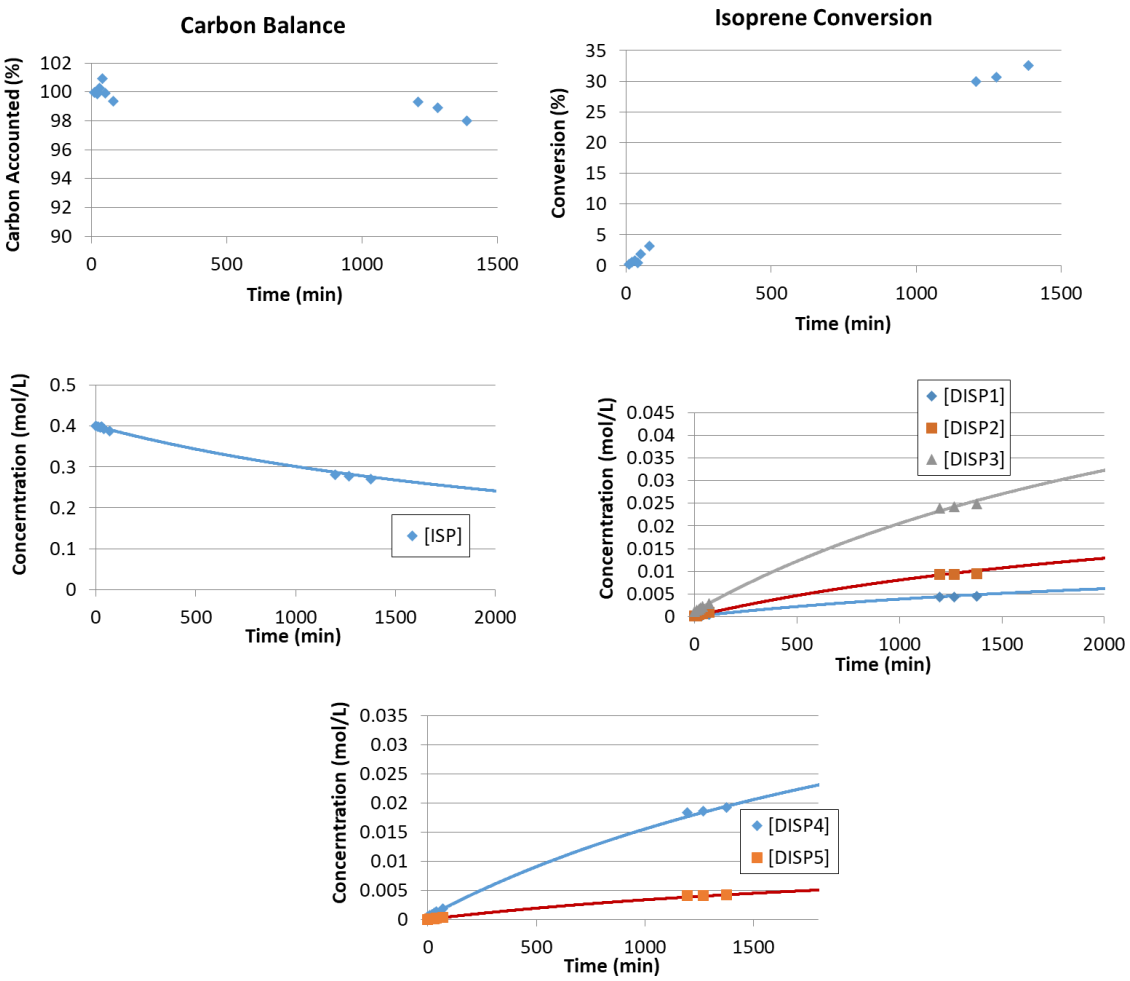

Figure 91: Isoprene dimerization in absence of air at 160 °C – Run 1.

Table 20: Fitted Rate Constants for Isoprene Dimerization in Absence of Air at 160 °C – Run 1

k_{DISP1}	$6.32 \cdot 10^{-5}$ 1/M·min
k_{DISP2}	$1.32 \cdot 10^{-4}$ 1/M·min
k_{DISP3}	$3.22 \cdot 10^{-4}$ 1/M·min
k_{DISP4}	$2.49 \cdot 10^{-4}$ 1/M·min
k_{DISP5}	$5.53 \cdot 10^{-5}$ 1/M·min

B.8 Isoprene-Cyclopentadiene Co-dimerization Experimental Data

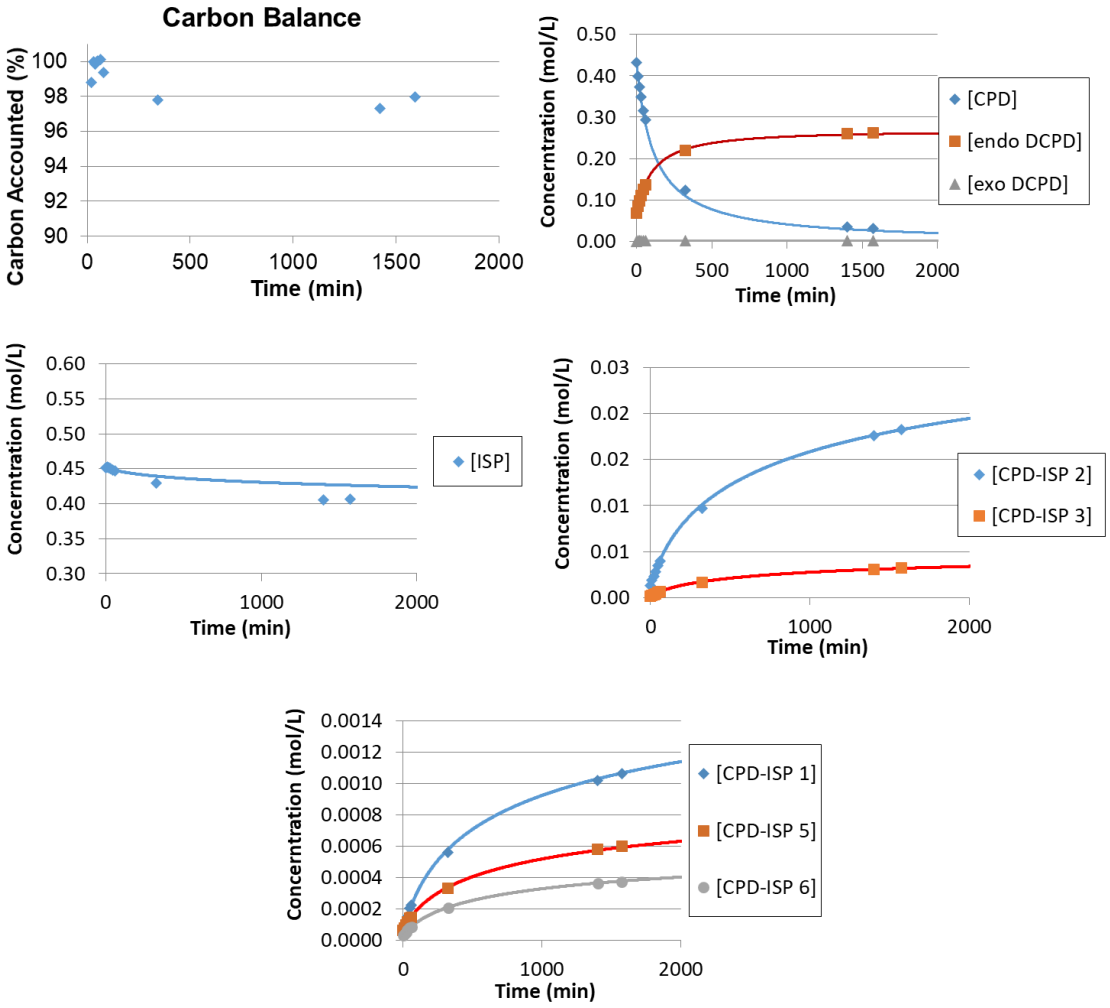

Figure 92: Cyclopentadiene-isoprene co-dimerization in absence of air at 100 °C – Run 1.

Table 21: Fitted Rate Constants for Cyclopentadiene-Isoprene Co-dimerization in Absence of Air at 100 °C – Run 1

$K_{CPD\text{-}ISP1}$	$1.80 \cdot 10^{-5}$ 1/M·min
$K_{CPD\text{-}ISP2}$	$3.01 \cdot 10^{-4}$ 1/M·min
$K_{CPD\text{-}ISP3}$	$5.34 \cdot 10^{-5}$ 1/M·min
$K_{CPD\text{-}ISP5}$	$9.42 \cdot 10^{-6}$ 1/M·min
$K_{CPD\text{-}ISP6}$	$6.20 \cdot 10^{-6}$ 1/M·min
$K_{CI2\text{-}CI3}$	--

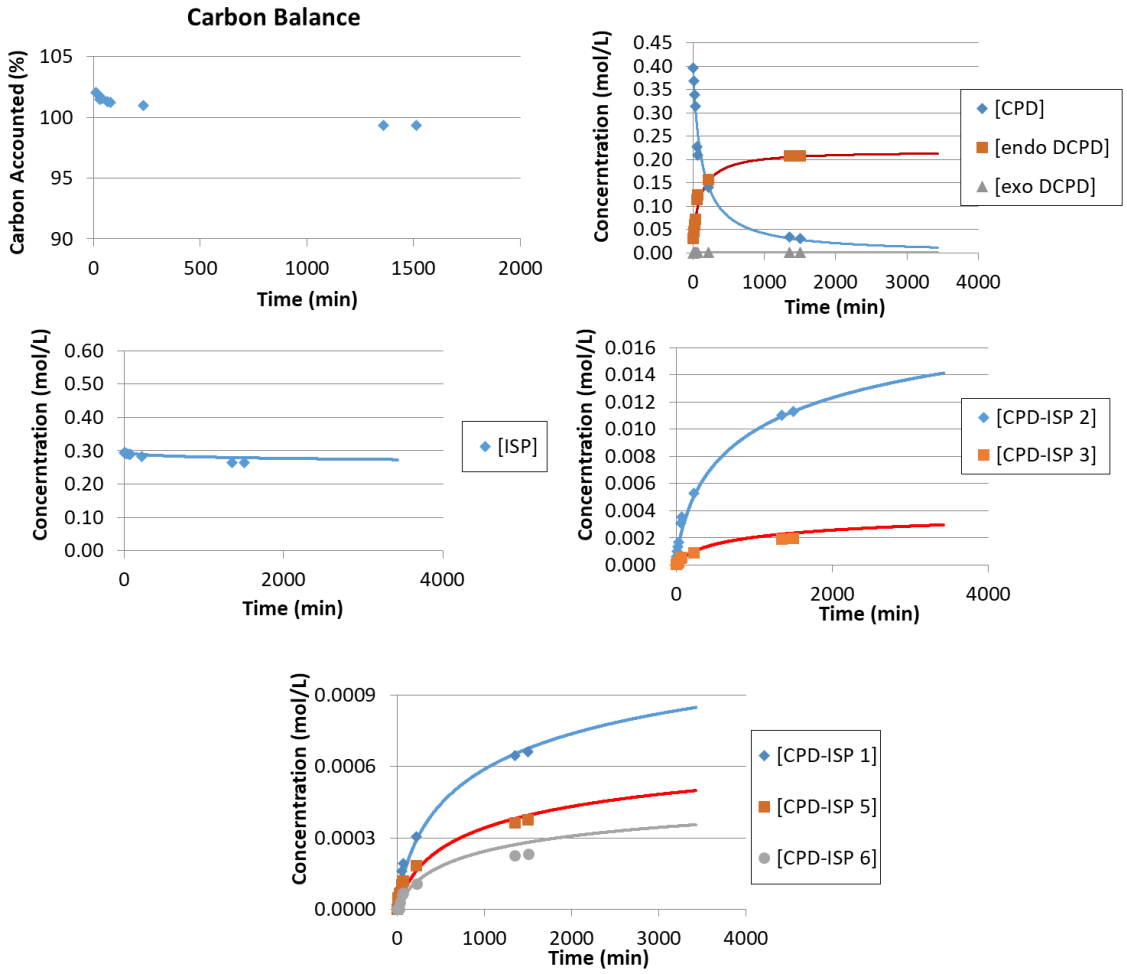

Figure 93: Cyclopentadiene-isoprene co-dimerization in absence of air at 100 °C – Run 2.

Table 22: Fitted Rate Constants for Cyclopentadiene-Isoprene Co-dimerization in Absence of Air at 100 °C – Run 2

$K_{CPD-ISP1}$	$1.84 \cdot 10^{-5}$ 1/M·min
$K_{CPD-ISP2}$	$3.00 \cdot 10^{-4}$ 1/M·min
$K_{CPD-ISP3}$	$6.46 \cdot 10^{-5}$ 1/M·min
$K_{CPD-ISP5}$	$1.11 \cdot 10^{-5}$ 1/M·min
$K_{CPD-ISP6}$	$7.90 \cdot 10^{-6}$ 1/M·min
$K_{CI2-CI3}$	--

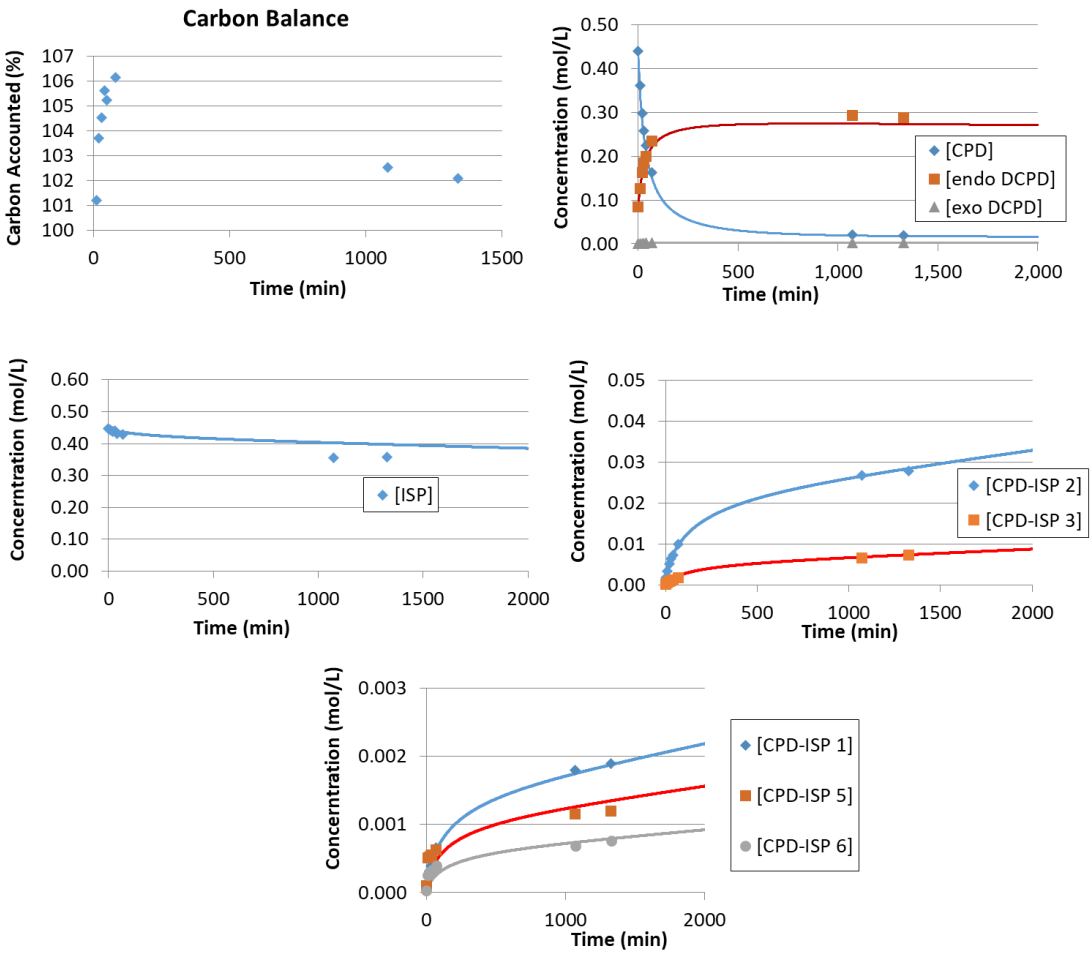

Figure 94: Cyclopentadiene-isoprene co-dimerization in absence of air at 120 °C – Run 1.

Table 23: Fitted Rate Constants for Cyclopentadiene-Isoprene Co-dimerization in Absence of Air at 120 °C – Run 1

$K_{CPD-ISP1}$	$6.95 \cdot 10^{-5}$ 1/M·min
$K_{CPD-ISP2}$	$1.04 \cdot 10^{-3}$ 1/M·min
$K_{CPD-ISP3}$	$2.67 \cdot 10^{-4}$ 1/M·min
$K_{CPD-ISP5}$	$4.82 \cdot 10^{-5}$ 1/M·min
$K_{CPD-ISP6}$	$2.93 \cdot 10^{-5}$ 1/M·min
$K_{CI2-CI3}$	$9.42 \cdot 10^{-6}$ 1/M·min

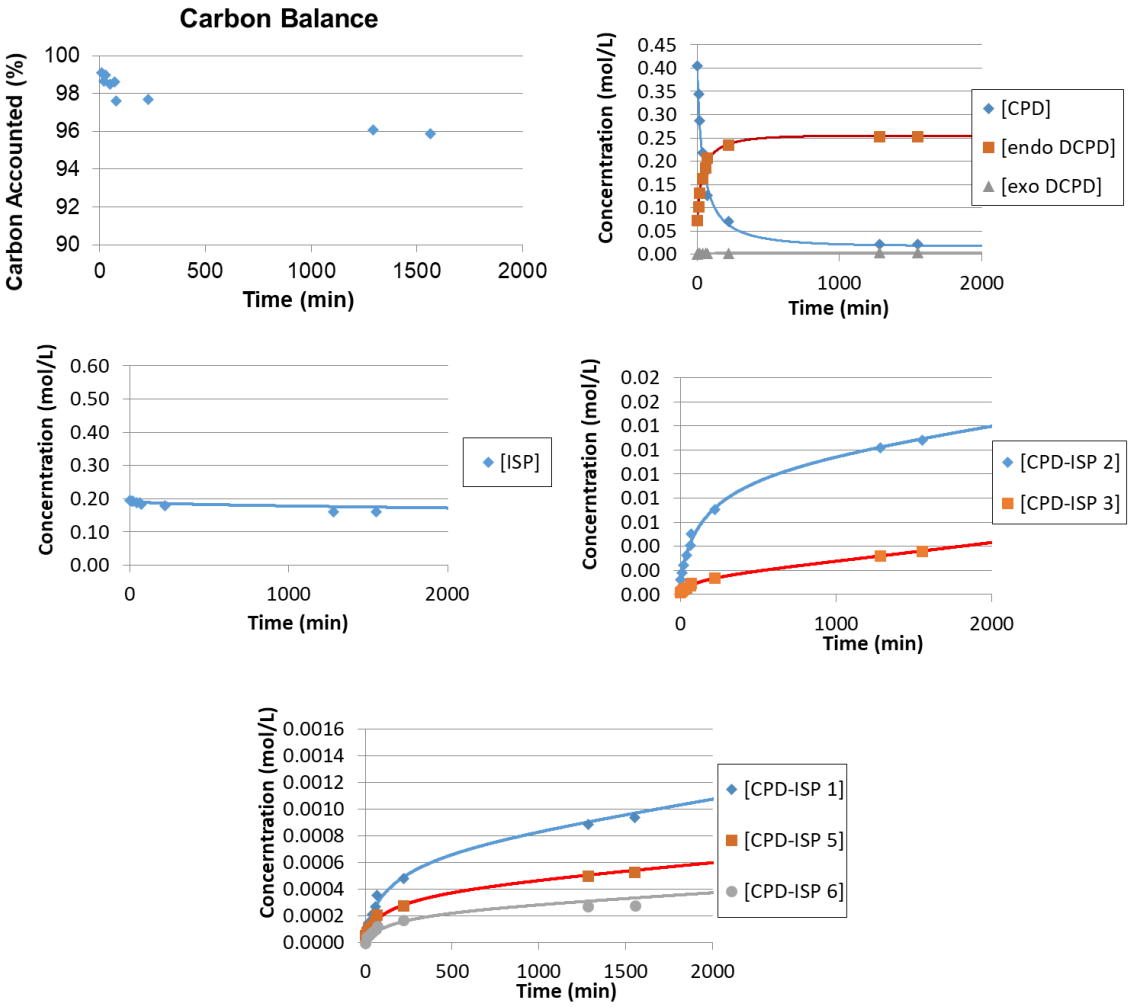

Figure 95: Cyclopentadiene-isoprene co-dimerization in absence of air at 120 °C – Run 2.

Table 24: Fitted Rate Constants for Cyclopentadiene-Isoprene Co-dimerization in Absence of Air at 120 °C – Run 2

$K_{CPD-ISP1}$	$7.34 \cdot 10^{-5}$ 1/M·min
$K_{CPD-ISP2}$	$1.04 \cdot 10^{-3}$ 1/M·min
$K_{CPD-ISP3}$	$1.87 \cdot 10^{-4}$ 1/M·min
$K_{CPD-ISP5}$	$3.99 \cdot 10^{-5}$ 1/M·min
$K_{CPD-ISP6}$	$2.71 \cdot 10^{-5}$ 1/M·min
$K_{CI2-CI3}$	$7.26 \cdot 10^{-5}$ 1/M·min

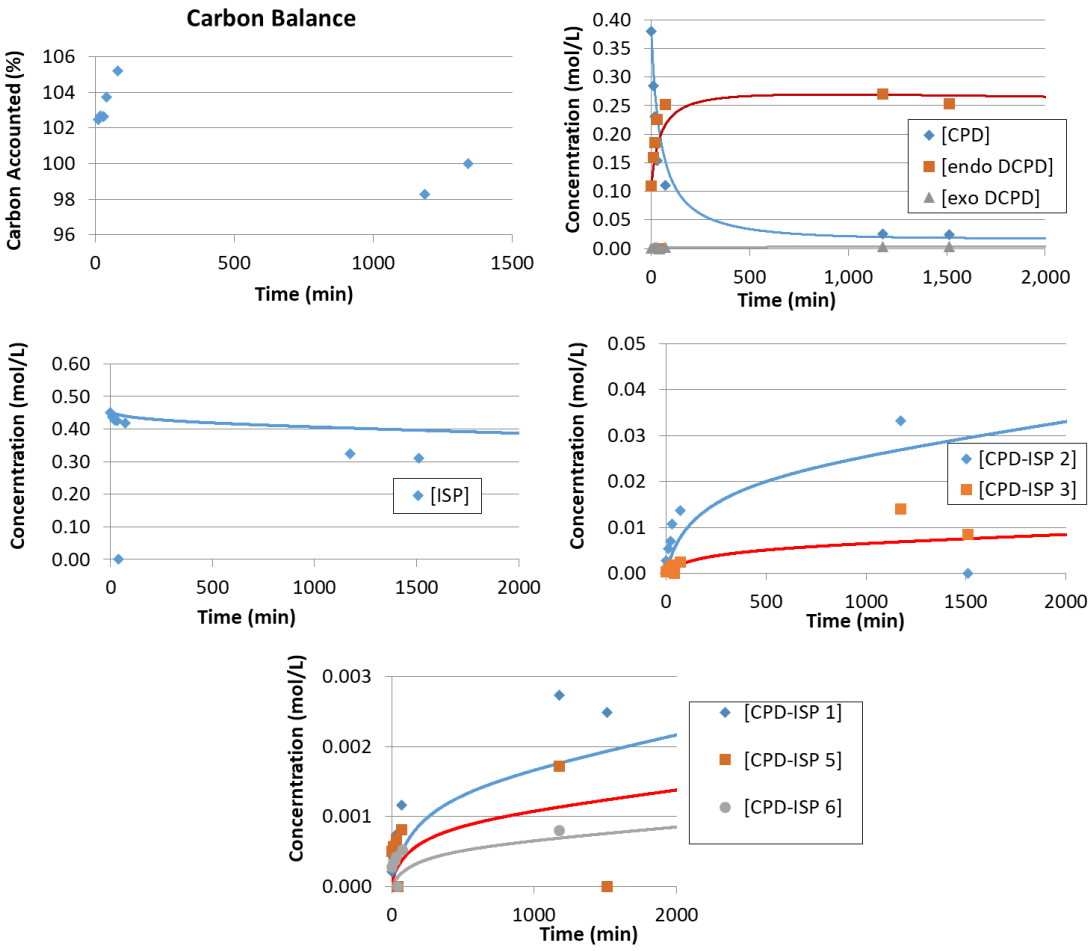

Figure 96: Cyclopentadiene-isoprene co-dimerization in absence of air at 130 °C – Run 1.

Table 25: Fitted Rate Constants for Cyclopentadiene-Isoprene Co-dimerization in Absence of Air at 130 °C – Run 1

$K_{CPD-ISP1}$	$6.71 \cdot 10^{-5}$ 1/M·min
$K_{CPD-ISP2}$	$1.01 \cdot 10^{-3}$ 1/M·min
$K_{CPD-ISP3}$	$2.62 \cdot 10^{-4}$ 1/M·min
$K_{CPD-ISP5}$	$4.03 \cdot 10^{-5}$ 1/M·min
$K_{CPD-ISP6}$	$2.62 \cdot 10^{-5}$ 1/M·min
$K_{CI2-CI3}$	--

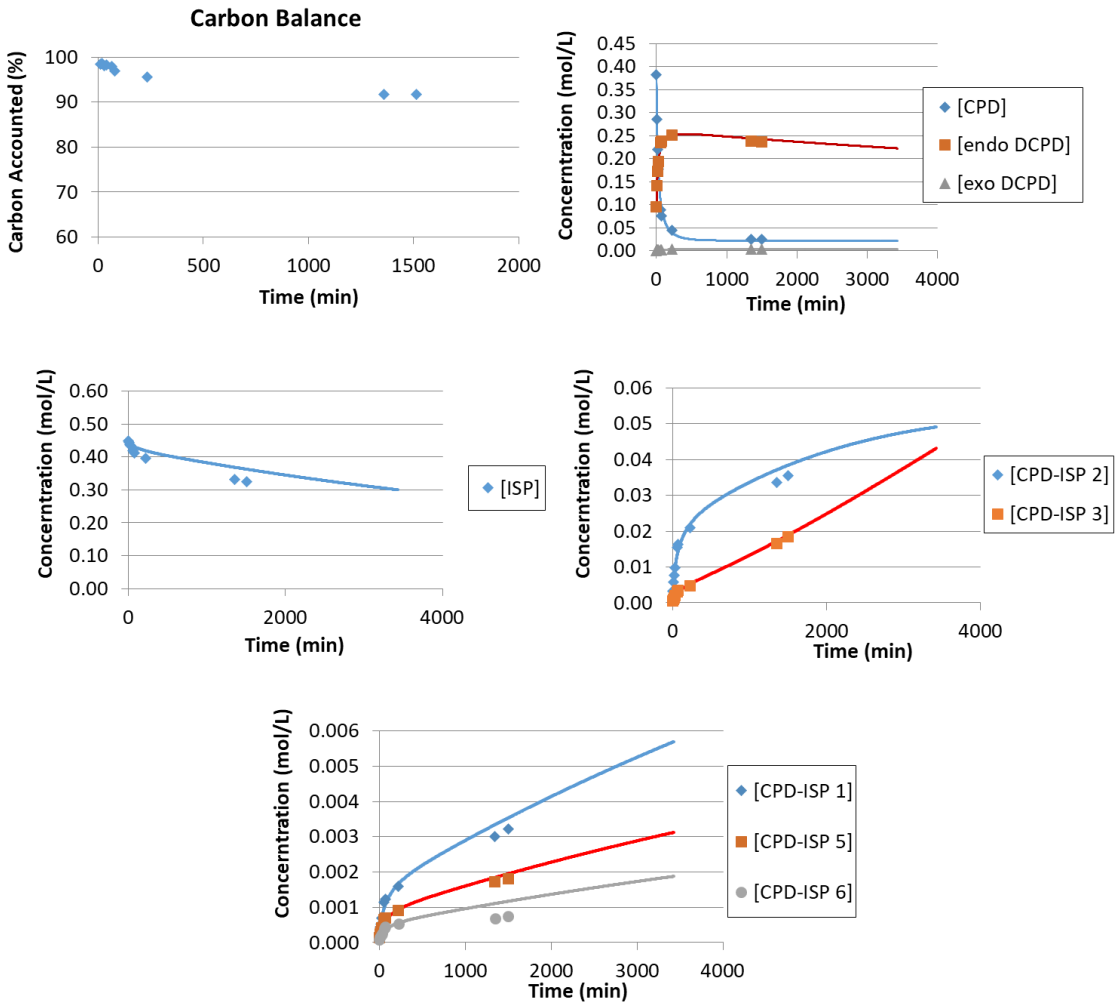

Figure 97: Cyclopentadiene-isoprene co-dimerization in absence of air at 130 °C – Run 2.

Table 26: Fitted Rate Constants for Cyclopentadiene-Isoprene Co-dimerization in Absence of Air at 130 °C – Run 2

$K_{CPD-ISP1}$	$1.55 \cdot 10^{-4}$ 1/M·min
$K_{CPD-ISP2}$	$2.08 \cdot 10^{-3}$ 1/M·min
$K_{CPD-ISP3}$	$4.18 \cdot 10^{-4}$ 1/M·min
$K_{CPD-ISP5}$	$8.41 \cdot 10^{-5}$ 1/M·min
$K_{CPD-ISP6}$	$5.07 \cdot 10^{-5}$ 1/M·min
$K_{CI2-CI3}$	$2.14 \cdot 10^{-4}$ 1/M·min

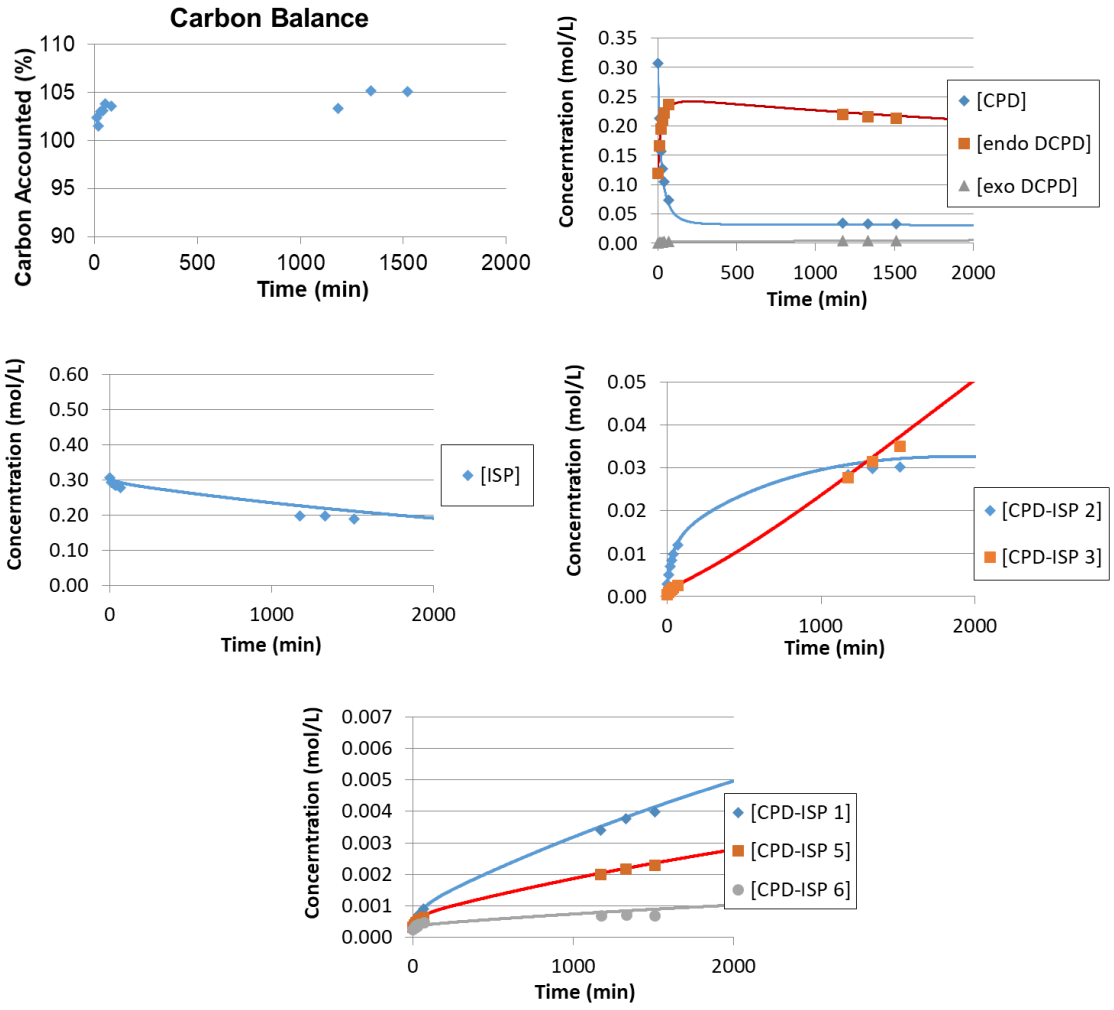

Figure 98: Cyclopentadiene-isoprene co-dimerization in absence of air at 140 °C – Run 1.

Table 27: Fitted Rate Constants for Cyclopentadiene-Isoprene Co-dimerization in Absence of Air at 140 °C – Run 1

$K_{CPD-ISP1}$	$2.68 \cdot 10^{-4}$ 1/M·min
$K_{CPD-ISP2}$	$3.86 \cdot 10^{-3}$ 1/M·min
$K_{CPD-ISP3}$	$6.54 \cdot 10^{-4}$ 1/M·min
$K_{CPD-ISP5}$	$1.39 \cdot 10^{-4}$ 1/M·min
$K_{CPD-ISP6}$	$4.26 \cdot 10^{-5}$ 1/M·min
$K_{CI2-CI3}$	$7.10 \cdot 10^{-4}$ 1/M·min

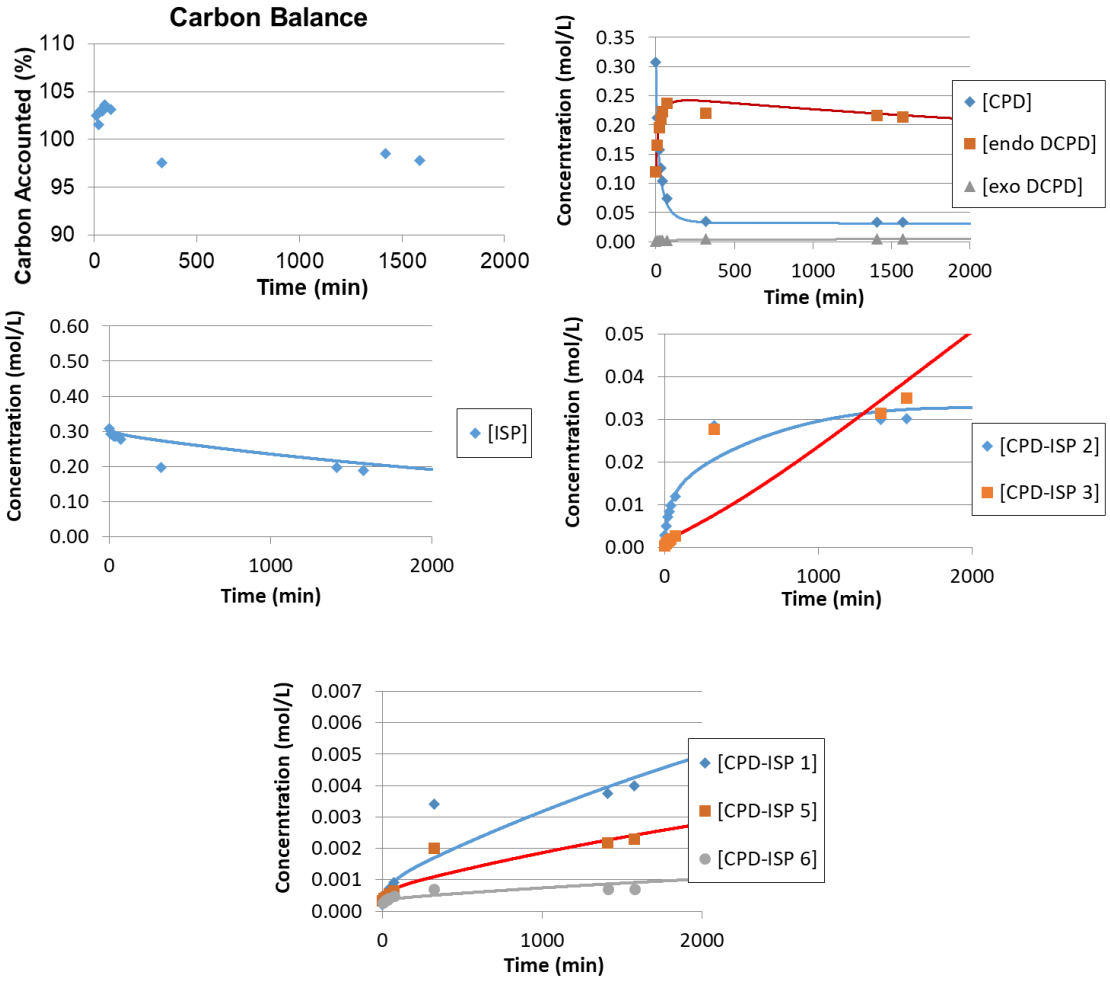

Figure 99: Cyclopentadiene-isoprene co-dimerization in absence of air at 140 °C – Run 2.

$K_{CPD-ISP1}$	$2.68 \cdot 10^{-4}$ 1/M·min
$K_{CPD-ISP2}$	$3.86 \cdot 10^{-3}$ 1/M·min
$K_{CPD-ISP3}$	$6.54 \cdot 10^{-4}$ 1/M·min
$K_{CPD-ISP5}$	$1.39 \cdot 10^{-4}$ 1/M·min
$K_{CPD-ISP6}$	$4.26 \cdot 10^{-5}$ 1/M·min
$K_{CI2-CI3}$	$7.10 \cdot 10^{-4}$ 1/M·min

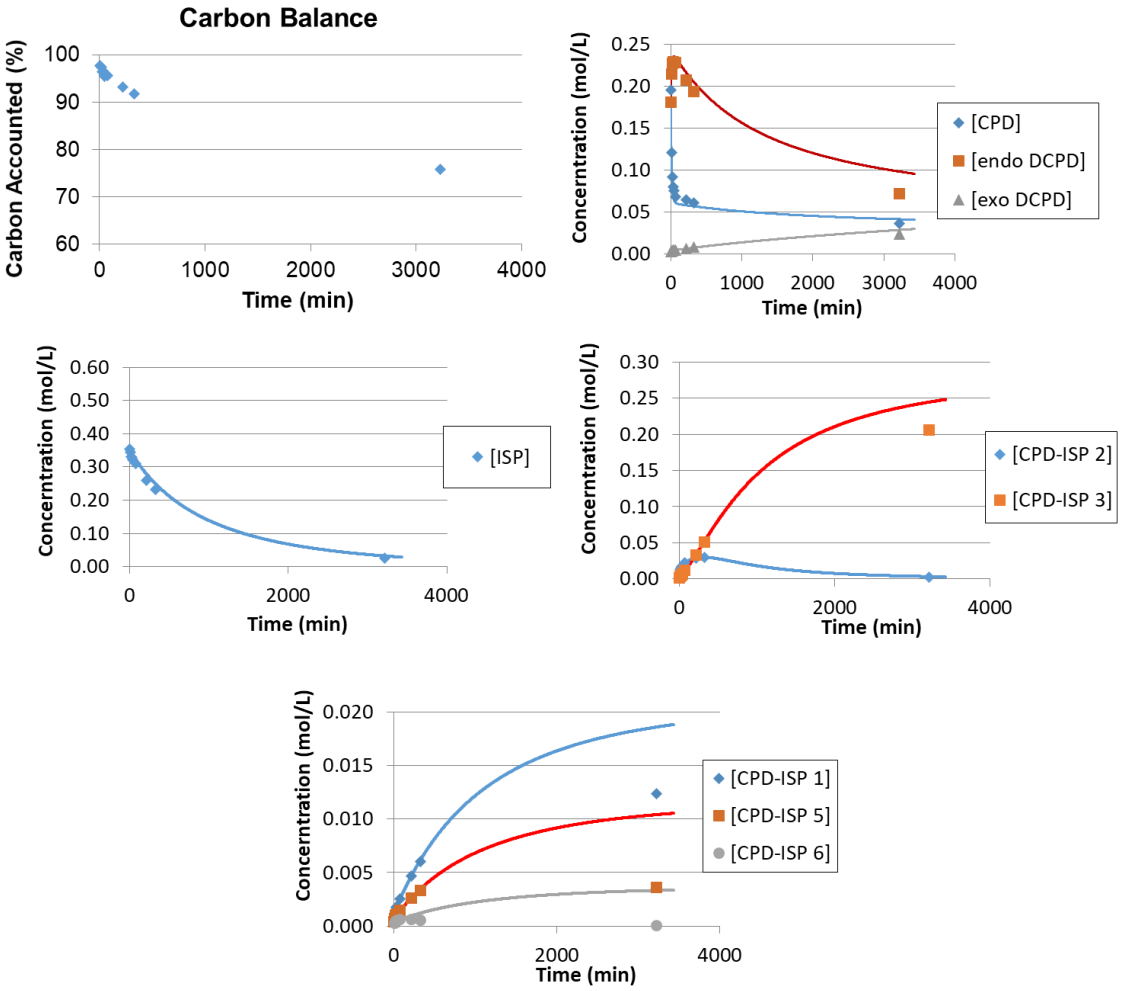

Figure 100: Cyclopentadiene-isoprene co-dimerization in absence of air at 160 °C – Run 1.

Table 28: Fitted Rate Constants for Cyclopentadiene-Isoprene Co-dimerization in Absence of Air at 160 °C – Run 1

$K_{CPD\text{-}ISP1}$	$8.92 \cdot 10^{-4}$ 1/M·min
$K_{CPD\text{-}ISP2}$	$9.94 \cdot 10^{-3}$ 1/M·min
$K_{CPD\text{-}ISP3}$	$1.92 \cdot 10^{-3}$ 1/M·min
$K_{CPD\text{-}ISP5}$	$4.98 \cdot 10^{-4}$ 1/M·min
$K_{CPD\text{-}ISP6}$	$1.53 \cdot 10^{-4}$ 1/M·min
$K_{CI2\text{-}CI3}$	$4.77 \cdot 10^{-3}$ 1/M·min

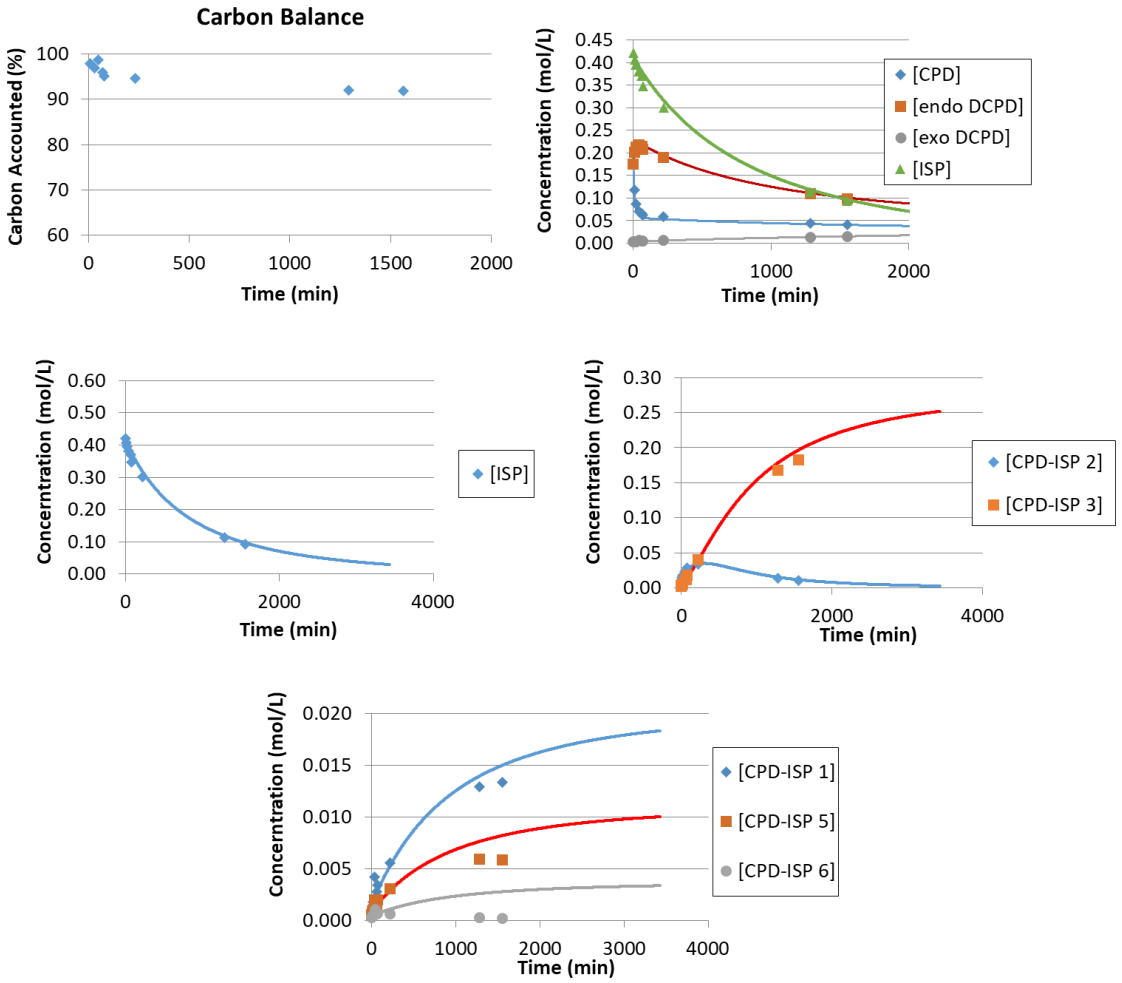

Figure 101: Cyclopentadiene-isoprene co-dimerization in absence of air at 160 °C – Run 2.

Table 29: Fitted Rate Constants for Cyclopentadiene-Isoprene Co-dimerization in Absence of Air at 160 °C – Run 2

$K_{CPD-ISP1}$	$8.69 \cdot 10^{-4}$ 1/M·min
$K_{CPD-ISP2}$	$9.89 \cdot 10^{-3}$ 1/M·min
$K_{CPD-ISP3}$	$2.19 \cdot 10^{-3}$ 1/M·min
$K_{CPD-ISP5}$	$4.74 \cdot 10^{-4}$ 1/M·min
$K_{CPD-ISP6}$	$1.51 \cdot 10^{-4}$ 1/M·min
$K_{CI2-CI3}$	$4.25 \cdot 10^{-3}$ 1/M·min

B.9 Trans-1,3-pentadiene Self-Dimerization Experimental Data

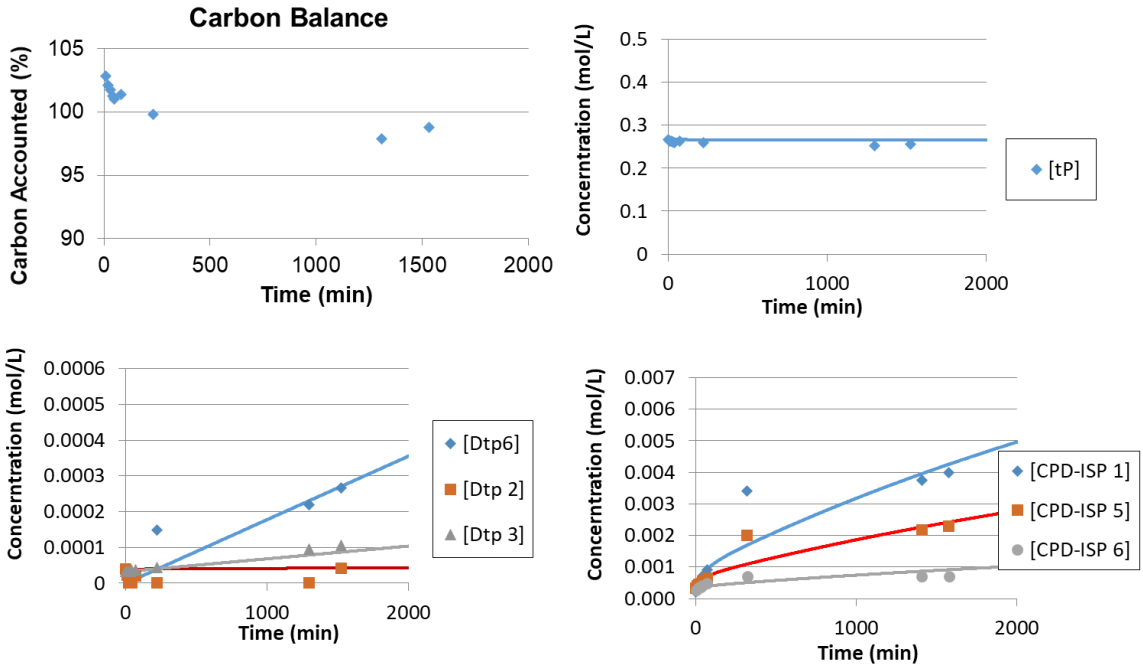

Figure 102: Trans-1,3-pentadiene dimerization in absence of air at 100 °C – Run 1.

Table 30: Fitted Rate Constants for Trans-1,3-pentadiene Dimerization in Absence of Air at 100 °C – Run 1

K_{Dtp1}	$1.27 \cdot 10^{-7}$ 1/M·min
K_{Dtp2}	$6.00 \cdot 10^{-8}$ 1/M·min
K_{Dtp3}	$1.00 \cdot 10^{-6}$ 1/M·min
K_{Dtp4}	--
K_{Dtp5}	$8.74 \cdot 10^{-8}$ 1/M·min
K_{Dtp6}	$5.00 \cdot 10^{-6}$ 1/M·min
K_{Dtp7}	$7.95 \cdot 10^{-9}$ 1/M·min

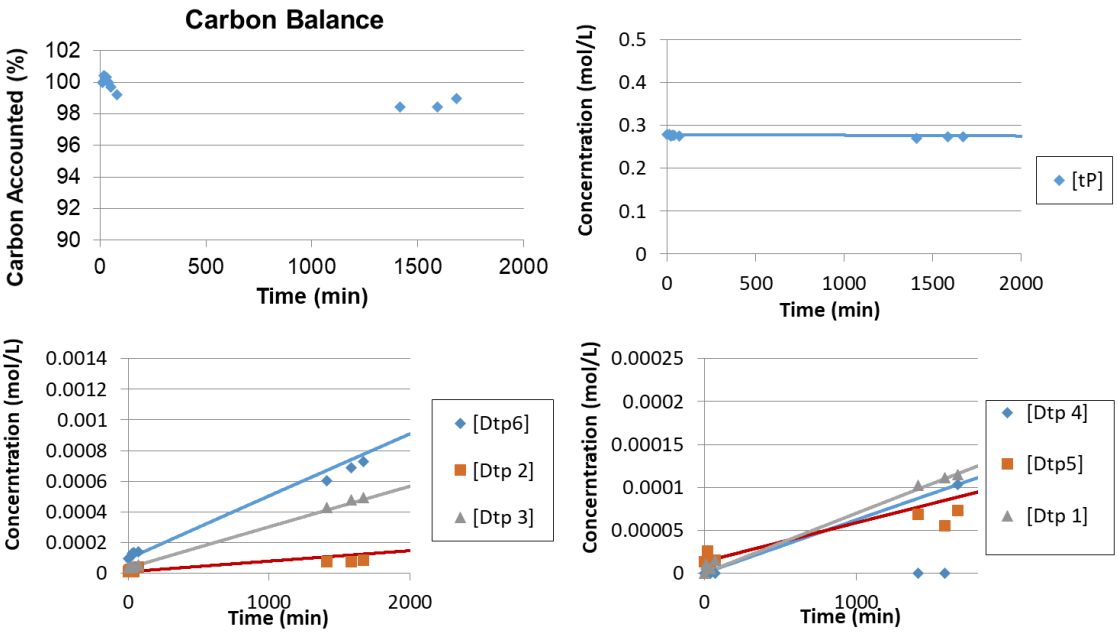

Figure 103: Trans-1,3-pentadiene dimerization in absence of air at 120 °C – Run 1.

Table 31: Fitted Rate Constants for Trans-1,3-pentadiene Dimerization in Absence of Air at 120 °C – Run 1

K_{Dtp1}	$1.80 \cdot 10^{-6}$ 1/M·min
K_{Dtp2}	$1.79 \cdot 10^{-6}$ 1/M·min
K_{Dtp3}	$6.93 \cdot 10^{-6}$ 1/M·min
K_{Dtp4}	$1.60 \cdot 10^{-6}$ 1/M·min
K_{Dtp5}	$1.17 \cdot 10^{-6}$ 1/M·min
K_{Dtp6}	$1.06 \cdot 10^{-5}$ 1/M·min
K_{Dtp7}	$3.00 \cdot 10^{-7}$ 1/M·min

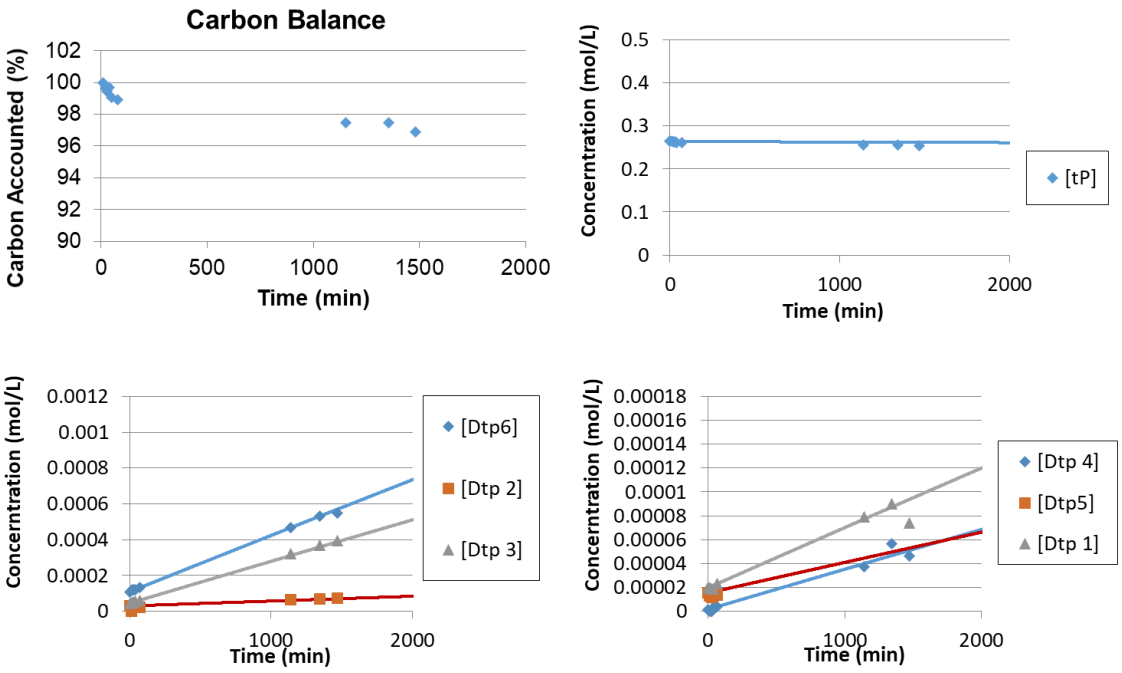

Figure 104: Trans-1,3-pentadiene dimerization in absence of air at 120 °C – Run 2.

Table 32: Fitted Rate Constants for Trans-1,3-pentadiene Dimerization in Absence of Air at 120 °C – Run 2

K_{Dtp1}	$1.46 \cdot 10^{-6}$ 1/M·min
K_{Dtp2}	$7.86 \cdot 10^{-7}$ 1/M·min
K_{Dtp3}	$6.74 \cdot 10^{-6}$ 1/M·min
K_{Dtp4}	$9.70 \cdot 10^{-7}$ 1/M·min
K_{Dtp5}	$7.38 \cdot 10^{-7}$ 1/M·min
K_{Dtp6}	$9.06 \cdot 10^{-6}$ 1/M·min
K_{Dtp7}	$3.00 \cdot 10^{-7}$ 1/M·min

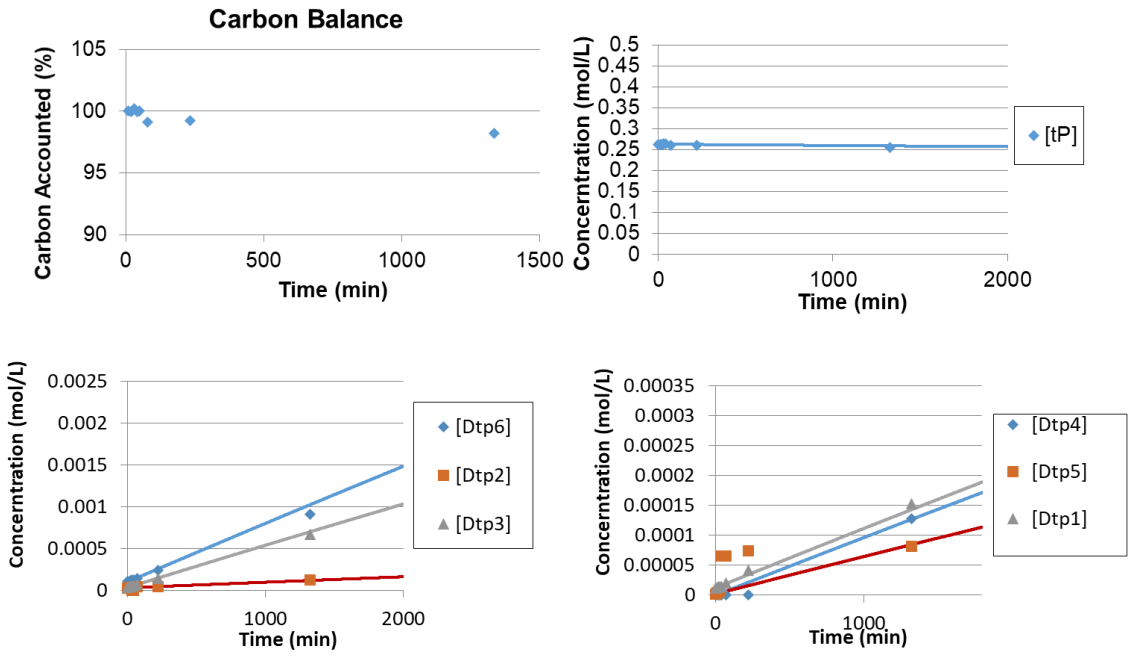

Figure 105: Trans-1,3-pentadiene dimerization in absence of air at 130 °C – Run 1.

Table 33: Fitted Rate Constants for Trans-1,3-pentadiene Dimerization in Absence of Air at 130 °C – Run 1

K_{Dtp1}	$2.90 \cdot 10^{-6}$ 1/M·min
K_{Dtp2}	$1.94 \cdot 10^{-6}$ 1/M·min
K_{Dtp3}	$1.47 \cdot 10^{-5}$ 1/M·min
K_{Dtp4}	$2.81 \cdot 10^{-6}$ 1/M·min
K_{Dtp5}	$1.83 \cdot 10^{-6}$ 1/M·min
K_{Dtp6}	$2.04 \cdot 10^{-5}$ 1/M·min
K_{Dtp7}	$8.54 \cdot 10^{-7}$ 1/M·min

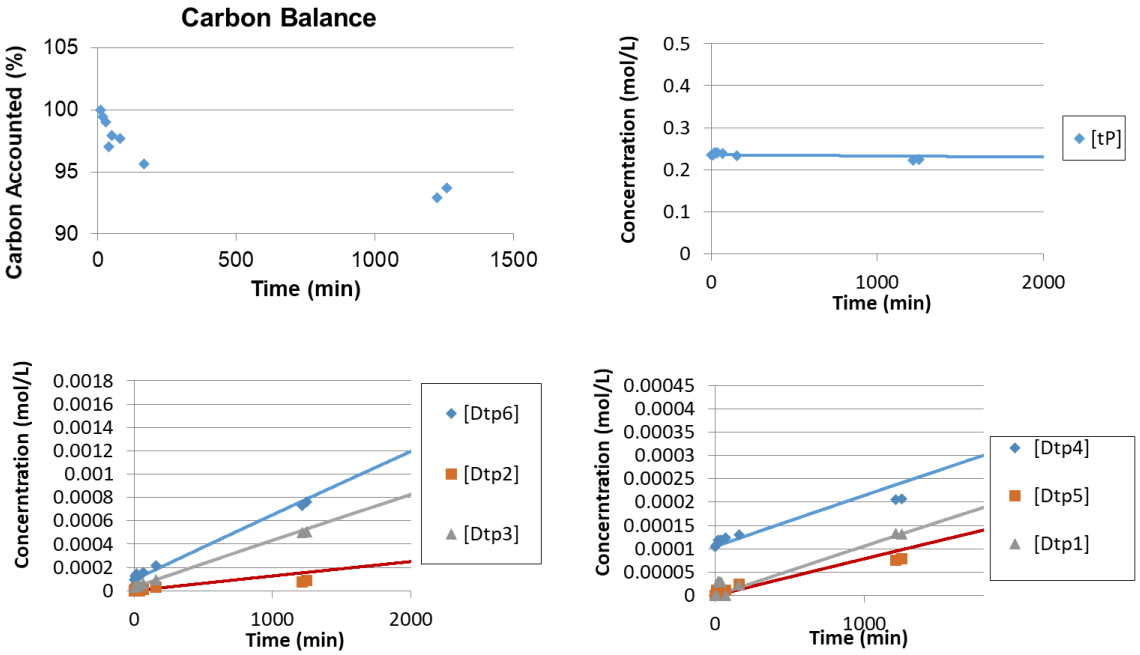

Figure 106: Trans-1,3-pentadiene dimerization in absence of air at 130 °C – Run 2.

Table 34: Fitted Rate Constants for Trans-1,3-pentadiene Dimerization in Absence of Air at 130 °C – Run 2

K_{Dtp1}	$3.86 \cdot 10^{-6}$ 1/M·min
K_{Dtp2}	$4.62 \cdot 10^{-6}$ 1/M·min
K_{Dtp3}	$1.47 \cdot 10^{-5}$ 1/M·min
K_{Dtp4}	$4.00 \cdot 10^{-6}$ 1/M·min
K_{Dtp5}	$2.87 \cdot 10^{-6}$ 1/M·min
K_{Dtp6}	$2.04 \cdot 10^{-5}$ 1/M·min
K_{Dtp7}	$8.54 \cdot 10^{-7}$ 1/M·min

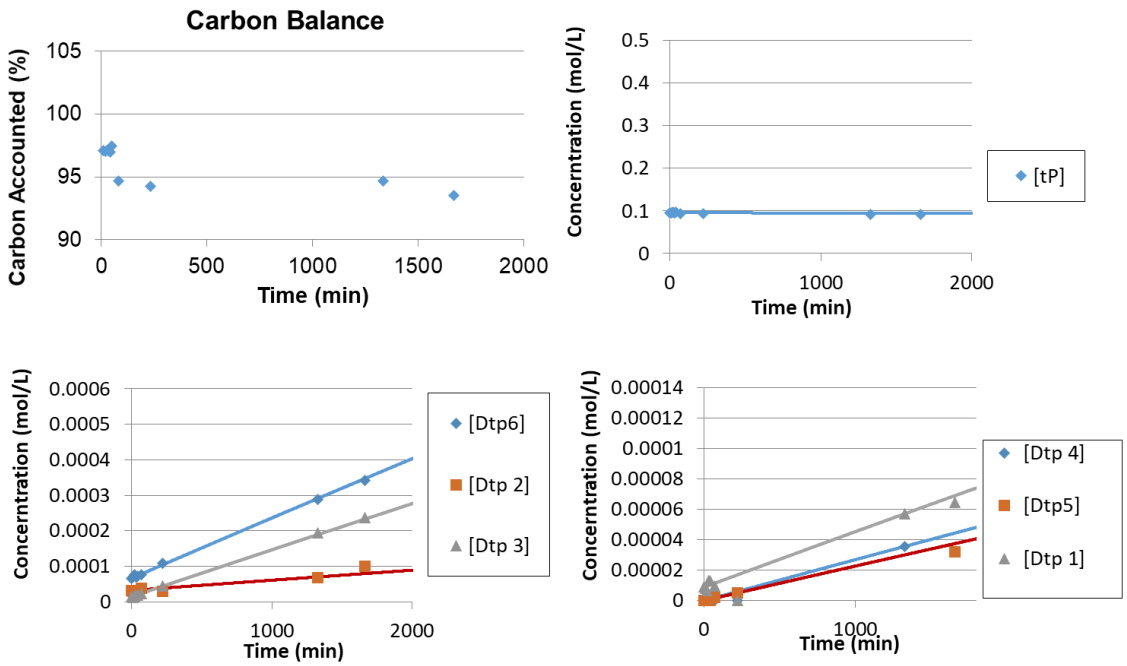

Figure 107: Trans-1,3-pentadiene dimerization in absence of air at 140 °C – Run 1.

Table 35: Fitted Rate Constants for Trans-1,3-pentadiene Dimerization in Absence of Air at 140 °C – Run 1

K_{Dtp1}	$8.00 \cdot 10^{-6}$ 1/M·min
K_{Dtp2}	$6.30 \cdot 10^{-6}$ 1/M·min
K_{Dtp3}	$2.91 \cdot 10^{-5}$ 1/M·min
K_{Dtp4}	$5.91 \cdot 10^{-6}$ 1/M·min
K_{Dtp5}	$4.99 \cdot 10^{-6}$ 1/M·min
K_{Dtp6}	$3.73 \cdot 10^{-5}$ 1/M·min
K_{Dtp7}	$2.00 \cdot 10^{-6}$ 1/M·min

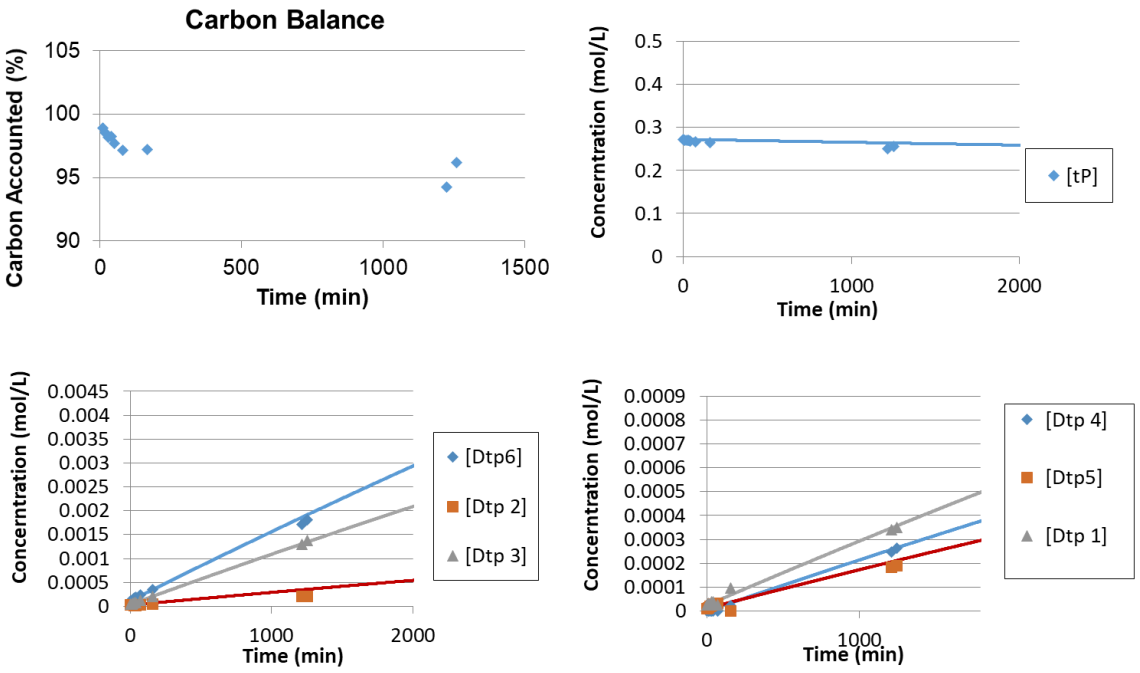

Figure 108: Trans-1,3-pentadiene dimerization in absence of air at 140 °C – Run 2.

Table 36: Fitted Rate Constants for Trans-1,3-pentadiene Dimerization in Absence of Air at 140 °C – Run 2

K_{Dtp1}	$7.40 \cdot 10^{-6}$ 1/M·min
K_{Dtp2}	$7.34 \cdot 10^{-6}$ 1/M·min
K_{Dtp3}	$2.91 \cdot 10^{-5}$ 1/M·min
K_{Dtp4}	$5.90 \cdot 10^{-6}$ 1/M·min
K_{Dtp5}	$4.46 \cdot 10^{-6}$ 1/M·min
K_{Dtp6}	$4.00 \cdot 10^{-5}$ 1/M·min
K_{Dtp7}	$2.08 \cdot 10^{-6}$ 1/M·min

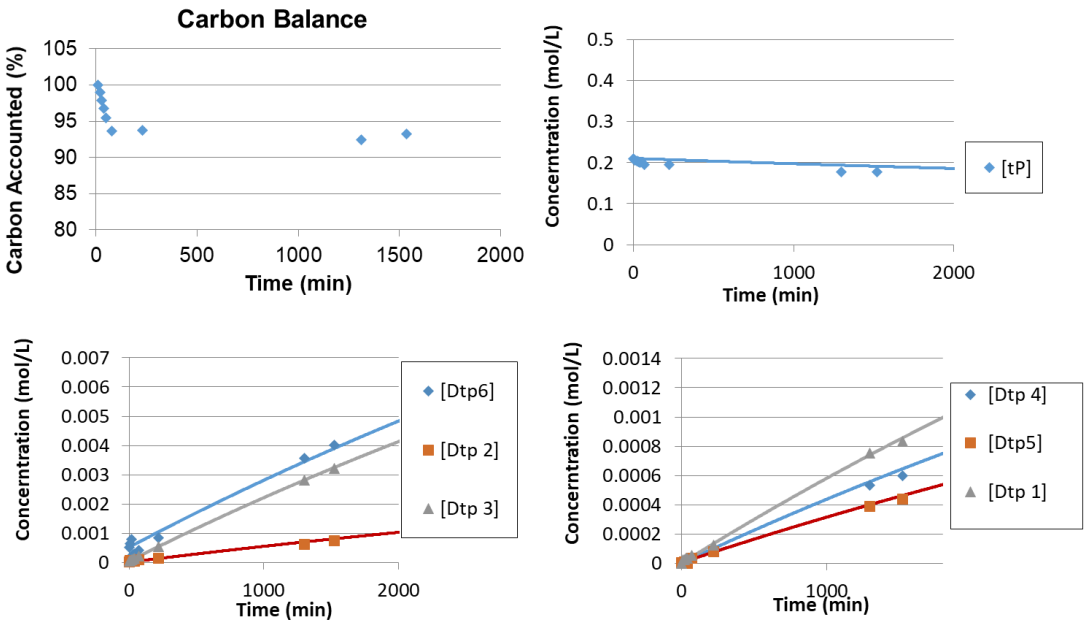

Figure 109: Trans-1,3-pentadiene dimerization in absence of air at 160 °C – Run 1.

Table 37: Fitted Rate Constants for Trans-1,3-pentadiene Dimerization in Absence of Air at 160 °C – Run 1

K_{Dtp1}	$2.79 \cdot 10^{-5}$ 1/M·min
K_{Dtp2}	$2.60 \cdot 10^{-5}$ 1/M·min
K_{Dtp3}	$1.04 \cdot 10^{-4}$ 1/M·min
K_{Dtp4}	$2.10 \cdot 10^{-5}$ 1/M·min
K_{Dtp5}	$1.49 \cdot 10^{-5}$ 1/M·min
K_{Dtp6}	$1.10 \cdot 10^{-4}$ 1/M·min
K_{Dtp7}	$1.00 \cdot 10^{-5}$ 1/M·min

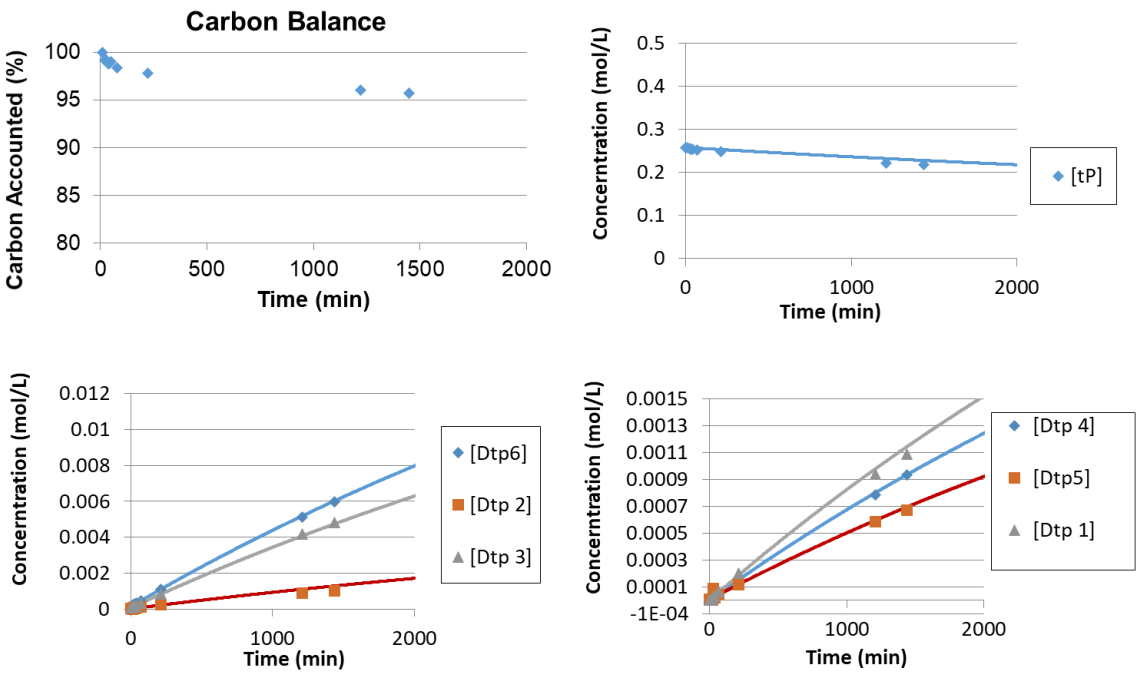

Figure 110: Trans-1,3-pentadiene dimerization in absence of air at 160 °C – Run 2.

Table 38: Fitted Rate Constants for Trans-1,3-pentadiene Dimerization in Absence of Air at 160 °C – Run 2

K_{Dtp1}	$2.70 \cdot 10^{-5}$ 1/M·min
K_{Dtp2}	$3.03 \cdot 10^{-5}$ 1/M·min
K_{Dtp3}	$1.11 \cdot 10^{-4}$ 1/M·min
K_{Dtp4}	$2.21 \cdot 10^{-5}$ 1/M·min
K_{Dtp5}	$1.63 \cdot 10^{-5}$ 1/M·min
K_{Dtp6}	$1.39 \cdot 10^{-4}$ 1/M·min
K_{Dtp7}	$1.10 \cdot 10^{-5}$ 1/M·min

B.10 Trans-1,3-pentadiene-Cyclopentadiene Co-dimerization Experimental Data

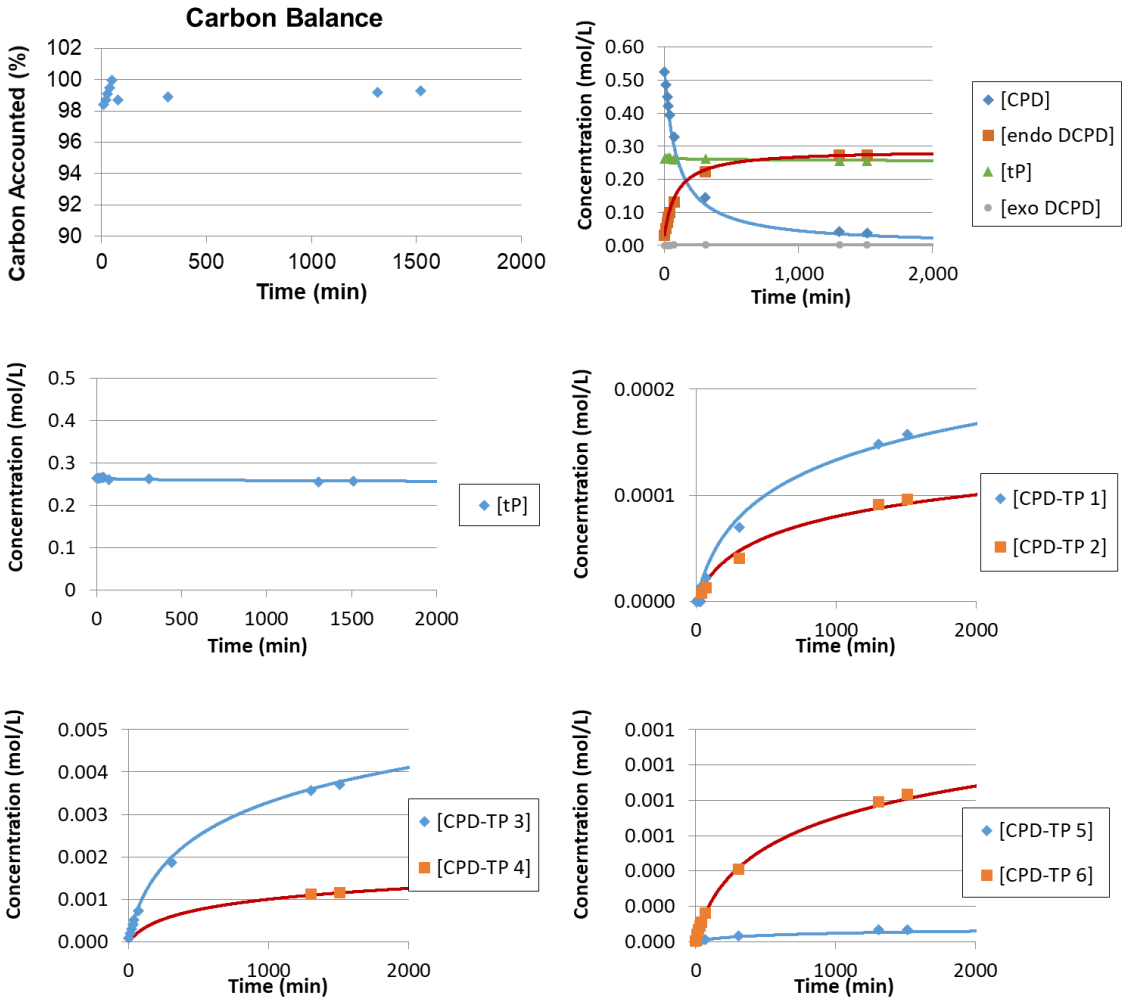

Figure 111: Cyclopentadiene-trans-1,3-pentadiene co-dimerization in absence of air at 100 °C – Run 1.

Table 39: Fitted Rate Constants for Cyclopentadiene-Trans-1,3-pentadiene Co-dimerization in Absence of Air at 100 °C – Run 1

K_{CPDtp1}	$4.21 \cdot 10^{-6}$ 1/M·min
K_{CPDtp2}	$2.52 \cdot 10^{-6}$ 1/M·min
K_{CPDtp3}	$1.01 \cdot 10^{-4}$ 1/M·min
K_{CPDtp4}	$3.15 \cdot 10^{-5}$ 1/M·min
K_{CPDtp5}	$1.49 \cdot 10^{-6}$ 1/M·min
K_{CPDtp6}	$2.20 \cdot 10^{-5}$ 1/M·min

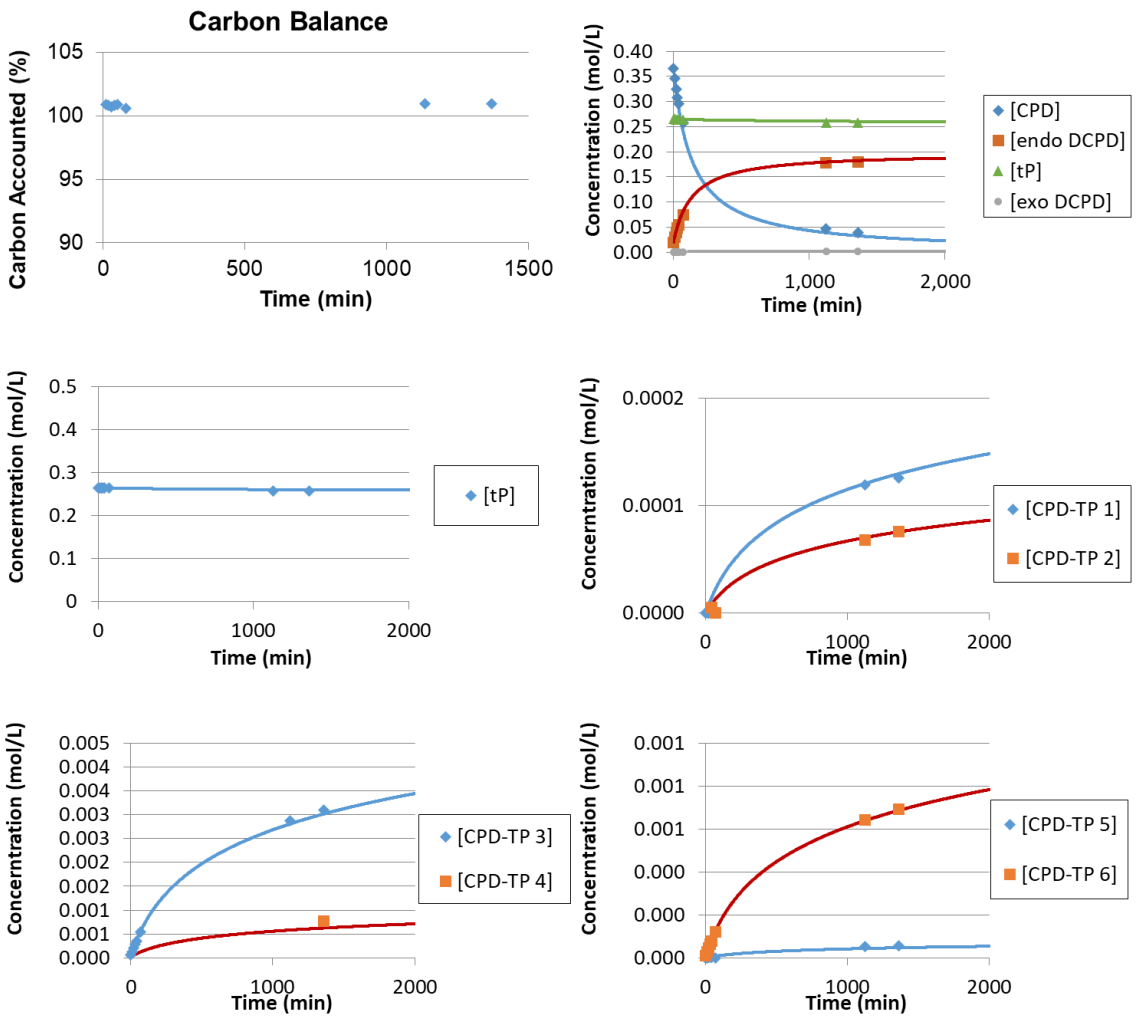

Figure 112: Cyclopentadiene-trans-1,3-pentadiene co-dimerization in absence of air at 100 °C – Run 2.

Table 40: Fitted Rate Constants for Cyclopentadiene-Trans-1,3-pentadiene Co-dimerization in Absence of Air at 100 °C – Run 2

K_{CPDtp1}	$4.16 \cdot 10^{-6}$ 1/M·min
K_{CPDtp2}	$2.42 \cdot 10^{-6}$ 1/M·min
K_{CPDtp3}	$9.50 \cdot 10^{-5}$ 1/M·min
K_{CPDtp4}	$1.93 \cdot 10^{-5}$ 1/M·min
K_{CPDtp5}	$1.51 \cdot 10^{-6}$ 1/M·min
K_{CPDtp6}	$2.17 \cdot 10^{-5}$ 1/M·min

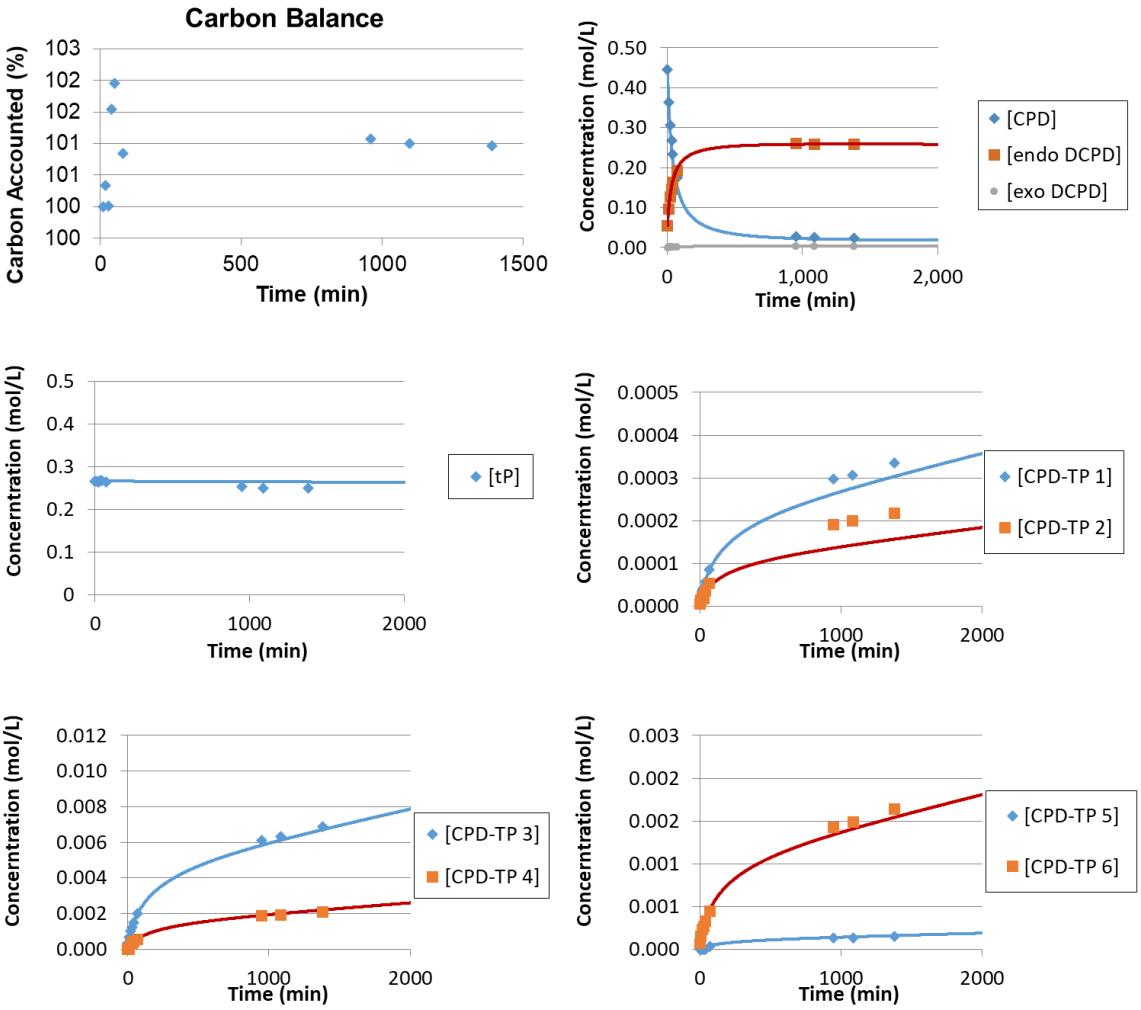

Figure 113: Cyclopentadiene-trans-1,3-pentadiene co-dimerization in absence of air at 120 °C – Run 1.

Table 41: Fitted Rate Constants for Cyclopentadiene-Trans-1,3-pentadiene Co-dimerization in Absence of Air at 120 °C – Run 1

K_{CPDtp1}	$1.69 \cdot 10^{-5}$ 1/M·min
K_{CPDtp2}	$8.59 \cdot 10^{-6}$ 1/M·min
K_{CPDtp3}	$3.64 \cdot 10^{-4}$ 1/M·min
K_{CPDtp4}	$1.26 \cdot 10^{-4}$ 1/M·min
K_{CPDtp5}	$9.06 \cdot 10^{-6}$ 1/M·min
K_{CPDtp6}	$8.38 \cdot 10^{-5}$ 1/M·min

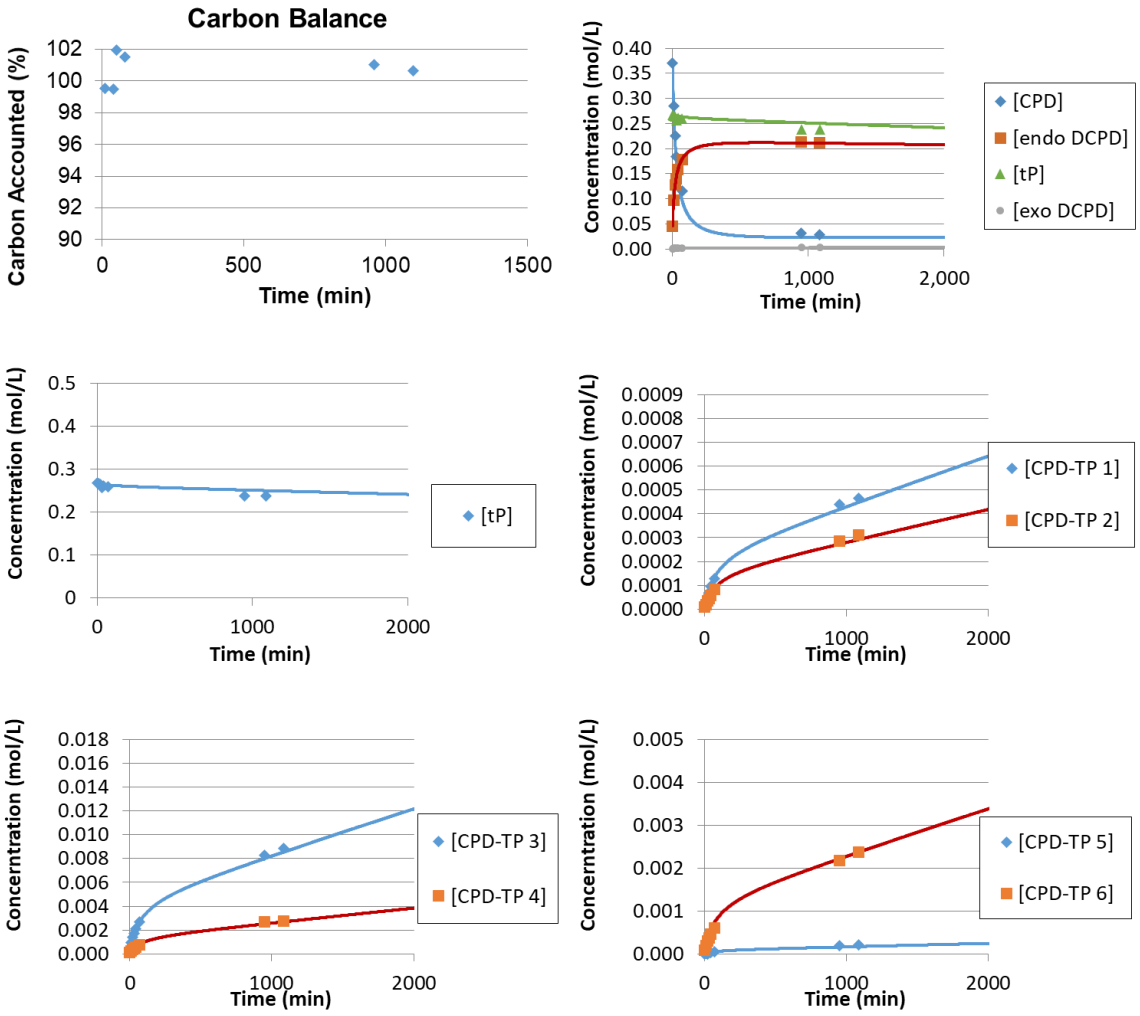

Figure 114: Cyclopentadiene-trans-1,3-pentadiene co-dimerization in absence of air at 130 °C – Run 1.

Table 42: Fitted Rate Constants for Cyclopentadiene-Trans-1,3-pentadiene Co-dimerization in Absence of Air at 130 °C – Run 1

K_{CPDtp1}	$3.83 \cdot 10^{-5}$ 1/M·min
K_{CPDtp2}	$2.49 \cdot 10^{-5}$ 1/M·min
K_{CPDtp3}	$7.13 \cdot 10^{-4}$ 1/M·min
K_{CPDtp4}	$2.27 \cdot 10^{-4}$ 1/M·min
K_{CPDtp5}	$1.47 \cdot 10^{-5}$ 1/M·min
K_{CPDtp6}	$2.00 \cdot 10^{-4}$ 1/M·min

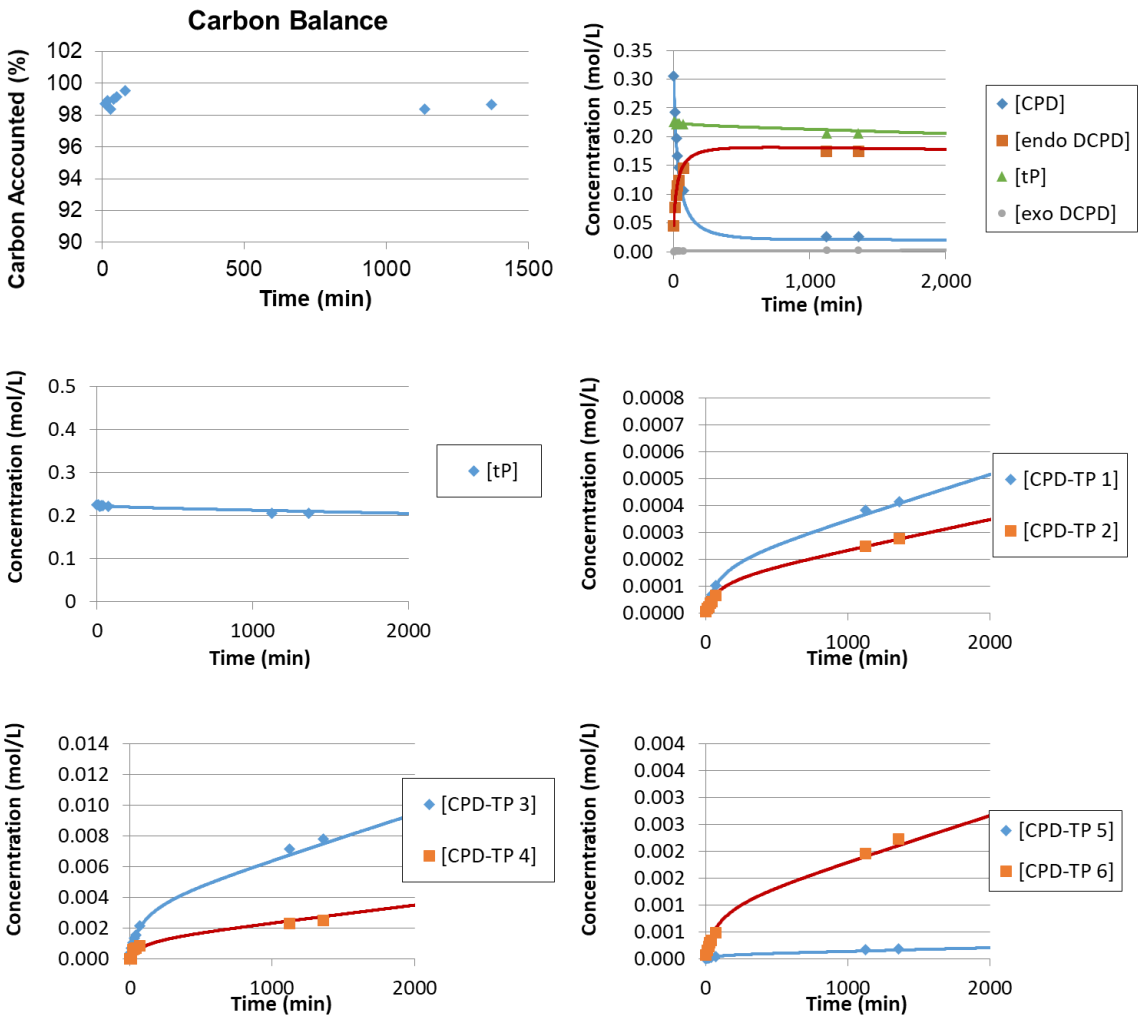

Figure 115: Cyclopentadiene-trans-1,3-pentadiene co-dimerization in absence of air at 130 °C – Run 2.

Table 43: Fitted Rate Constants for Cyclopentadiene-Trans-1,3-pentadiene Co-dimerization in Absence of Air at 130 °C – Run 2

K_{CPDtp1}	$3.89 \cdot 10^{-5}$ 1/M·min
K_{CPDtp2}	$2.62 \cdot 10^{-5}$ 1/M·min
K_{CPDtp3}	$6.97 \cdot 10^{-4}$ 1/M·min
K_{CPDtp4}	$2.67 \cdot 10^{-4}$ 1/M·min
K_{CPDtp5}	$1.54 \cdot 10^{-5}$ 1/M·min
K_{CPDtp6}	$1.98 \cdot 10^{-4}$ 1/M·min

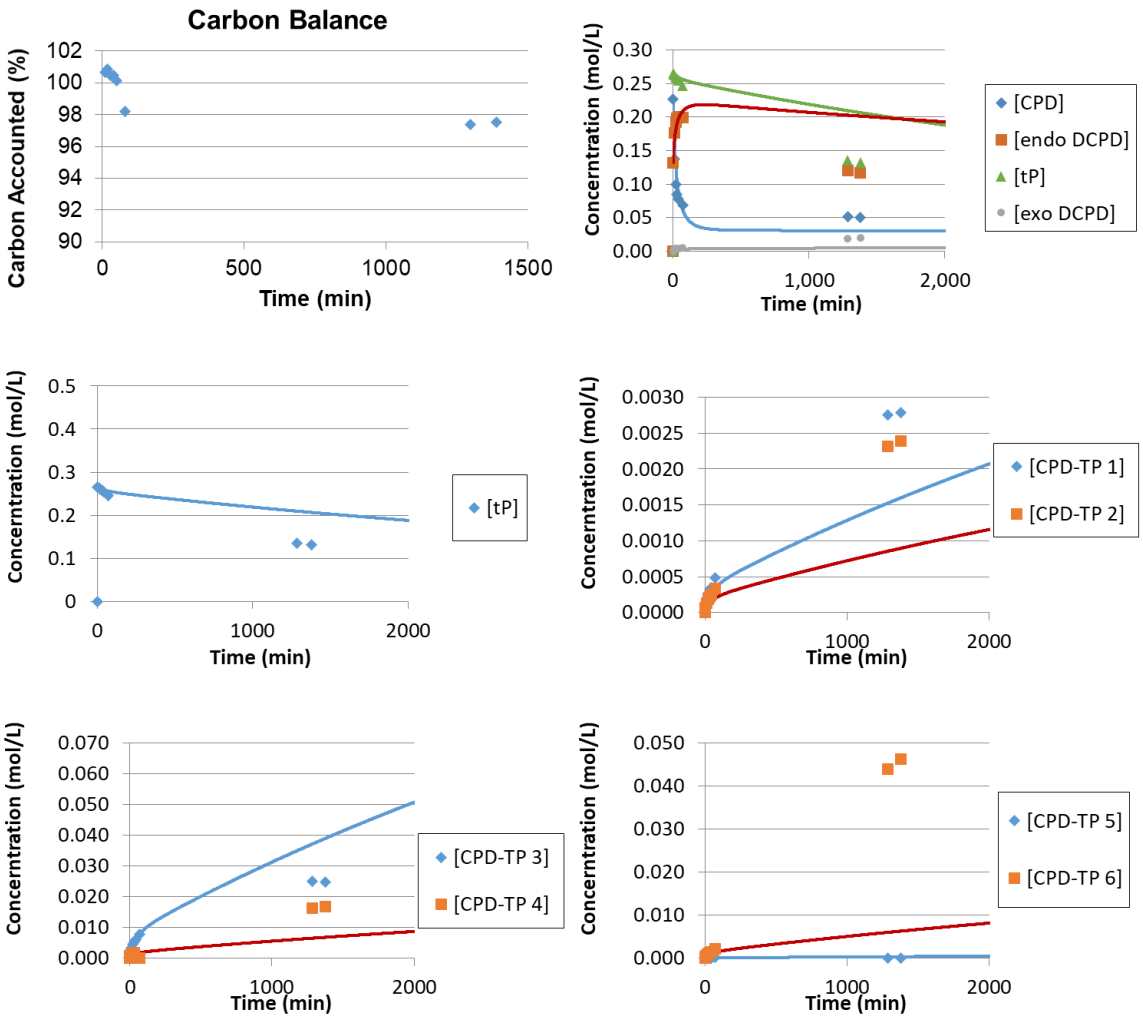

Figure 116: Cyclopentadiene-trans-1,3-pentadiene co-dimerization in absence of air at 140 °C – Run 1.

Table 44: Fitted Rate Constants for Cyclopentadiene-Trans-1,3-pentadiene Co-dimerization in Absence of Air at 140 °C – Run 1

K_{CPDtp1}	$1.28 \cdot 10^{-4}$ 1/M·min
K_{CPDtp2}	$7.06 \cdot 10^{-5}$ 1/M·min
K_{CPDtp3}	$3.15 \cdot 10^{-3}$ 1/M·min
K_{CPDtp4}	$5.10 \cdot 10^{-4}$ 1/M·min
K_{CPDtp5}	$3.01 \cdot 10^{-5}$ 1/M·min
K_{CPDtp6}	$5.02 \cdot 10^{-4}$ 1/M·min

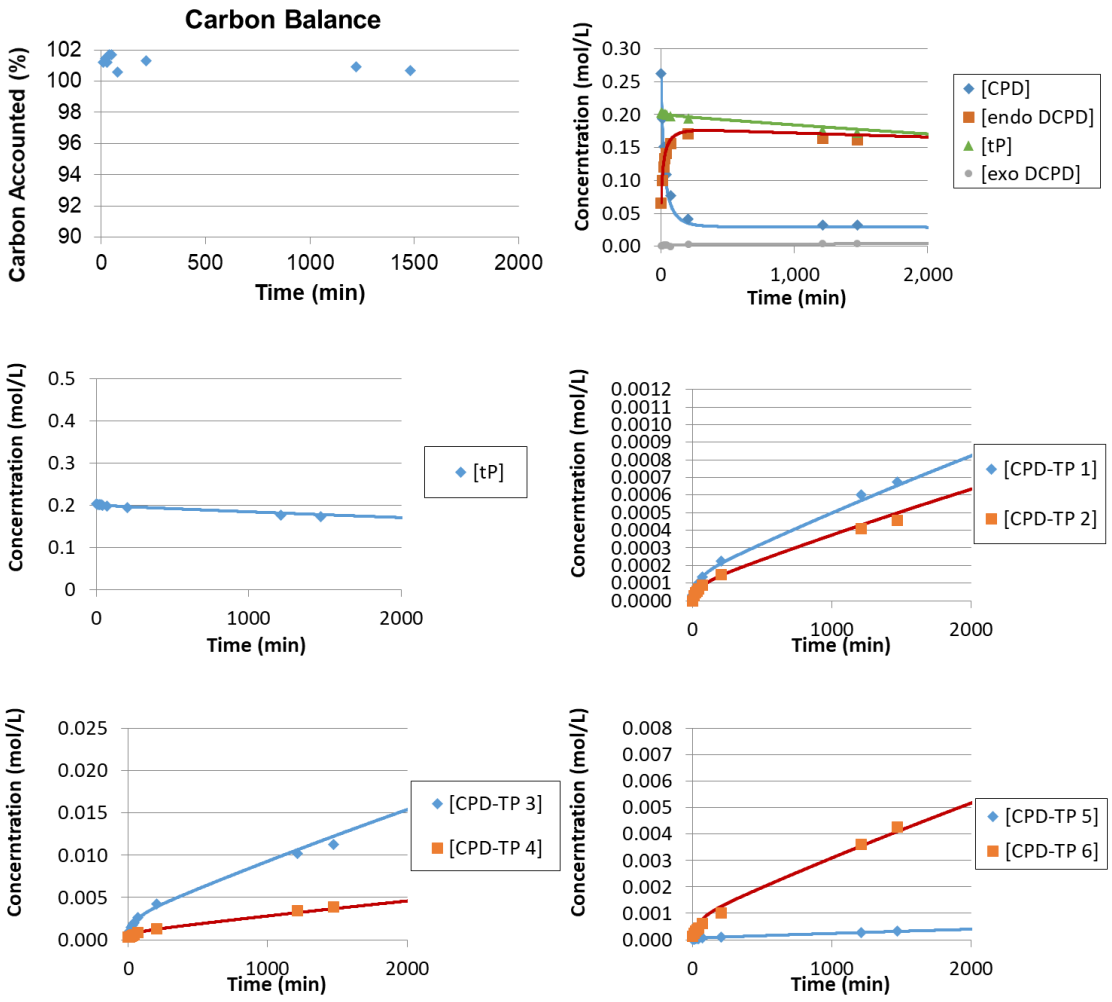

Figure 117: Cyclopentadiene-trans-1,3-pentadiene co-dimerization in absence of air at 140 °C – Run 2.

Table 45: Fitted Rate Constants for Cyclopentadiene-Trans-1,3-pentadiene Co-dimerization in Absence of Air at 140 °C – Run 2

K_{CPDtp1}	$6.29 \cdot 10^{-5}$ 1/M·min
K_{CPDtp2}	$5.04 \cdot 10^{-5}$ 1/M·min
K_{CPDtp3}	$1.18 \cdot 10^{-3}$ 1/M·min
K_{CPDtp4}	$3.43 \cdot 10^{-4}$ 1/M·min
K_{CPDtp5}	$3.09 \cdot 10^{-5}$ 1/M·min
K_{CPDtp6}	$4.03 \cdot 10^{-4}$ 1/M·min

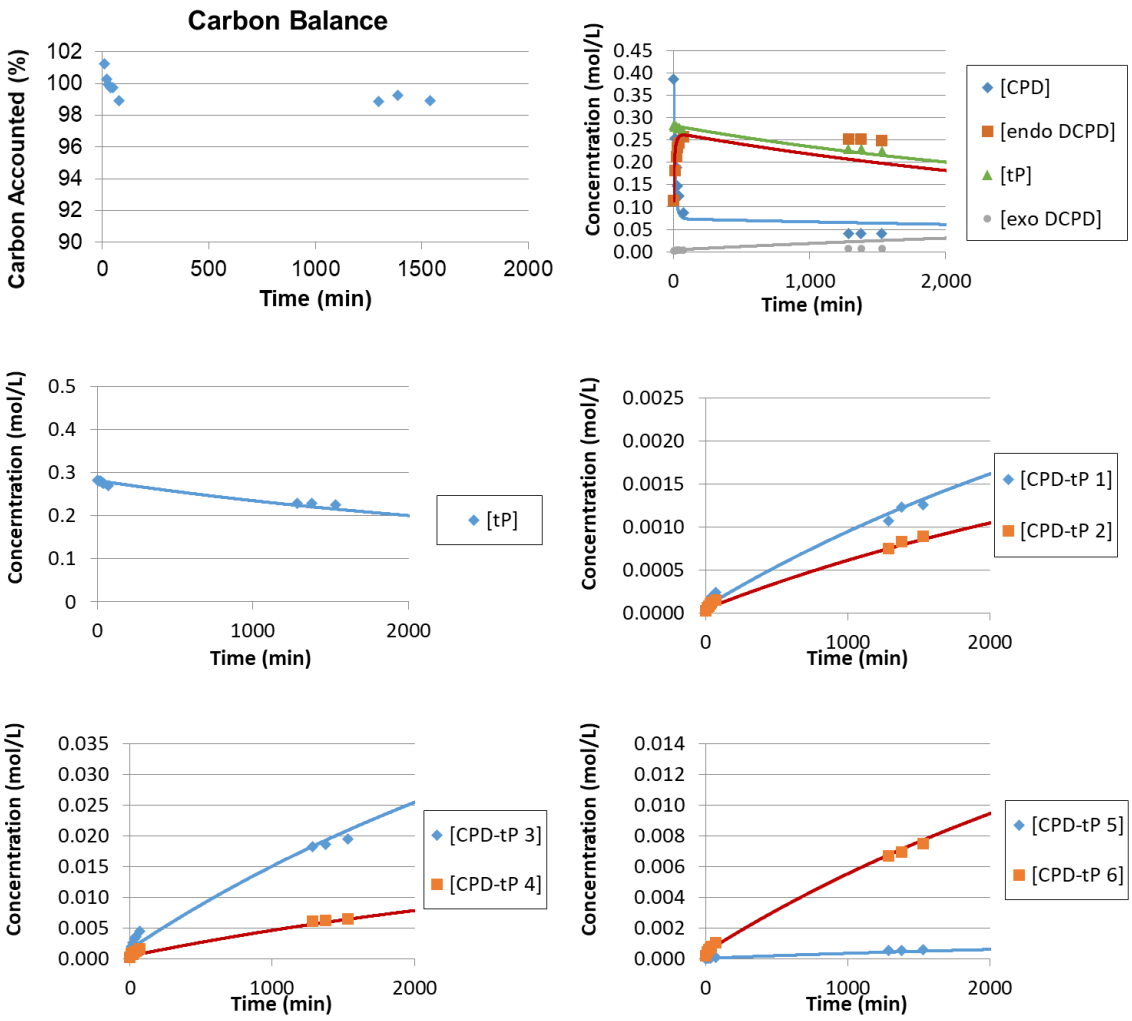

Figure 118: Cyclopentadiene-trans-1,3-pentadiene co-dimerization in absence of air at 160 °C – Run 1.

Table 46: Fitted Rate Constants for Cyclopentadiene-Trans-1,3-pentadiene Co-dimerization in Absence of Air at 160 °C – Run 1

K_{CPDtp1}	$4.82 \cdot 10^{-5}$ 1/M·min
K_{CPDtp2}	$3.12 \cdot 10^{-5}$ 1/M·min
K_{CPDtp3}	$7.46 \cdot 10^{-4}$ 1/M·min
K_{CPDtp4}	$2.31 \cdot 10^{-4}$ 1/M·min
K_{CPDtp5}	$1.81 \cdot 10^{-5}$ 1/M·min
K_{CPDtp6}	$2.81 \cdot 10^{-4}$ 1/M·min

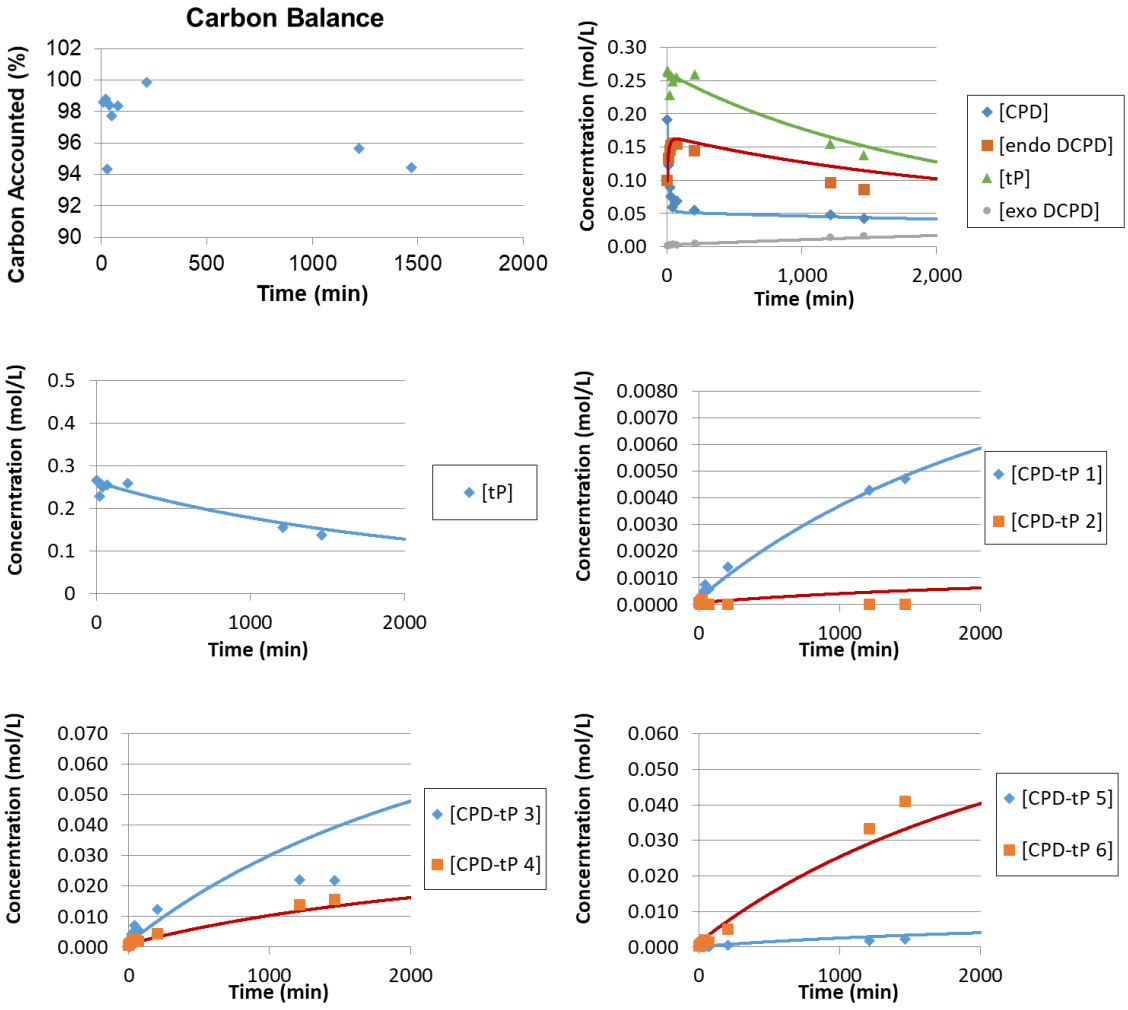

Figure 119: Fitted Rate Constants for Cyclopentadiene-Trans-1,3-pentadiene Co-dimerization in Absence of Air at 160 °C – Run 2

K_{CPDtp1}	$3.27 \cdot 10^{-4}$ 1/M·min
K_{CPDtp2}	$3.19 \cdot 10^{-5}$ 1/M·min
K_{CPDtp3}	$2.69 \cdot 10^{-3}$ 1/M·min
K_{CPDtp4}	$8.85 \cdot 10^{-4}$ 1/M·min
K_{CPDtp5}	$2.25 \cdot 10^{-4}$ 1/M·min
K_{CPDtp6}	$2.26 \cdot 10^{-3}$ 1/M·min

B.11 Cyclopentadiene-1-pentene Co-dimerization Experimental Data

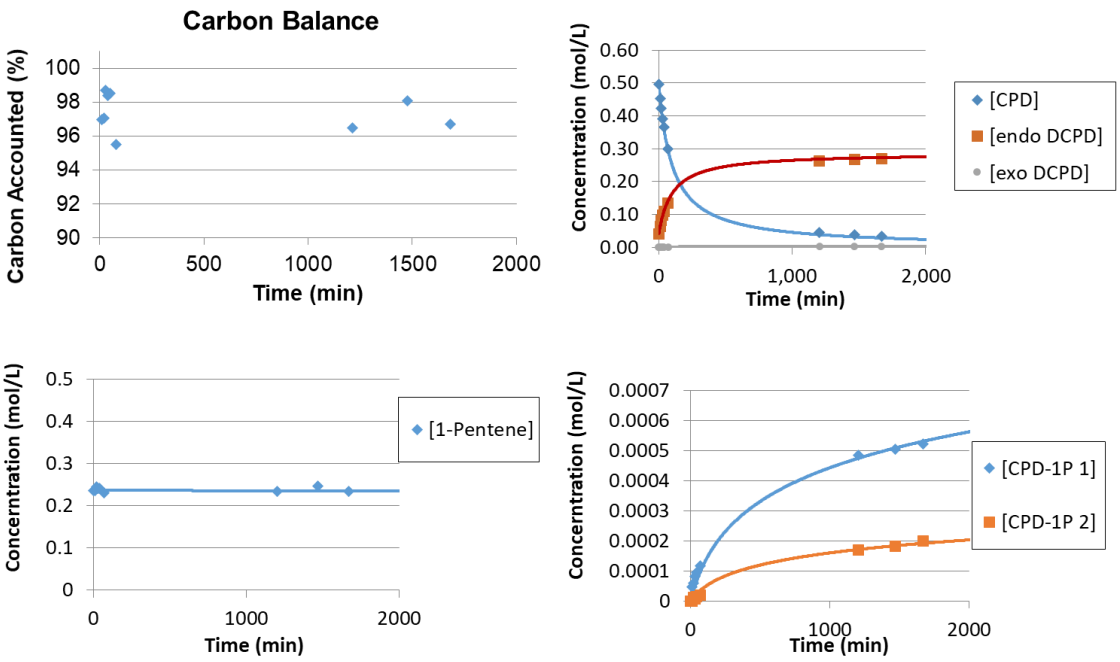

Figure 120: Cyclopentadiene-1-pentene co-dimerization in absence of air at 100 °C – Run 1.

Table 47: Fitted Rate Constants for Cyclopentadiene-1-Pentene Co-dimerization in Absence of Air at 100 °C – Run 1

K_{CPD1p1}	$1.57 \cdot 10^{-5}$ 1/M·min
K_{CPD1p2}	$5.66 \cdot 10^{-6}$ 1/M·min

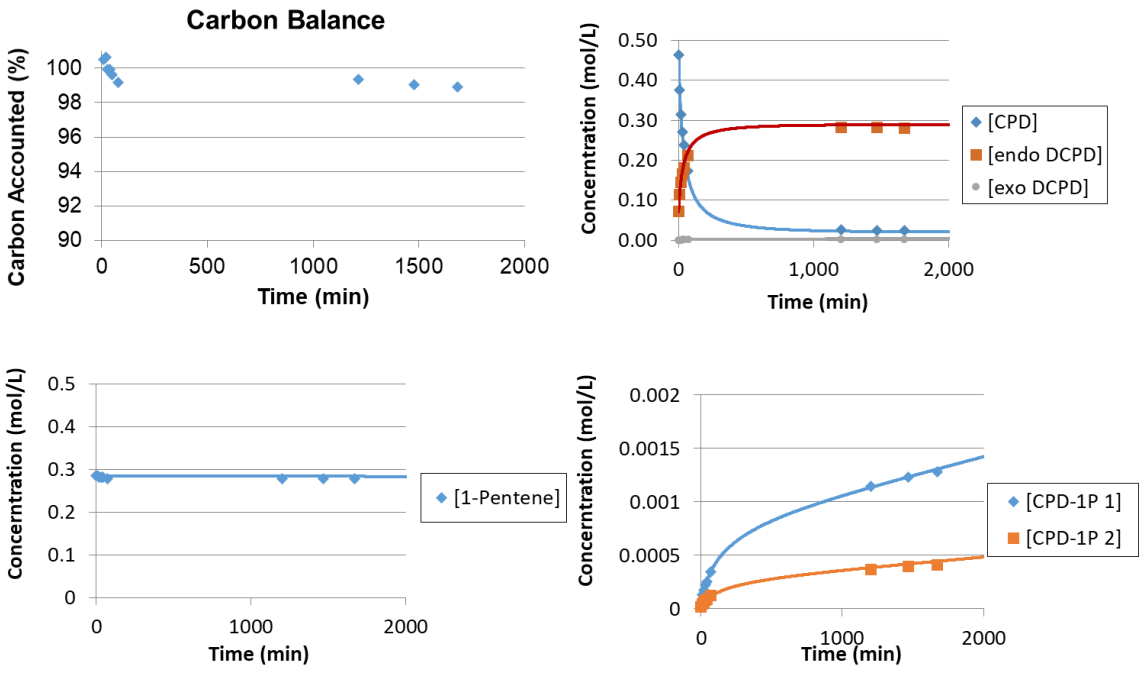

Figure 121: Cyclopentadiene-1-pentene co-dimerization in absence of air at 120 °C – Run 1.

Table 48: Fitted Rate Constants for Cyclopentadiene-1-Pentene Co-dimerization in Absence of Air at 120 °C – Run 1

K_{CPD1p1}	$5.86 \cdot 10^{-5}$ 1/M·min
K_{CPD1p2}	$2.00 \cdot 10^{-5}$ 1/M·min

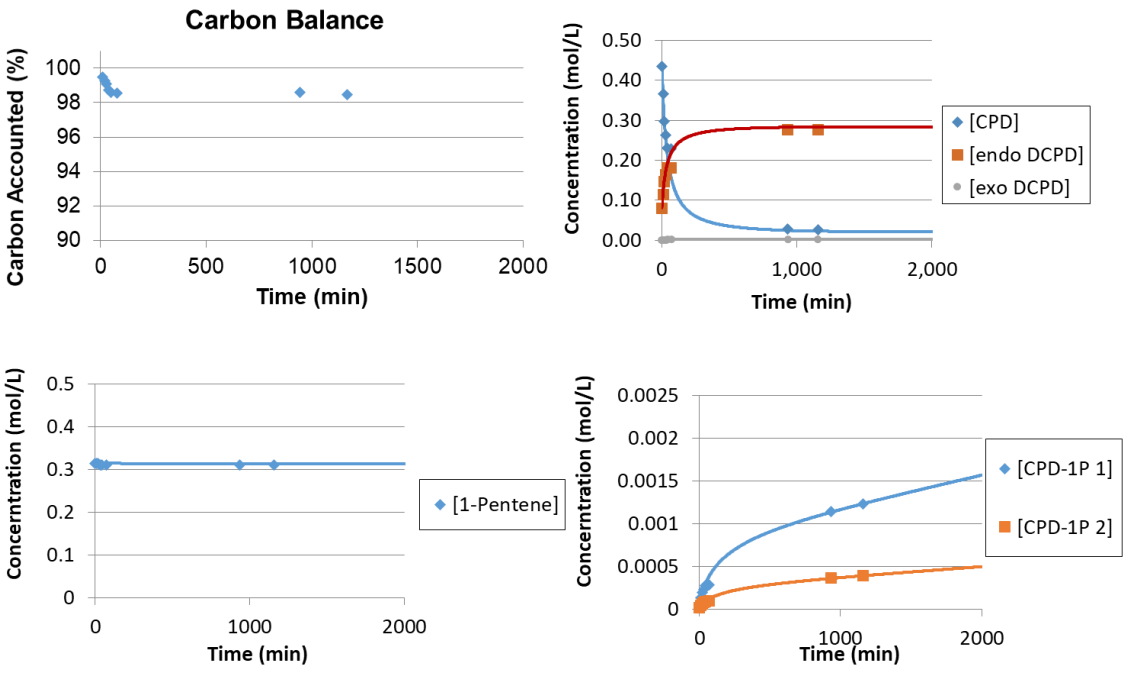

Figure 122: Cyclopentadiene-1-pentene co-dimerization in absence of air at 120 °C – Run 2.

Table 49: Fitted Rate Constants for Cyclopentadiene-1-Pentene Co-dimerization in Absence of Air at 120 °C – Run 2

K_{CPD1p1}	$5.88 \cdot 10^{-5}$ 1/M·min
K_{CPD1p2}	$1.88 \cdot 10^{-5}$ 1/M·min

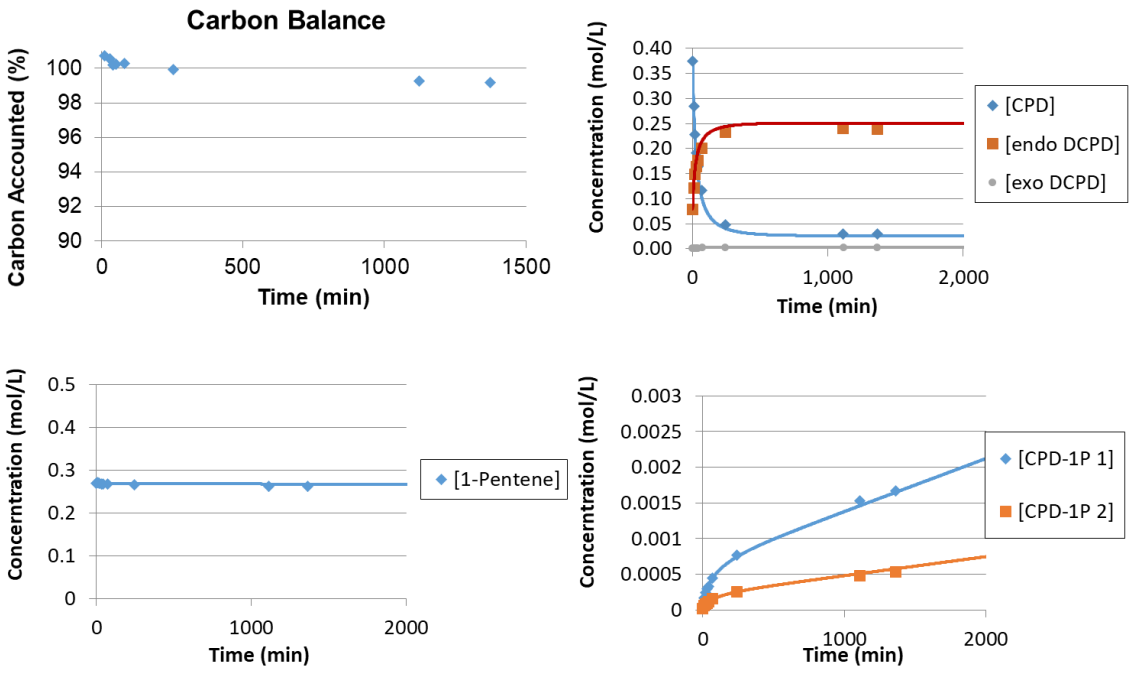

Figure 123: Cyclopentadiene-1-pentene co-dimerization in absence of air at 130 °C – Run 1.

Table 50: Fitted Rate Constants for Cyclopentadiene-1-Pentene Co-dimerization in Absence of Air at 130 °C – Run 1

K_{CPD1p1}	$1.07 \cdot 10^{-4}$ 1/M·min
K_{CPD1p2}	$3.85 \cdot 10^{-5}$ 1/M·min

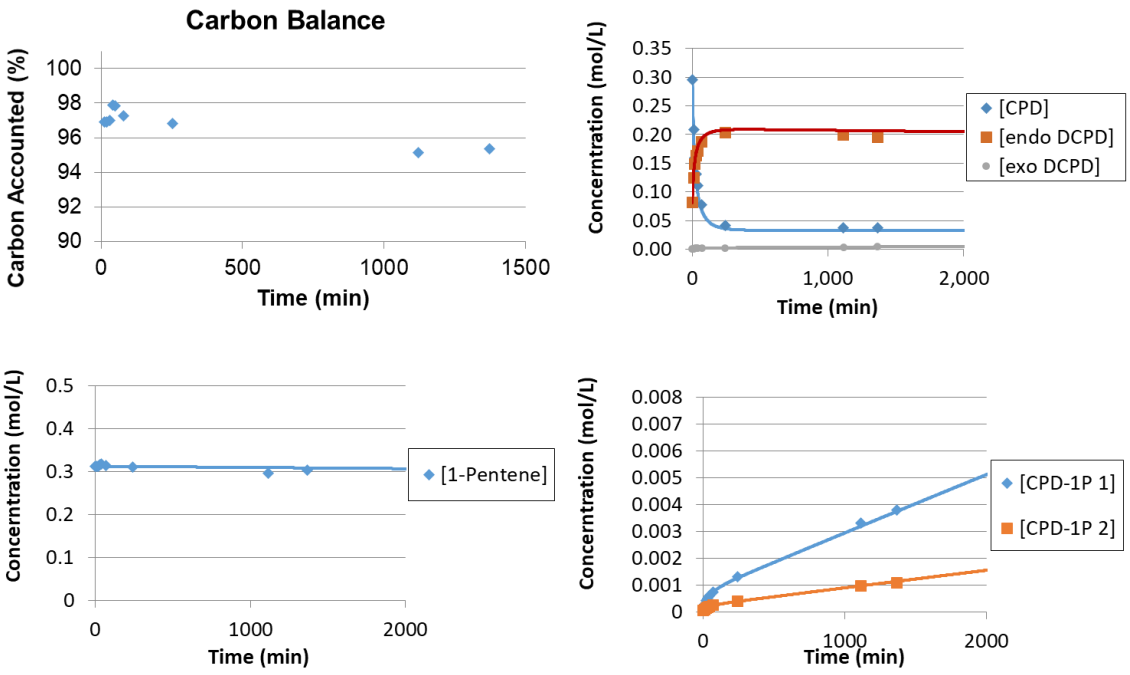

Figure 124: Cyclopentadiene-1-pentene co-dimerization in absence of air at 140 °C – Run 1.

Table 51: Fitted Rate Constants for Cyclopentadiene-1-Pentene Co-dimerization in Absence of Air at 140 °C – Run 1

K_{CPD1p1}	$2.14 \cdot 10^{-4}$ 1/M·min
K_{CPD1p2}	$6.44 \cdot 10^{-5}$ 1/M·min

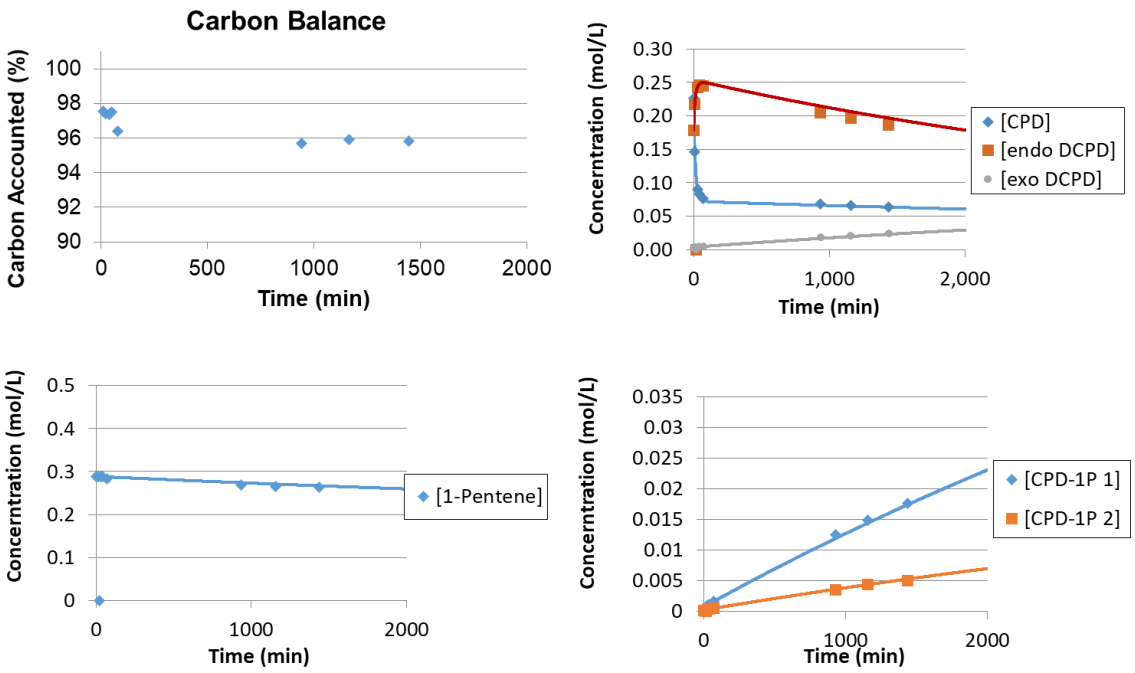

Figure 125: Cyclopentadiene-1-pentene co-dimerization in absence of air at 160 °C – Run 1.

Table 52: Fitted Rate Constants for Cyclopentadiene-1-Pentene Co-dimerization in Absence of Air at 160 °C – Run 1

K_{CPD1p1}	$6.17 \cdot 10^{-4}$ 1/M·min
K_{CPD1p2}	$1.87 \cdot 10^{-4}$ 1/M·min

REFERENCES

1. Loudon, M., *Organic Chemistry*. Fifth ed. 2009: Roberts and Company Publishers.

2. Krupka, J., *Kinetics of Thermal Dimerizations of Cyclopentadiene and Methylcylopentadienes and their codimerization.* Petroleum & Coal, 2010. **52**(4): p. 290-306.

3. Jamroz, M.E., S. Galka, and J.C. Dobrowolski, *On dicyclopentadiene isomers.* Journal of Molecular Structure-Theochem, 2003. **634**: p. 225-233.

4. Herndon, W.C., C.R. Grayson, and J.M. Manion, *Retro-Diels-Alder reactions. 3. Kinetics of Thermal Decompositions of Exo- and Endo- Dicylopentadiene.* Journal of Organic Chemistry, 1967. **32**(3): p. 526-&.

5. Liang, G., et al., *Intrinsic Kinetic Modeling of Thermal Dimerization of C5 Fraction.* China Petroleum Processing & Petrochemical Technology, 2016. **18**(1): p. 92-99.

6. Krupka, J., et al., *Kinetics of Cycloaddition Reactions of Conjugated C5 Dienes.* Petroleum & Coal, 2014. **56**(4): p. 428-441.

7. Krupka, J., *Kinetics of Diels-Alder reactions between 1,3-cyclopentadiene and isoprene.* Reaction Kinetics Mechanisms and Catalysis, 2015. **116**(2): p. 315-326.

8. Tseng, F.P., et al., *Preparation and epoxy curing of p-nonylphenol/dicyclopentadiene adducts.* Journal of Applied Polymer Science, 1999. **74**(9): p. 2196-2206.

9. Akizuki, M., N. Fujioka, and Y. Oshima, *Catalytic Effect of the SUS316 Reactor Surface on the Hydrolysis of Benzamide in Sub- and Supercritical Water*. Industrial & Engineering Chemistry Research, 2016. **55**(39): p. 10243-10250.

10. Krupka, J. and J. Kolena, *Gas Chromatographic Data and Identification of Isomeric Products of Cycloaddition Reactions of Conjugated C5 Dienes.* Petroleum & Coal, 2012. **54**(5): p. 385-396.

11. Muja, I., et al., *Kinetics and Thermodynamics of some Diels-Alder reactions: Kinetic study of the dimerization of cyclopentadiene and the codimerization of cyclopentadiene-isoprene.* Revista de chimie, 1975. **26**(12): p. 981-985.

12. Reichardt, C., *Solvents and Solvent Effects in Organic Chemistry*. 3rd ed. 2003: Wiley-VCH Publishers.

13. Hsu, H.C., et al., *Simplification and Intensification of a C5 Separation Process.* Industrial & Engineering Chemistry Research, 2015. **54**(40): p. 9798-9804.